Mag. rer. nat. Simon Leimgruber

Investigation of Elastomer-Metal Adhesion Interfaces and Development of Bifunctional Adhesion Promoter

DOCTORAL THESIS

to achieve the university degree of

Doktor der technischen Wissenschaften

submitted to

Graz University of Technology

Supervisor

Assoc. Prof. DI Dr. Gregor Trimmel

Institute for Chemistry and Technology of Materials
Graz University of Technology

Graz, August 2015

AFFIDAVIT

I declare that I have authored this thesis independently, that I have not used other than the declared sources/resources, and that I have explicitly indicated all material which has been quoted either literally or by content from the sources used. The text document uploaded to TUGRAZonline is identical to the present doctoral thesis.

Date	Signature

To my Family

ACKNOWLEDGEMENTS

Als erstes möchte ich mich beim Herrn Assoc. Prof. Dr. Gregor Trimmel vom Institut für Chemische Technologie von Materialien (ICTM) der Technischen Universität Graz für die Bereitstellung der Doktorarbeit in einem überaus interessanten und anwendungsorientierten Forschungsbereich sowie für die hervorragende Betreuung bedanken.

Gleich großer Dank gilt an Prof. Dr. Wolfgang Kern und Mag. Martin Payer vom Polymer Competence Center Leoben GmbH (PCCL) für die finanzielle Unterstützung. Die vorliegende akademische Arbeit wurde im COMET-Projekt „Interfacial Engineering towards improved adhesion between polymers and inorganic substrates“ (Projekt-Nr.: 4.02/1.06) am Polymer Competence Center Leoben GmbH im Rahmen des Kompetenzzentren-Programms COMET des Bundesministeriums für Verkehr, Innovation und Technologie und Bundesministeriums für Wirtschaft, Familie und Jugend unter Beteiligung der Technischen Universität Graz (ICTM) und Semperit Technische Produkte GmbH erstellt und mit Mitteln des Bundes und der Länder Steiermark, Niederösterreich und Oberösterreich gefördert.

Hier geht noch ein besonderer Dank an Herrn Dr. Armin Holzner, Dr. Roman Hochenauer, Dr. Michael Melmer, Ing. Michaela Jagschitz, Ing. Daniela Oehsl sowie vielen weiteren Mitgliedern der Semperit-Group in Wimpassing für die stete Hilfsbereitschaft und Unterstützung, ohne welche eine reibungslose Projektdurführung nicht möglich gewesen wäre.

Des Weiteren möchte ich mich beim gesamten ICTM-Team, im speziellen bei meiner Arbeitsgruppe für die jederzeit vorhandene Hilfsbereitschaft sowie die hervorragende Arbeitsatmosphäre bedanken. Besonderer Dank gilt hier an Sebastian Dunst und Manuel Hollauf, die ständing ein offense Ohr für meine Anliegen und Probleme hatten.

Viele Untersuchungen, welche im Zusammenhang mit dieser Arbeit stehen, wären ohne Kollaborationen nicht möglich gewesen. Deshalb möchte ich mich bei Ao. Univ.-Prof. Dr. Franz-Andreas Mautner und Dr. Brigitte Bitschnau (Institut für Physikalische und Theoretische Chemie) für die Röntgenbeugungsanalysen, bei Univ.-Doz. Dr. Peter Pölt und Dr. Angelika Reichmann (Institut für Elektronenmikroskopie) für die detailierten

SEM-EDX Messungen sowie bei Ing. Josefine Hobisch (ICTM) für die Thermogravimetrischen Analysen bedanken.

Meinen Eltern Olga und Nikolaus sowie meiner Schwester Lissi möchte ich ein besonders wertvolles Dankeschön für die unermüdliche Unterstützung aussprechen. Ohne euch wäre dies keinesfalls möglich gewesen.

Zuletzt möchte ich mich noch bei meiner Freundin Eva für die wunderbaren und abenteuerlichen gemeinsamen Jahre bedanken. Deine Geduld mit meiner Person, deine Toleranz für meine unzähligen Bergtouren sowie deine Energie und positive Lebenseinstellung geben mir Tag für Tag von neuem Kraft um meine privaten, sportlichen und beruflichen Ziele zu erreichen. Danke Eva!

ABSTRACT

Technical rubber products such as tires, hydraulic hoses, conveyor belts and hand rails are usually reinforced by brass-coated steel wires to improve their strength, persistence and dimensional stability. In order to meet the high mechanical requirements an outstanding and durable adhesion between the rubber compound and the metallic reinforcing device is mandatory.

Therefore, the principle topic of this thesis was to investigate and optimize the rubber-to-metal adhesion. The conventional adhesion mechanism is based on mechanical interlocking of the cross-linked rubber macromolecules on a rough Cu_xS-interface, created during the sulfur vulcanization of rubber. Here, the adhesion performance depends mainly on the composition of the rubber compound as well as on the wire properties. Regarding the wire samples, it was observed that various brass-plated steel wires with the same specifications show different adhesion performances. For this reason the work was focused firstly on the question, where are the differences between these wire samples.

Further, the rubber-brass adhesion strongly depends on the composition of the elastomer mixture. Hence, in a further study, the influences of various components on the rubber-brass adhesion interface were investigated using the olefin-metathesis method. Due to the strong adhesive strength of the rubber on the wire, it is challenging to uncover the brass-surface which is necessary to study the adhesion layer. The olefin-metathesis method is an excellent tool to degrade the cross-linked rubber network and to uncover the adhesion layer in a gentle way. Thus, it was possible to investigate different rubber types such as NR, NBR and SBR as well as additives and filler materials as carbon black, silica, cobalt-salts, and formaldehyde resins. However, the main focus was set on the investigation of the adhesion properties between nitrile butadiene rubber and brass, which shows some anomalies compared to other diene elastomers.

The third part of this thesis was to develop new bonding systems based on organic bifunctional molecules. Thereby, the rubber-metal adhesion is not achieved by mechanical interlocking of the rubber macromolecules in the brass layer but by chemical linkage. In doing so, the adhesion performance becomes less dependent from rubber compositions, wire properties, and aging processes. In order to transfer the manual dip-coating procedure to a continuous process also an automatic dip-coating machine was designed and constructed.

KURZFASSUNG

Technische Gummiprodukte wie Reifen, Hydraulikschläuche, Förderbänder und Handläufe sind in der Regel mit messingbeschichteten Stahldrähten verstärkt um deren Festigkeit, Beständigkeit sowie Formstabilität zu verbessern. Um den höchsten Standard an mechanischen Eigenschaften zu gewährleisten ist dabei eine hervorragende Haftung zwischen dem Gummi und den metallischen Verstärkungselementen erforderlich.

Das Thema dieser Arbeit war es die Gummi-Metall Haftung zu untersuchen und neue Haftsysteme zu entwickeln. Der konventionelle Haftmechanismus beruht auf eine mechanische Verhakung der vernetzten Kautschuk-Makromolekülen in eine raue Cu_xS-Adhäsionsschicht, welche sich während der Schwefelvulkanisation von Kautschuk ausbildet. Die Haftung wird dabei stark von den Drahteigenschaften beeinflusst, weshalb zunächst eine Reihe von vermessingten Stahldrähten auf Unterschiede in deren Materialeigenschaften untersucht wurde.

Des Weiteren hängt die Gummi-Messing Haftung von der Zusammensetzung der Kautschukmischung ab. Deshalb wurden in einem weiteren Schritt die Einflüsse der verschiedenen Mischungskomponenten auf die Gummi-Messing Haftschicht unter Verwendung des Olefin-Metathese Abbaus untersucht. Aufgrund der im Allgemeinen sehr starken Haftung des Gummis auf dem Draht ist es schwierig die Adhäsionschicht ohne gravierende Manipulation der Oberflächenstrukturen freizulegen. Der Olefin-Metathese-Abbau ermöglicht es jedoch, die vernetzten Kautschuknetzwerke abzubauen und die Haftschicht auf schonende Weise freizulegen. Dadurch war es möglich, den Einfluss verschiedener Kautschukarten wie NR, NBR und SBR sowie Additive und Füllstoffe wie Ruß, Silika, Kobalt-Salze und Formaldehyd-Harze auf die Gummi-Metall Adhäsion zu untersuchen.

Ziel im dritten Teil dieser Arbeit war es, neue Haftsysteme auf Basis von organischen bifunktionellen Molekülen herzustellen. Dabei wird die Gummi-Metall Haftung nicht durch mechanische Verhakung der Kautschukpolymere in die Messingschicht sondern durch chemische Bindung erreicht. Dadurch ist das Haftvermögen zu einem geringeren Maß von der Zusammensetzung der Kautschukmischung, den Drahteigenschaften und den Alterungsprozessen abhängig. Zur Automatisierung des Beschichtungsprozesses wurde in weiterer Folge eine eigen entwickelte Drahtbeschichtungsanlage verwendet.

ABBREVIATIONS

A	Bis[3-(trimethoxysilyl)propyl]amine
AAMS	Aminoethylaminopropyltrimethoxysilane
AAS	Atom absorption spectroscopy
ADMET	Acyclic diene metathesis
APS	Aminopropyltrimethoxysilane
ATR-IR	Attenuated total reflection – Infrared spectroscopy
BR	Butadiene rubber
bs	Broad singlet
CBS	Cyclohexylbenzothiazole
COC	Cyclooctene
CPE	Cyclopentene
CTA	Chain transfer agent
d	Doublet
DCBS	N-dicyclohexylbenzothiazole 2-sulfenamide
DMF	N,N-Dimethylformamide
DOA	Dioctyl adipate
DSA	Drop shape analysis
EDX	Energy dispersive X-ray spectroscopy
ELT	End-of-life tire
ENR	Epoxidized natural rubber
EPDM	Ethylene propylene diene monomer
EPR	Ethylene propylene rubber
GC	Gas chromatography
GPC	Gel permeation chromatography
HMMM	Hexamethoxymethylmelamine
HNBR	Hydrogenated nitrile butadiene rubber
HPLC	High performance liquid chromatography

IR	Isoprene rubber
Iso	3-(triethoxysilyl)propyl isocyanate)
KMR	Kaolin modified resin
m	Multiplet (NMR), middle (IR)
MAS	3-Methacryloxypropyltrimethoxysilane
MAS	3-(trimethoxysilyl)propyl methacrylate
MBS	2-Morpholinothiobenzothiazole
MBT	Mercaptobenzothiazole
MBTS	2,2-Dithiobenzothiazole
MeCN	Acetonitrile
MEKO	2-butanone oxime
MeOH	Methanol
MS	Mass spectrometry
NAAPS	N-allylamino propyl trimethoxysilane
NBDC	Bisdecyl norbornene dicarboxylate
NBE	Norbornene
NBR	Nitrile butadiene rubber
NMR	Nuclear magnetic resonance spectroscopy
NR	Natural rubber
p-TCN	p-Tolunitrile
PA	Phosphonic acid
PB	Polybutadiene
phr	Parts per hundred rubber
PI	Polyisoprene
q	Quadruplet
RAFT	Reversible addition-fragmentation chain transfer
RCM	Ring closing metathesis
RF	Resorcin – formaldehyde
ROMP	Ring opening metathesis polymerization
s	Singlet (NMR), strong (IR)

S_4-Si	Bis[3-(triethoxysilyl)propyl] tetrasulfide
SAM	Self-assembled monolayer
SBR	Styrene butadiene rubber
SCN	Succinonitrile
SEM	Scanning electron microscopy
t	Triplet
t-BA	*tertiary*-Butyl acrylate
TGA	Thermal gravimetric analysis
THF	Tetrahydrofuran
TMSBr	Bromotrimethylsilane
TOF-SIMS	Time of flight – Secondary ion mass spectrometry
VOC	Volatile organic compound
w	Weak
wt	Weight
XPS	X-ray photoelectron spectroscopy
XRD	X-ray diffraction
γ-MPS	Mercaptopropyltrimethoxysilane

CONTENTS

1 INTRODUCTION

Rubber is already used for more than one century in many technical products due to its versatile and unique properties. The requirements as well as the diversity of such products increased over time, especially from 1900 onwards due to the development of the automobile. During the First World War, Germany was isolated from the natural rubber supply and thus Bayer started the first large-scale production of synthetic rubber. Consequently, in the following years, natural rubber has been replaced more and more by synthetic elastomers due to their functionalities, availability, and affordability [1].

Nevertheless, natural rubber is still competitive with the synthetic counterparts. This can be seen in Figure 1, which shows the development of the worldwide consumption of natural and synthetic rubber since 2000. The consumption increases constantly in every year except one small slump, which was caused by the commercial crisis in 2008 and 2009.

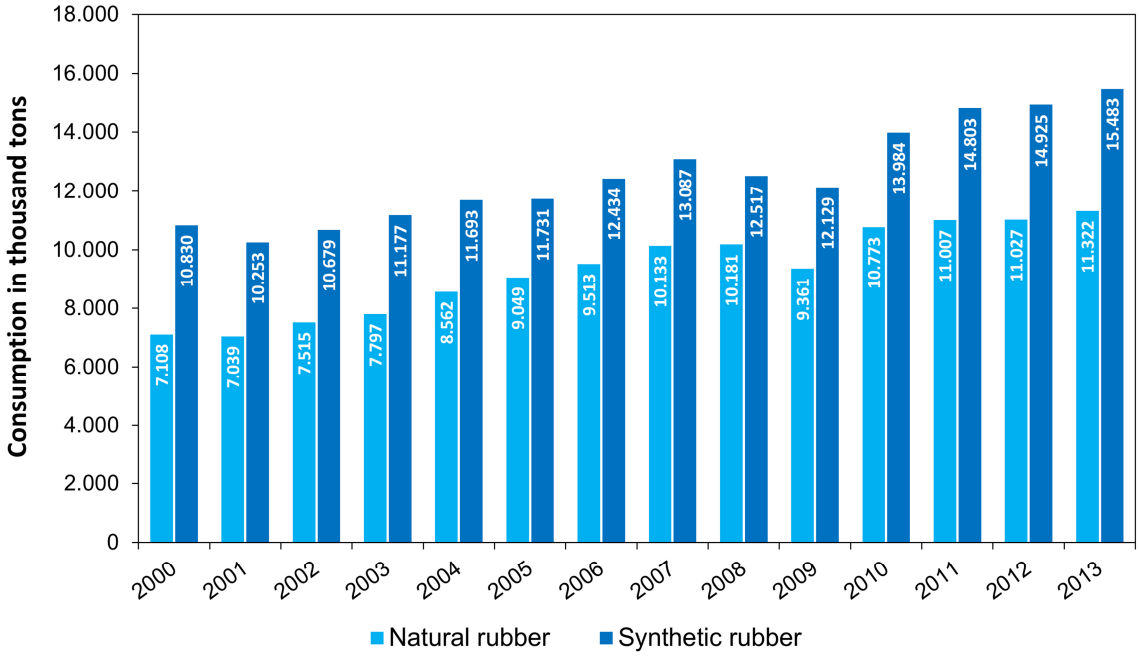

Figure 1 Development of the natural and synthetic rubbers` worldwide consumption from 2000 to 2013 (data taken from Statista) [2].

The high consumption of both natural and synthetic rubber implicates that also the number of elastomeric products continuously increased. Elastomers are frequently used in tires but also in many applications as damping systems and seals for gases, liquids,

and solids. Many of these applications, however, need mechanical reinforcements to achieve the required performances. These are very often products for automotive, aerospace, and industrial applications, which we can find in our everyday life, e.g. tires, hydraulic hoses, and handrails. The increased use of rubber products has also driven the requirements for powerful and robust bonds between rubber and metal [3]. The bonding mechanism of metals to elastomers was subject of many studies but still there are many unanswered questions. As a consequence, the rubber industry has to work with empirical knowledge. This is not surprising, as small variations in the rubber mixture or metal surface result in totally different bonding properties.

As far as it is currently known, the conventional rubber-to-metal adhesion is accomplished by a mechanical interlocking mechanism of the elastomers at the adhesion interface [4]. A chemical bonding contribution between brass and rubber is assumed to be only a minor factor [5]. In order to further improve and optimize the adhesion interface a method is needed, where the build-up interface can be uncovered without manipulations. This is a serious challenge, since it is located between the rubber network and the metal surface. One method, which meets all these requirements is based on the olefin-metathesis and is used in this study to illuminate new details of the rubber-to-metal bonding mechanism.

However, in case of the mechanically interlocking mechanism the rubber mixture has to be optimized for the adhesion performance rather than for the rubber properties as e.g. abrasion resistance and thermal ageing. Further, this adhesion system is limited to unsaturated elastomers, sulfur vulcanizations as well as specific metal surfaces. Using chemical adhesion promoters, both the rubber-brass adhesion properties as well as the rubber properties can be optimized simultaneously. Thus, outstanding product performances can be achieved for a wide variety of substrates and elastomers. Such coupling agents are based on bifunctional molecules and are already used commercially to enhance filler-to-rubber interactions. In this study, commercially available as well as in house developed organofunctional silanes and phosphonic acids are investigated and optimized in order to be used as coupling agents for peroxide and sulfur vulcanisable rubber types.

2 THEORETICAL BACKGROUND

2.1 Rubber-brass adhesion

2.1.1 Introduction

In rubber technology, the elastomer-metal bonding is of great importance as many rubber products such as tires, hydraulic hoses, and handrails are reinforced by wires or cords. In order to achieve outstanding mechanical properties the adhesion between rubber and metals plays a crucial role. In general, pure steel wires could be used as reinforcing devices in rubber products. Unfortunately, rubber adheres very poorly on steel for which it cannot be used without any modification (Figure 2) [6]. However, it has been shown that under certain conditions rubber adheres very well on brass, for which the steel wires are simply coated with a thin layer of brass. For some applications – especially if excellent corrosion resistance is required – zinc-plated steel wires are used [7] but most of the time brass is applied to achieve high adhesion performances. Beside this, various alternative alloys were investigated to reach good rubber-to-metal bindings. Thus, for example, a third alloy-component was simply added to brass as 2 wt% cobalt in the study of Jeon *et al* [8] or 12 wt% Ni in experiments of van Ooij and Kleinhesselink [9]. Further, van Ooij investigated – in cooperation with Giridhar – a Cu-free alloy system on the basis of NiZn/ZnCo [10-12]. However, none of these systems was able to replace brass as top-coating for rubber reinforcing devices. The reasons are mainly that brass leads to good adhesion performances, has a reasonable corrosion resistance and can act as drawing agent during the manufacturing process of the wire samples [13].

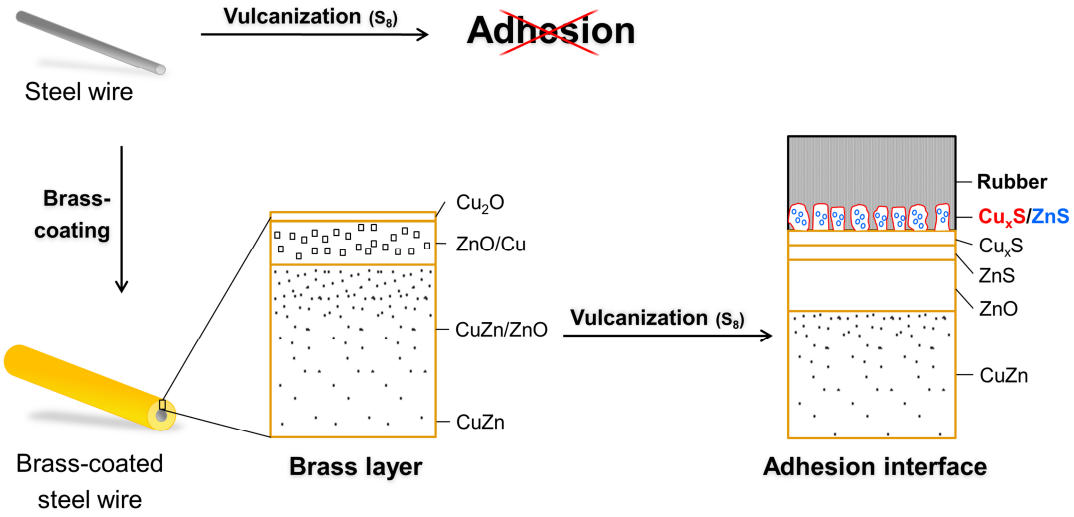

Figure 2 Principle of the rubber-brass adhesion.

As illustrated in Figure 2, the surface of brass consists normally of a layer system based on different oxides [14]. The outermost layer is based on Cu_2O, which is with approximately 1 nm very thin. Between the copper oxide layer and the brass bulk there is an intermediate layer of zinc oxide with copper inclusions, which is formed during surface oxidation processes of brass.

At the beginning of the vulcanization reaction – also known as scorch – copper and zinc ions diffuse together with free electrons to the brass surface, at which they react with the active sulfiding species of the rubber mixture. Thereby, in a first step, ZnS is formed but this layer is immediately overgrown by a very rough and non-stoichiometric Cu_xS ($x \rightarrow 1.8$) layer [14]. Initially, the copper ions diffuse very slowly through the ZnS layer. However, from that point where the copper ions migrate into the Cu_xS layer the diffusion rate drastically increases due to the non-stoichiometry of the copper sulfide layer [15]. This process holds until the entire copper inclusions of the zinc oxide intermediate layer are used up for which reason the copper content in the ZnO layer is of crucial relevance for the formation of a well-defined and strong adhesion interface [15,16].

Although many studies focused on the investigation of the rubber-brass bonding mechanism, it is still not thoroughly clarified in detail how the adhesion is accomplished. The most likely theory was proposed by van Ooij in 1984. According to its examination results the rubber interlocks mechanically in the Cu_xS-structures, which are build-up during the sulfur vulcanization [14]. Here, the often proposed covalent

bindings [1,16] between rubber and brass were determined to play a minor role in the adhesion mechanism or, at least, that covalent bindings are a minor factor. One hint therefore, e.g., is that a minimum critical thickness of the copper sulfide layer has to be reached to ensure good adhesion properties [17]. But if covalent bindings would be mainly responsible for the adhesion, a Cu_xS monolayer should be sufficient [14].

However, the performance of the rubber-brass adhesion depends on many parameters, mainly on the vulcanization conditions, on the composition and properties of the rubber compound as well as on the wires` properties. Concerning the wire characteristics, the composition of the brass-alloy is of great importance. In general, the occurrence of α-brass is preferred because β-brass is rather brittle and easily detaches from the wire surface. Such labile parts may cause material failure at the metal interface [18].

The optimal copper content was found to be between 60 and 70 %. Beside others, the constitution of the brass layer strongly influences the size of the Cu_xS-structures and consequently the quality of adhesion. If the copper level in the brass-coating is low, the diffusion of the copper ions deteriorates and thus no Cu_xS is formed. On the other side, at high copper contents the copper sulfides grow too fast which results in a brittle adhesion interface [4].

Additionally, for a satisfactory adhesion performance the plating thickness should be in the range of 0.2 to 0.3 µm [15] and the thickness of the ZnO layer has to be chosen optimally for a particular application because as mentioned before, ZnO has a mediating effect on the sulfidation reaction and therefore its condition is of considerable importance for the bonding strength [14]. Also drawing additives, which remain on the wire surface after the manufacturing process, may have an influence on the adhesion but this has never been really confirmed [15].

Concerning the composition of the rubber compound, van Ooij mentioned the importance of the high sulfur to accelerator ratio (> 4 phr) as well as a high degree of unsaturation of the rubber polymers for good adhesions [19]. Beside this, also the accelerator type or the amount of stearic acid can have a strong impact on the build-up of the adhesion interface [14,19,20]. In particular, almost every compound ingredient influences the overall quality of adhesion for which there are still many unsolved issues concerning the adhesion mechanism. Although the general adhesion mechanism has been studied extensively [4-9, 21], there are still disagreements concerning some

important aspects. However, before these aspects of the rubber-metal adhesion will be discussed in detail, the fundamental reaction of rubber technology is presented, the vulcanization.

2.1.2 Rubber vulcanization

The accidental discovery of the sulfur vulcanization of rubber by Goodyear in 1839 was a milestone in polymer technology [22]. Due to the fact that rubber products can be found in the majority of technical devices they are irreplaceable. However, since the invention of the sulfur vulcanization several other crosslinking techniques have been developed. Thus, the formation of the covalent bridging bonds between the rubber macromolecules can be achieved by different chemical reactions. The greatest significance has still the vulcanization using sulfur-accelerator-systems, cross-linking with peroxides comes in second place. For some special applications, also energetic radiation, diisocyanates and resins are used, to name just a few. The selection of the cross-linking system depends mainly on the rubber and processing method and influences the elastomer properties significantly. So the elastomer properties are mainly determined by the type of polymer (basis material) but also by the crosslinking density and the chemical structures of the cross-linking sites. Procedure relevant is e.g. the sensitivity of the cross-linking system against oxygen and high processing temperatures as well as the influence of the vulcanization time [1]. However, in this contribution only sulfur-accelerator systems – for natural rubber (NR), nitrile butadiene rubber (NBR), and styrene butadiene rubber (SBR) – and peroxide curing systems – for ethylene propylene diene monomer (EPDM) rubber – are applied for which their functionality is described more detailed.

Sulfur vulcanization

The most important cross-linking reagent is still sulfur. In particular, there is one prerequisite for the implementation of the sulfur vulcanization, namely that the elastomers contain double bonds either in their main chain (diene rubbers) or double bonds – more precisely allyl-hydrogen atoms – in their side chains as for example in EPDM. One big advantage of the sulfur vulcanization is its insensitivity to most of the mixture components as well as to oxygen and moisture. However, alkaline ingredients have an accelerating effect and acids a retarding effect. In order to achieve particular

mechanical, chemical and dynamic properties but also to speed up the cross-linking reaction accelerators and activators are indispensable. The sulfur vulcanization without accelerators is due to the associated disadvantages as long reaction times and bad ageing behavior only of scientific interest.

Compared to other types of curing systems, cross-linking of rubber using sulfur-accelerator-systems has the advantage that by using different accelerators the processing and product properties can be varied over a wide range. Especially the combination of accelerators is of great interest because it enables to adjust the scorch-time as well as the reaction rate. The ratio of sulfur to accelerator controls the structure of the sulfide bridges. Thus, rubber engineers have a wide variety of variables to find a compromise between processing parameters, economic reaction times, and well-balanced product properties.

Until today, the mechanism of the sulfur vulcanization is subject of numerous studies and research projects. There are many postulates, which explain the reaction mechanism of the sulfur vulcanization in a different way. But most probably the sulfur transmission is achieved by an active sulfur-accelerator-complex. In the literature, there are many proposals about exact compositions and modes of operation for these complexes. However, up to the present, two things have been clear: in the presence of zinc ions complexes are formed that are soluble in rubber and which have a structure as depicted in Figure 3 [23-28].

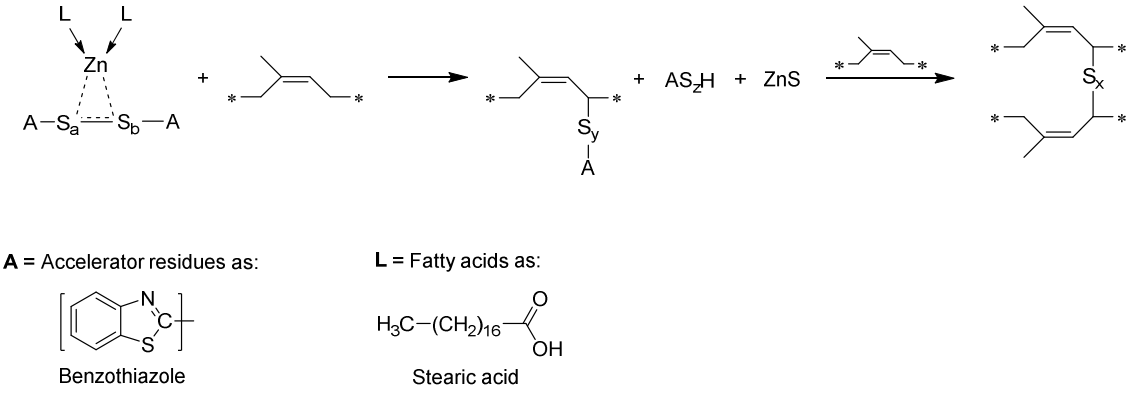

Figure 3 Proposed mechanism of the sulfur bridge formation via the active sulfur-accelerator complex (without illustrating the electrical charges) [29].

The active sulfur-accelerator complex transfers sulfur to the rubber and subsequently cross-linking starts. Beside this simplified reaction process further consecutive and

parallel reactions take place [29]. These reactions have different activation energies and therefore they depend on the particular reaction time and temperature. Thus, different reaction products can be formed and therefore the investigation of the correct and detailed mechanism is very difficult and highly complicated [30,31].

Recently, Ideka *et al* published a new possible mechanism for the sulfur vulcanization of isoprene rubber (synthetic natural rubber). Accordingly, zinc forms together with stearic acid an intermediate complex, which may play a significant role in accelerating the sulfur cross-linking reaction (Figure 4) [32].

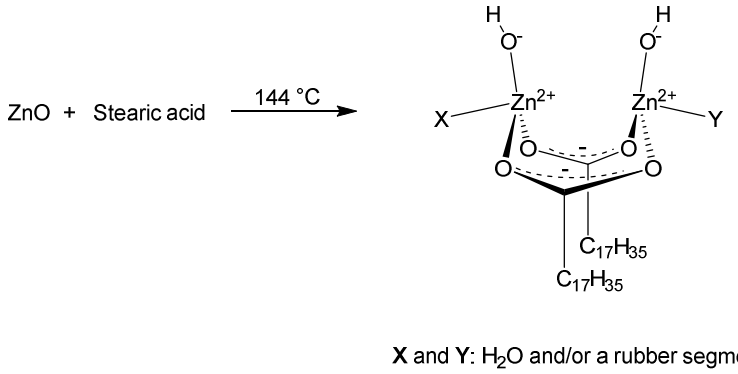

Figure 4 Formation of the ZnO-stearic acid intermediate complex [32].

Unfortunately, also by using this approach the entire mechanism of the sulfur vulcanization cannot be explained, for which reason this topic will still be of interest for detailed investigation.

Peroxide crosslinking

Peroxides were used for the first time in 1915 to crosslink natural rubber [33]. In the following years, this approach was used not very frequently to crosslink NR because of serious disadvantages compared to the sulfur vulcanization. Only after the development of saturated rubber polymers peroxide crosslinking became a topic again. Today, peroxides are also used for the cross-linkage of diene rubbers. The efficiency of the cross-linkage can be significantly improved by using radical transferring compounds, so called coagents. Peroxide cross-linked elastomers have – compared to sulfur cross-linked elastomers – a better thermal stability, the deformation remains low and the covalent bridges are formed irreversible. Disadvantages are lower tensile strengths and tear resistance, an unfavorable processing window, and the necessity to exclude oxygen during the curing process.

The mechanism of the peroxide cross-linkage was investigated in many studies. The reaction is initiated by thermal breakup of the peroxide, which leads to the formation of two radicals (Figure 5). The transfer of the radical on the polymer is based either on the substitution of a hydrogen atom or by addition on the double bond. However, now, cross-linking takes places via bimolecular reactions, which compete with side reactions. Cross-linking occurs if allylic or secondary hydrocarbon radicals are formed. It is the core reaction of the peroxide vulcanization in which the degree of cross-linking depends on many parameters. The type of termination, in contrary, depends on the radical structure (steric factors), the radical concentration as well as on the used coagents [34-37].

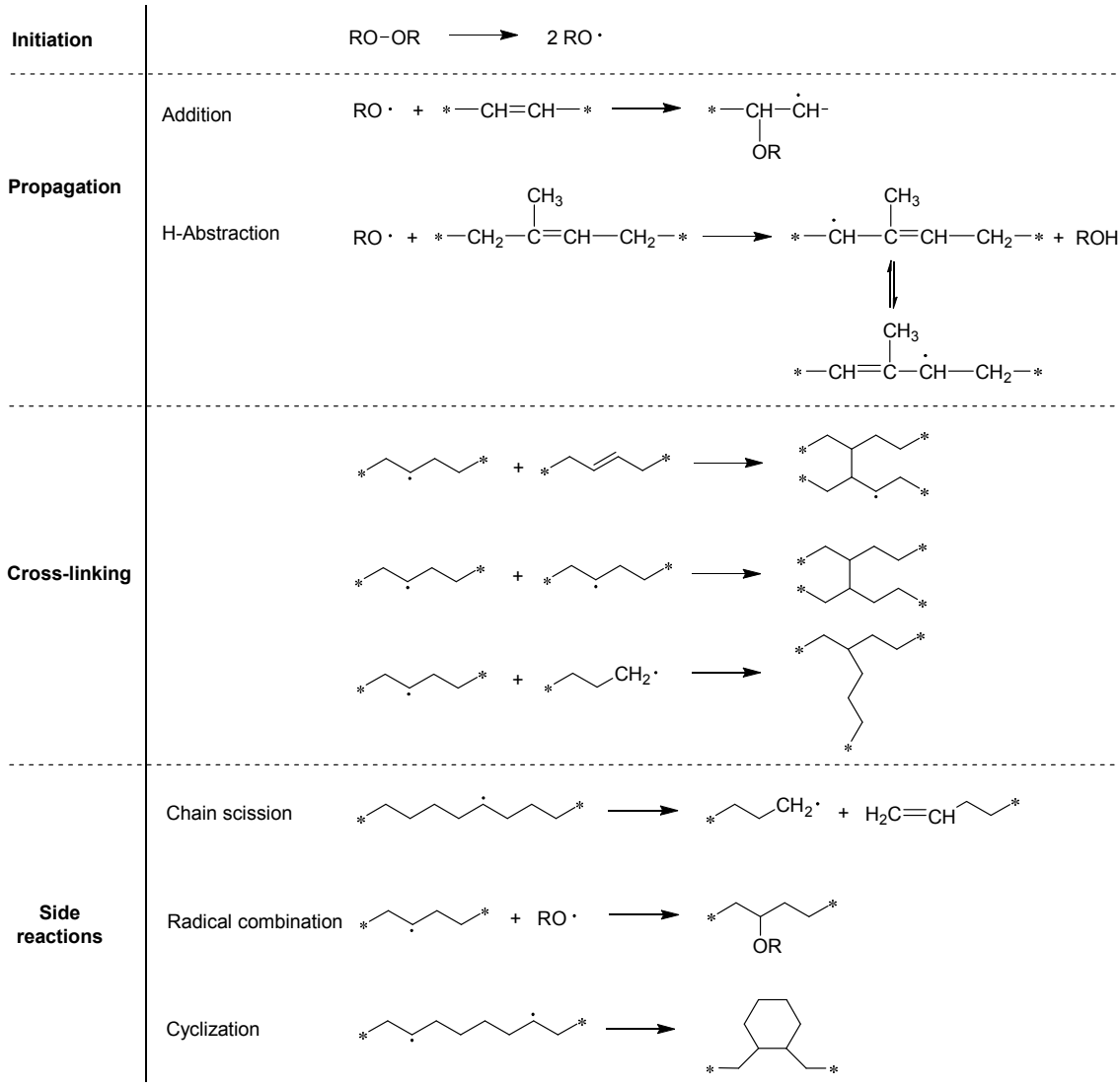

Figure 5 Reaction process of the peroxide crosslinking without using coagents [1].

2.1.3 Adhesion interface build-up

As the vulcanization of rubber, also the bonding of rubber to metal was invented by accident in the mid-19th century. Thus, NR was bonded to brass during the sulfur vulcanization reaction. This process was commercialized quite late in the 1930s when steel substrates were brass-plated via a galvanic process. Even though this technique is relatively old it is still the most used adhesion system for metal reinforced rubber products. The rubber-to-brass bond has – under certain conditions – very good mechanical properties, is very durable and resistant to high temperatures. Therefore, the areas of application are mainly in the section of tires but also in some other technical rubber products.

The formation of the adhesion interface during the sulfur vulcanization of rubber was not really understood for a long time. However, van Ooij postulated in 2001 a mechanism, which correlates very well with the experimental observations. In his explanations he used cyclohexylbenzothiazole sulfenamide (CBS) as accelerator because it suits very well for the build-up of an efficient rubber-to-brass bonding. Other sulfonamide accelerators perform equally but at different paces [19,38].

According to van Ooij the sulfidation process of the brass surface can be divided into five steps. As can be seen in Figure 6, first of all the high electron density of the rubber double bonds (π-orbital) polarize the S-N bond of the accelerator in which the cleavage of the covalent bond is supported. Thus the sulfonamide residue gets charged negatively because of two reasons. Once, sulfur is a relatively large atom compared to nitrogen and secondly due to the possibility of resonance induced charge delocalization [6,14]. As a result of this cleavage 2-mercaptobenzothiazole (MBT) is formed which reacts with another accelerator molecule (CBS) to form 2,2-dithiobenzothiazole (MBTS). Now, the accelerator intermediate is activated via complexation with zinc ions and serves either to form Cu_xS-structures on the brass surface or to crosslink the rubber macromolecules.

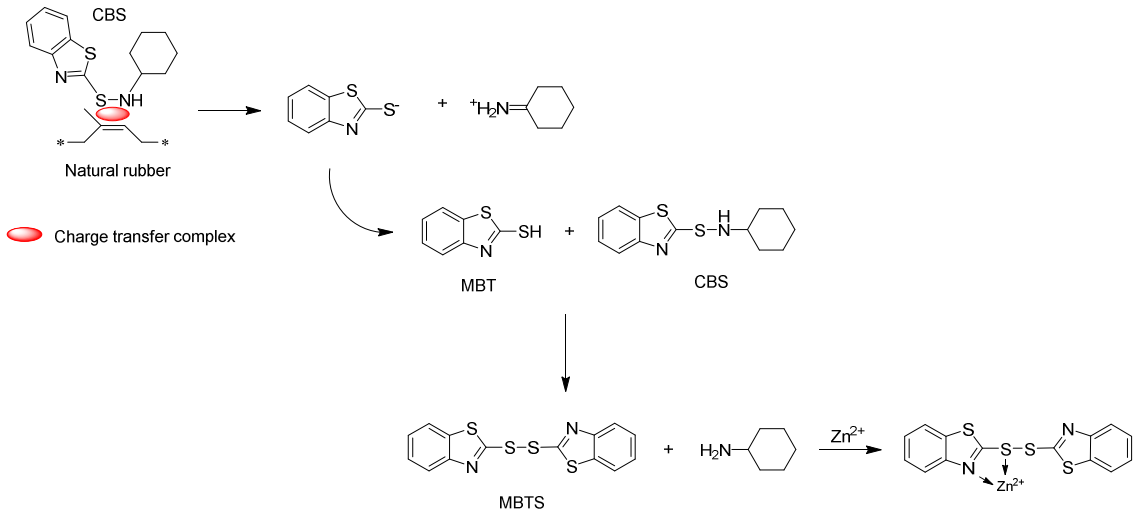

Figure 6 Step 1: formation of the active intermediate of the accelerator.

Figure 7 depicts step two to four of the adhesion interface build-up. Initially, stearic acids dissolve partially the surface oxides – Cu_2O and ZnO – in order to expose the brass layer. Subsequently afterwards MBTS or MBT adsorb on the exposed brass surface.

Afterwards, in the third step, the brass-to-sulfur bonds open the sulfur-rings and so they enable the insertion of sulfur. Very often, zinc ions support this reaction by complexing with the nitrogen and sulfur atoms of MBT. However, usually not the entire S_8-ring is inserted between the metal-to-sulfur bond but a smaller fragment.

The formation of the Cu_xS-structures starts finally in stage four at increased temperatures. The adsorbed accelerator-sulfur-metal complexes are disassembled building metal sulfides and active accelerator-S_{y-1} fragments. This active accelerator radical adsorbs once more on the surface to react with another copper atom, which has diffused to the brass surface. In doing so copper sulfides are formed up to the point where no fresh accelerator, MBT or sulfur is available any more. Alternatively, the active accelerator-S_{y-1} fragment can initiate the curing process of the rubber polymers.

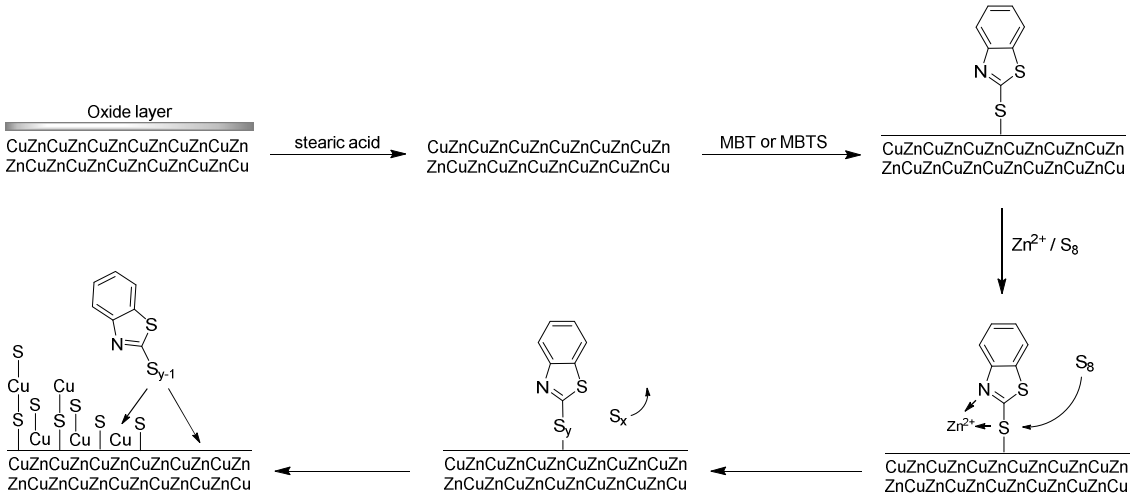

Figure 7 Step two to four of the adhesion interface build-up.

Crosslinking of rubber was defined as step five of the adhesion interface build-up process because there the sulfiding species from step one as well as the active accelerator-S_{y-1} fragments from step four are involved (compare Chapter 2.1.2). Thus, a rubber network is formed which interlocks in the rough nonstoichiometric copper sulfide layer. Here one has to note that close to the adhesion interface the concentration of the active crosslinking species is significant higher then on the other regions, which results in increased crosslinking densities of the elastomers close to the wire surface.

Moreover, the brass sulfidation reaction (step 4) competes with the vulcanization reaction (step 5), which complicates controlling the respective reaction.

By watching this proposed mechanism of the adhesion interface build-up one cannot exclude the formation of covalent copper-sulfur-rubber bonds. In literature, the presence of such chemical bindings is discussed [5], but it is believed that they are of minor importance for the overall rubber-to-brass adhesion performance.

The mechanism proposed by van Ooij is based on natural rubber systems and does not consider substituents on the polymer backbone. There is practical no literature regarding the build-up mechanism of binding layers for functionalized elastomers. However, the general mechanism could be the same unless there appear undesired interactions between rubber, brass, and the sulfiding species. In order to explore such interactions, the adhesion performance of SBR and NBR to brass was investigated in detail.

2.1.4 Influence of compound composition

A conventional rubber compound consists of many components, which differ in their functionality and interact in a very complicated way. Thus, most of the ingredients have an influence on the adhesion performance between rubber and brass. One good example is the correlation between the thickness of the adhesion layer (size of Cu_xS-structures) and the sulfur content of the rubber mixture [4]. It is generally known that for a high quality of adhesion an optimal size of the Cu_xS-structures is mandatory. Just by adding at least 3 to 4 phr sulfur, the critical size for the sulfuric structures can be achieved [39]. In contrast, excessively high sulfur levels in the compound lead to very large Cu_xS-structures and as a result they become brittle and consequently break easily [4]. Additionally, as already mentioned before, it was observed that the sulfur to accelerator ratio is of enormous importance. In order to obtain well bonding properties, here, the ratio has to exceed 4 [14].

Also the type of accelerator plays a crucial role in the formation of the sulfuric adhesion interface. Based on the mechanism for the rubber-brass adhesion interface build-up proposed by van Ooij (Chapter 2.1.3), delayed-action accelerators – most likely sulfonamides – have to be used. Fast accelerators, e.g. thiurams, leading to short scorch times result in bad adhesions because there the rubber cures faster than the Cu_xS-structures are formed and consequently the mechanical interlocking of the elastomers in the binding layer is deteriorated. However, in order to achieve good adhesion performances, N-dicyclohexylbenzothiazole 2-sulfenamide (DCBS) was found to be one of the best accelerator candidates [14].

Another important factor for good adhesions is a high degree of unsaturation. Since the double bonds are a major prerequisite to polarize the S-N bond of the accelerator and thus to enable a good sulfidation reaction, their absence leads to decreased accelerator decomposition. Therefore, the speed of the Cu_xS formation is reduced with decreasing number of double bonds in the polymer backbone [40].

ZnO is mixed as activator into rubber compounds. It influences the rubber-to-brass bonding as well as the rubber properties [40]. Concerning the adhesion interface build-up, zinc ions support the formation of activated sulfiding species by creating chelate complexes [19]. In order to achieve good bonding characteristics, it was found that high

zinc oxide contents, small ZnO particle sizes [4] as well as a high zinc oxide to stearic acid ratio are of great advantage [14].

Beside these, filler materials such as carbon black and silica are supposed to have a positive impact on the quality of adhesion. Similar to the double bonds, carbon black supports the accelerator decomposition and thus the formation of the adhesive structures [40]. Further, carbon black reinforces the rubber network and consequently it improves the adhesion properties as well by reducing the modulus-differences between rubber and metal. Silica is also used very often in elastomer mixtures. Beside its beneficial properties to adjust the modulus, tensile strength as well as the elongation at break it also affects the rubber-to-brass adhesion strength. It was found that with increasing silica content of the rubber mixture the pull-out force as well as the rubber coverage raises too [41,42]. The reason therefore is that silica increases the zinc and oxygen levels but decreases the total amount of sulfur in the rubber compound. As a consequence, the copper sulfide structures are smaller [43] which results in a higher stability of the adhesion interface with increasing silica loading [42].

The improved adhesion properties by using moderate amounts of silica (20-50 phr) are also caused – as for the carbon black filled rubber mixtures – by an increased modulus of the rubber network at increased filler loadings. Thus, the modulus of the rubber resembles more closely the modulus of the adhesive which reduces differential stress at the adhesion interface [44].

If the rubber compound is targeted on the improvement of the elastomer-brass adhesion, very often cobalt salts are used as adhesion promoter. They show positive effects on the initial bonding strength and on the durability of the adhesion, especially after thermal and humidity ageing [15,45]. In literature, many different cobalt salts were already investigated regarding their strengthening effects on the adhesion layer. Thus, cobalt stearate, cobalt naphthenate, cobalt resinat, cobalt neodecanoate as well as cobalt boroacylate are the most frequently applied salts. Apart from the influence of the cobalt salts on the rheological properties [45,46] and curing characteristics of the rubber mixture [40,45-50] they affect the growth behavior of the sulfuric structures. The reason for that is the change of the diffusion rate of copper and zinc ions because of the incorporation of cobalt ions into the adhesion interface [14,15]. Thus, according to Hotaka *et al*, more Cu_2S is formed instead of CuS. Since Cu_2S is mainly responsible for

the adhesion [51], the adhesion performance is increased by cobalt ions [50]. Also in respect to ageing, cobalt has the property to preserves the adhesion performance. During thermal ageing, the copper sulfide structures continue growing and thus the adhesion interface becomes brittle and loses its adhesion strength. Using cobalt salts this reaction is drastically slowed down [48]. However, there are many other theories about the influence of cobalt salts on the rubber-brass adhesion, which correlate more or less well with the experimental observations [45-47,50,52].

Very recently, Darwish *et al* developed a new promoter for enhancing the adhesion between NR and brass-coated steel cords, which enables replacement of cobalt salts by kaolin in rubber compounds. Thus, kaolin modified resins (KMRs) are produced by reacting acrylonitrile with a cross-linking agent followed by adding $FeCl_3$. The so formed modified kaolin/resin-iron chelate showed excellent adhesion properties in natural rubber mixtures compared to conventional cobalt salts. This is caused by the presence of Fe-chelating compounds which facilitate the formation of cross-links between the elementary sulfur in the rubber compound and the brass layer [53].

As just indicated, resins represent another very efficient group of additives to promote the adhesion strength between elastomers and metals. In the majority of cases methylene donors, as e.g. hexamethoxymethylmelamine (HMMM), are applied in combination with a methylene acceptor, typically resorcinol [54]. Beside this, condensation products based on resorcinol and formaldehyde (RF resins) are used rather often in order to reduce the fuming [15]. Loading the rubber compound with such resin systems leads to the formation of a dense and highly cross-linked network which improves the adhesion strength [55].

There exists another category of adhesion promoter, namely the chemical adhesion promoters based on multifunctional molecules, which will be discussed more detailed in the next chapter.

2.2 Chemical bonding systems

2.2.1 Introduction

The rubber-to-brass adhesion is the most frequently used bonding system in rubber technology due to its very good mechanical properties, durability, and resistance to high temperatures. Therefore, the areas of application are mainly in the section of tires but also in some other technical rubber products. For products as e.g. in suspension bushings, engine mounts, and transmission seals, however, the conventional brass-plating technique reaches its limits, for which alternative adhesion systems have to be used. As practical alternative solvent-based or waterborne adhesives have been investigated, which offer a much broader range of elastomer-metal combinations. Hereafter, the limitations of the rubber-brass adhesion system are summarized:

- Rubber binds only to brass if the rubber macromolecules are highly unsaturated. Consequently, this adhesion system is limited to unsaturated elastomers.
- The typical sulfuric structures, which are mainly responsible for the rubber-brass adhesion, are only formed using the sulfur vulcanization. Further, high sulfur levels and accelerators of specific type are mandatory for a good adhesion performance.
- The composition and characteristics of the brass layer is also of great importance.
- Very well established rubber-to-brass adhesion promoters are cobalt salts. While this additive improves the stability of the rubber-brass bond, especially in a corrosive environment, it exerts a negative effect on the stability of the rubber network, in that it accelerates reversion phenomena especially in the presence of oxygen and at elevated temperatures.
- Brass is only to a low extent corrosion-resistant for which it protects the underlying steel device only marginally from water, humidity, and steam, especially if the brass layer is porous. Consequently, the brass-plating of the steel wires or cords may detach or even result in wire breakage.

Nevertheless, the advantages of this conventional adhesion system as e.g. the simple technical implementation, the durability as well as the mostly sufficient adhesion performance lead to a still essential role in rubber technology. However, in case of the brass-plating technique the rubber mixture has to be compounded in order to get a compromise between the adhesion properties and the rubber properties as e.g. crack

growth resistance, abrasion resistance, and thermal ageing. Using adhesion promoter based on chemical linkage both the rubber-brass adhesion performance as well as the rubber properties can be optimized simultaneously. Thus, outstanding product performances for a wide variety of substrates and elastomers can be achieved [44].

Chemical adhesion promoters – also known as coupling agents – are compounds that enhance the adhesion performance between an inorganic substrate and an organic polymer via covalent bindings. Due to the great differences in the chemical, mechanical, and physical properties of the organic and inorganic materials the formation of a strong, efficient, and durable covalent bond is rather tricky. Ideally, a chemical adhesion promoter should be able to build a durable and powerful chemical bond between the organic-inorganic interface so that the final product performance achieves its desired quality. In other words, the coupling agent should act as a "glue" to provide outstanding adhesions. Furthermore, chemical adhesion promoters must overcome environmental and other destructive influences, e.g. moisture, heat, and irradiation, which often lead to the loss of adhesion strength [56].

In general, one can distinguish between solvent-based or waterborne adhesives. Until the beginning of the 1990s, elastomer-to-metal adhesives have been prepared nearly exclusively in organic solvents. During the last three decades the use of volatile organic compounds (VOCs) was restricted by law and aqueous based adhesives became more interesting.

A further distinction can be made between primer/cover-coat systems and single coat systems. In case of the primer/cover-coat, the primer – mostly a mixture of resins and functionalized polymers [44] – binds in a first step to the metal surface. Thus, the cured primer coating has a modulus closer to that one of the metal. In a second step, the cover-coat is coated on the primer-layer, that connects the primer with the rubber macromolecules and which has a modulus closer to the rubber matrix. Consequently, the advantage of this adhesion system is the gradation in the modulus between the elastomer and metal, which provides a better stress distribution.

One-coat adhesives, on the other hand, are traditionally made out of both materials, namely the one which binds to the metal surface and that which reacts with the rubber polymers. The great advantage of these adhesion systems is the requirement of only one coating step and consequently only one processing machine. Thus, the process can be

performed faster and more cost efficient. However, one coat adhesives based on a mixture of adhesive materials have in many cases a very bad long-term stability, which is a significant drawback of these bonding systems. Therefore, the trend is moving towards one coat adhesives which consist of only one component, namely on bifunctional molecules. These compounds are already used in many technical areas as coupling agents, for surface modifications, and for polymer cross-linking. They can be produced out of mostly low-concentrated aqueous solutions by simple e.g. dip, spray or spin coating and are therefore very promising candidates to bind elastomers efficiently on metal substrates [44].

However, by using chemical bonding systems as adhesion promoter the adhesion performance is significantly influenced by another very important factor, the cleanliness. Whether for one or two component coatings, contaminations on the adhesion system are “poisoning” the covalent bond formation. Even if the reinforcing devices are coated with polymeric or monomolecular adhesives, it must be ensured that the coating does not get contaminated prior to molding. Dirt and dust particles as well as oil and moisture might be entrapped between the rubber compound and the adhesive coating preventing the formation of a resistant chemical linkage. If the coated components have to be stored and transported for a longer period and under ambient conditions, they have to be protected from heat, moisture, and irradiation. This is very important to consider for the use of adhesion promoters in real technical applications.

2.2.2 Adhesion promoter based on bifunctional organic molecules

Bifunctional organic molecules have the property of connecting the inorganic with the organic world. They feature a functional group (head group) to bind the adhesive to the polymer, an anchor group (terminal group) that links the adhesion promoter to the inorganic substrate, and a spacer which connects the functional with the anchor group (Figure 8).

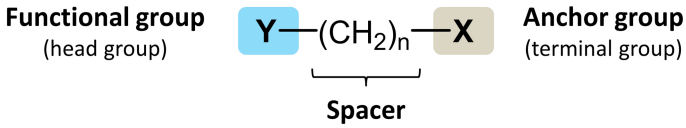

Figure 8 Principal structure of an organofunctional (bifunctional) molecule.

As anchor groups, very often silanes, phosphonics acids and thiols are used. They exhibit e.g. methoxy, ethoxy, hydroxyl, or thiol groups, which enable the binding on various metal and metal oxide surfaces via chemisorption. These chemical bonds differ from physical bindings in high resistances against the attack of moisture, heat, irradiation, and chemicals. Consequently, they cannot be destroyed easily by environmental forces. Depending on the type of anchor group, the multifunctional molecules form sol-gel networks or self-assembled monolayers (SAMs) on the substrate. Silanes, for example, are very well known to build sol-gel networks in the presence of a catalyst. They are very versatile in their functionality which enables them to form high-tech coatings for a wide variety of applications. Further, (organo)silanes show high physical and chemical stability and can be deposited on a broad variety of substrates. The most common chemical structure of silane coupling agents consist of three hydrolysable alkoxy groups (methoxy or ethoxy) on the silicon atom which react with the inorganic surface and one non-hydrolysable organofunctional group that interacts with the polymer matrix (Figure 9) [56,57].

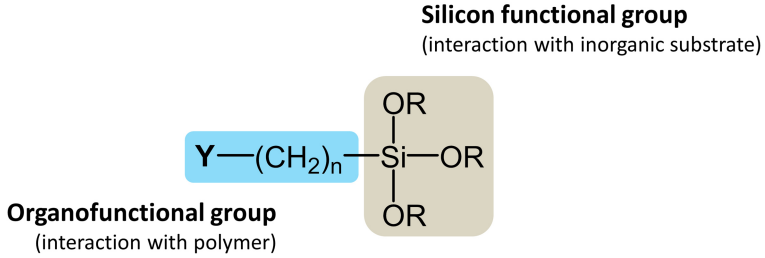

Figure 9 General structures of silane coupling agents.

This special property to have inorganic but also organic reactivities in one compound makes this type of molecules very suitable as adhesion promoters. The reaction, which leads to the chemisorption of the silane to the substrate is based on the sol-gel process. First, in the presence of water and a catalyst (acid or alkaline) the alkoxy groups of the silane react to hydroxyl groups under elimination of alcohols (Figure 11). This process is also known as hydrolysis. Since the hydroxyl groups of the silanetriols are highly reactive with inorganic materials that feature hydroxyl groups as e.g. Si-OH and metal-OH, they are able to bind covalently to these substrates via the so called condensation reaction. Thus, water is split off and the organosilane is now strongly linked to the substrate surface via a silicon-oxygen-metal bond. Beside this, the silanetriols are able to condense with other silanetriols to form siloxanes (Si-O-Si), which is the reason that silanes prefer to form networks rather than monolayers (Figure 10).

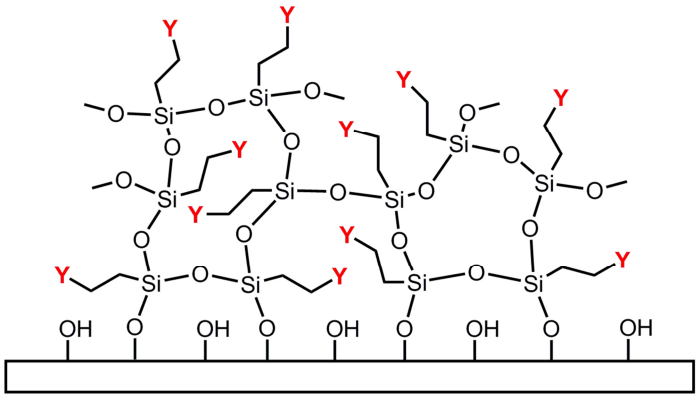

Figure 10 Network of organofunctional silanes; **Y** corresponds to a functional group (head group).

In general, the hydrolysis and the condensation reaction appear simultaneously directly after initiating the hydrolysis. Further, as mentioned before, alcohol and water are generated during the hydrolysis and condensation reaction. After drying, these small molecules are driven off and the organosilane network shrinks as further condensation may occur. These processes are generally affected by the reaction conditions, such as pH, temperature, solvent composition, and molar ratios of reactants, just to name a few.

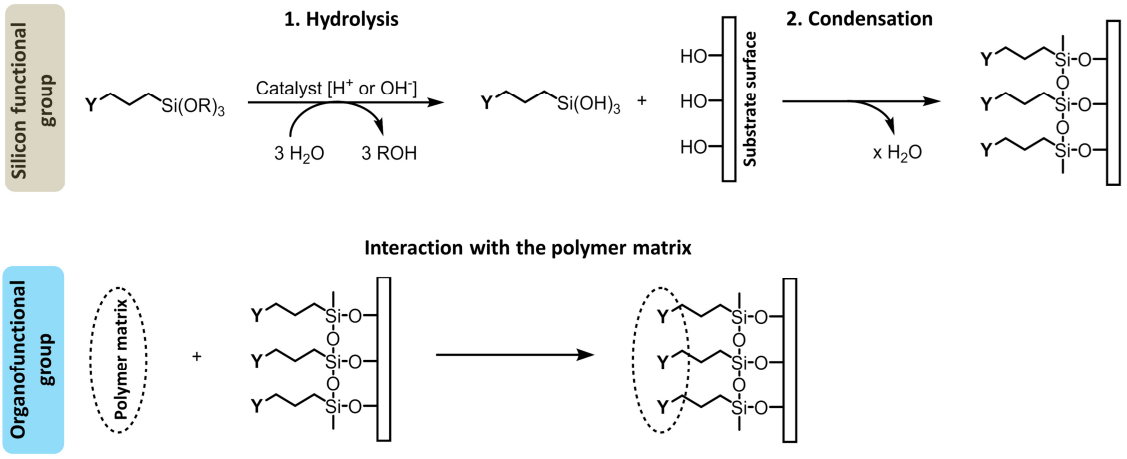

Figure 11 Hydrolysis and condensation reaction of organofunctional silanes as well as interaction with a polymer matrix; **Y** corresponds to a functional group (head group).

Very well-known candidates that form SAMs, on the other hand, are thiols and phosphonic acids. Thiols became very famous for their good-adhesion properties on gold. However, their ability to form well-defined monolayers are limited to only a few metals, they lack long-term stability due to high sensitivity against oxygen, and detach readily from the surface in aqueous environments. On the contrary, phosphonic acids are getting more and more popular. This is because the phosphonate group is able to form strong chemical bonds with a variety of metal oxides which is very robust to external influences as heat, oxygen, and irradiation. The chemical structure of the organophosphorous compounds – in this case of organofunctional phosphonic acids – consists of two hydroxyl groups, one double bonded oxygen atom as well as a non-hydrolysable organofunctional group (Figure 12).

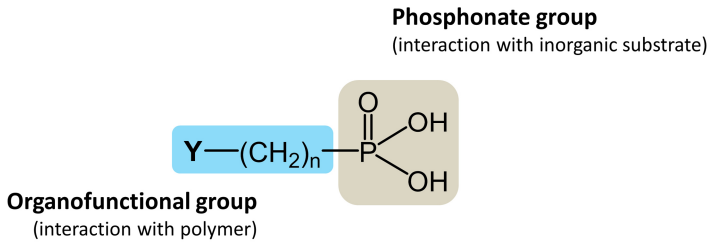

Figure 12 General structures of organofunctional phosphonates.

Due to the fact that phosphonic acids contain three potential binding sites, various types of coordination have been proposed which differ depending on the exposed crystallographic planes and type of metal oxide, and most notably which strongly depend on the reaction conditions. As depicted in Figure 13, the nature of adsorption is

based on mono-, di-, or tridentate coordination via bridging or chelating. Thus, binding of phosphonic acids results from the phosphonates ability to displace hydroxide ions that coordinate to the metal exposed on the surface, with the simultaneous release of water molecules (in the case of phosphonate esters alcohols are released) [58,59].

This condensation reaction depends – amongst others – on the pH and temperature. It must be noted that some authors recommend subsequent heat treatment to increase the deprotonation rate of the P-OH groups, which results in the formation of metal-O-P bonds as well as P-O-P bonds and enhances the stability of the monolayer [60,61].

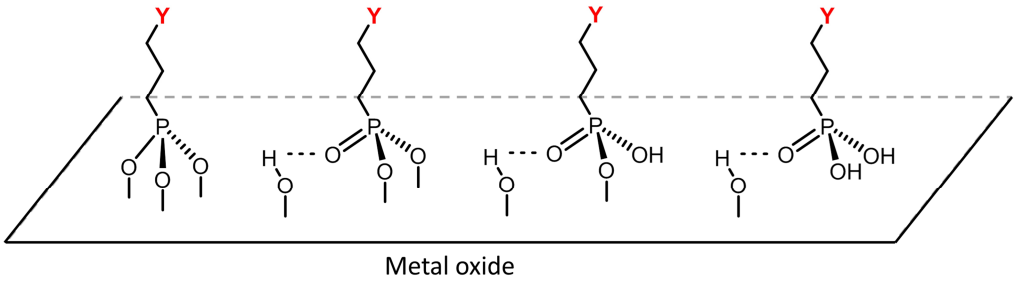

Figure 13 Scheme of some proposed binding modes of phosphonic acids to metal oxides, ranging from tridentate coordination to hydrogen bonds[62]; **Y** corresponds to a functional group (head group).

A significant advantage of these monolayers compared to silanes is the simple applicability. SAMs are not that strongly influenced by process parameters as sol-gel networks for which the reproducibility of the silane coatings is generally low and the formation of dry films is very often connected with high drying temperatures or the addition of drying supporter. Phosphonic acids have the advantage that the organofunctional groups have a well-defined orientation in the direction of the polymer matrix whereas functional groups in the silane network do not point necessarily in the direction of the organic bulk, which may deteriorate the adhesion performance. However, inter-diffusion of single polymer chains into the silane network further improves the adhesion performance of the silane based systems, which is a great benefit [56].

In order to bind the bifunctional molecules to the polymers, the anchor groups must feature also a non-hydrolysable organofunctional group that is directly linked to the central atom (Si-C, P-C). Figure 14 depicts some frequently used functional groups as amines, methacrylates, epoxides, vinyles, thiols, polysulfides and isocyanates, to name just a few.

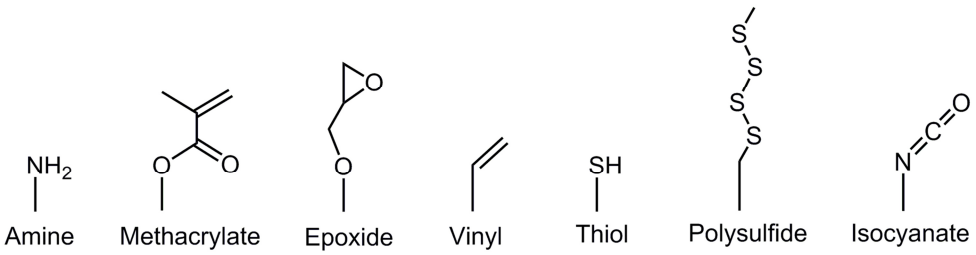

Figure 14 Frequently used functional groups for chemical adhesion promoters.

Organic spacer groups as alkyl-chains usually separate the functional group from the silicon atom in which the chain-length is responsible for how strong the central atom of the anchor group (Si or P) influences the functional group. Generally one can say that if the spacer group is not less than three carbons in length, the reaction behavior of the functional group in the silane is similar as in carbon chemistry. Nevertheless, independently on the dimension of the spacer group the interaction of the adhesion promoter with polymers is very complex, especially in case of silanes as the structure of the network can be of varying nature. However, in order to achieve outstanding adhesion properties the reactivity of the coupling reagents has to be compatible with the polymer. In the best case, the organofunctional groups of the coupling agents participate in the cross-linking mechanism or bind directly to the macromolecules by reacting with the polymer. Beside these covalent bindings, interdiffusion of single polymer chains into the silane network further improve the adhesion performance even though these interactions are not based on chemical reactions [56,63,64].

The choice of the appropriate functional group depends mainly on the characteristics of the polymers and is very often the tricky part when developing a new adhesion system. A wide variety of bifunctional molecules based on silanes, thiols, and phosphonic acids are already commercially available, but very often they have to be developed for a specific application. The functional groups, which are used to date in bifunctional molecules designed for special elastomer purposes are summarized in the next Chapter.

2.2.3 State of the art

Bifunctional molecules specially designed as adhesion promoter in rubber technology are able to bind to both, the substrate as well as the rubber network. Apart from the adhesives on the basis of functional polymers and/or resins there are only a few systems, which really work as coupling agents between reinforcing devices and rubber. Nevertheless, in the last 15 to 20 years some quite interesting multifunctional compounds were developed to improve the adhesion between different elastomers and substrates via covalent linkage.

One of the first valuable contributions for sulfur vulcanized rubber compounds was registered for patent approval by van der Aar and van Ooij [65] in 1997 and first published by Jayaseelan and van Ooij [66] in 2003. They coated various metal surfaces – e.g. brass, zinc, aluminum, and steel – with a mixture of bis-(triethoxysilylpropyl)tetrasulfide (Si 69) and bis-(trimethoxysilylpropyl)amine at a ratio of 3 to 1 prior to molding. By investigating the adhesion performance of this system to i.a. NR, NBR, SBR, and EPDM compounds they observed comparatively good results for brass but also for zinc and steel. Fortunately, these performances were not deteriorated by using cobalt-free compounds and mixtures with low sulfur values, which indicated that the adhesion strength originates from the silane coating. Thermal as well as humidity aging resulted in the majority of cases in cohesive failure which is characteristic for a strong bonding between rubber and metals. Originally, the sulfur functionalized organosilane bis-(triethoxysilylpropyl)tetrasulfide was developed – and is still used – to enhance the distribution of silica in rubber compounds [67]. There the high hydrophobicity is a great advantage due to the improved compatibility with the mostly nonpolar rubber macromolecules. For the hydrolysis, which is necessary to form a dry coating on the metal surface this is unfavorable because thus the reaction proceeds very slowly. Here the amino silane comes into play: it has the property to form dry films and the amino group further serves as catalyst for the hydrolysis/condensation reaction. Consequently, a dry sol-gel coating can be preserved by combining both silanes.

In the meantime, however, van Ooij *et at* [68,69] were able to optimize these silane coatings so that the adhesion performance is less dependent on the layer thickness. This was achieved by using the classical sol-gel process, i.e. the silanes are (partially)

hydrolyzed before they are mixed to one coating solution. Thus not only the adhesion performance increased but also an improved corrosion resistance [70,71] was achieved. The silane groups are responsible for the linkage between the adhesive and the metal substrate. For the bonding between the silane coating and the rubber on the other hand, the polysulfide silane is responsible. During the vulcanization process, in a first step, elementary sulfur is integrated into the polysulfide chain of the sulfur functionalized organosilane. Thus the affinity of the "activated" polysulfide chain to the allyl hydrogen atom of the rubber polymers increases and as a consequence the bonding reaction is possible (Figure 15).

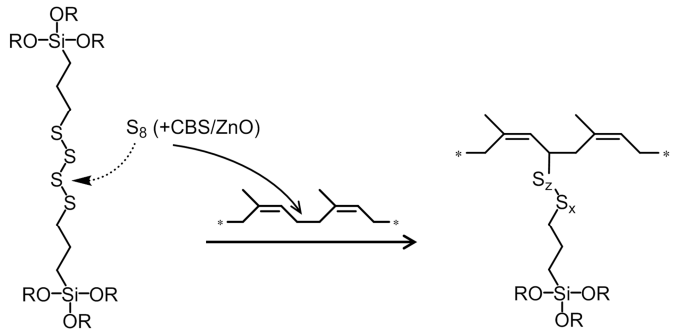

Figure 15 Scheme of polysulfide silane to rubber bonding.

Hence, using this adhesion system a throughout covalent binding between the rubber and the metal surface is provided. Additionally, the rough silane coating and the rubber network penetrate into each other, resulting in an additional enhancement of the adhesion performance.

A very similar approach was designed by Mutin in 2009. Instead of polysulfide silanes he used organophosphorous compounds containing a polysulfide bridge. In particular, the bonding mechanism between the rubber macromolecules and the polysulfide chain is the same as for the system invented by van Ooij *et al*. However, the phosphorous group – in this case phosphonic acid – is able to form self-assembled monolayers on the metal substrate and thus no drying additive has to be added. Although silane groups bind more efficiently to inorganic fillers (silica, clays), phosphonic acids show better adsorption behaviours to metal oxide surfaces. Therefore, this adhesion promoter is very promising to be applied in rubber products, which are vulcanized using sulfuric curing systems [72].

Simultaneously to Mutin, Najari *et al* published a concept to bind rubber via covalent bonds to metal surfaces by using bifunctional organosilanes as well as modified rubber polymers. Thus, a monolayer of aminopropyltrimethoxysilane (APS) or a bilayer of mercaptopropyltrimethoxysilane (γ-MPS) and APS were used to bind epoxidized natural rubber (ENR, 20% epoxy groups) to zinc. The used rubber compounds were usually based on both NR and ENR (20-50% ENR), but the amino groups bind only to the epoxy groups of ENR. As an alternative to APS *N*-allylaminopropyl trimethoxysilane (NAAPS) was also investigated. The corresponding experiments led to the conclusion that the adhesion of NR/ENR blends is significantly improved using a bilayer system where γ-MPS is bonded first to the zinc surface followed by a layer of APS and NAAPS, respectively. Compared to the monolayer, the adhesion strength increased 20-30%. The best results were obtained for the γ-MPS/NAAPS bilayer system, which further showed very good stabilities towards aggressive environments (heat and corrosion resistant). The achieved pull-out forces were really promising, but this adhesion system is restricted to epoxydized rubber polymers and thus not universally applicable unless ENR is used as blend [73].

Beside adhesive agents for sulfur vulcanized rubber compounds, adhesion promoter for peroxide cured rubber mixtures to metal substrates have been investigated. Here, again van Ooij published the first report of a well-functioning adhesion system [65]. As substrates steel, aluminium, and brass were used whereas the adhesion improvement was investigated to silica-filled EPDM, silicone rubber, fluorosilicone rubber and fluorocarbon rubber. The coating procedure was divided into two steps. First, the substrate was dipped into a bis-(triethoxysilyl) ethane solution followed by dipping in vinyl silane. However, the performance of this bonding system was not convincing for which reason it never found the way in real rubber products.

Only a few years later, at the turn of the millennium, Li *et al* patented an adhesion system for peroxide-cured rubber mixtures on the basis of organofunctional silanes. Interestingly, they limited their invention to fiber materials, e.g. polyesters, polyamides, polyaramids, glass fibers, and carbon fibers and did not apply their bonding system to metal substrates. Nevertheless, because of the very interesting and unique approach this system is mentioned here. First of all, aminoethylaminopropyltrimethoxysilane (AAMS) is mixed with 3-methacryloxypropyltrimethoxysilane (MAS) in the ratio

7 to 3. Afterwards, 1000 parts of water are added in order to preserve a stable silane dispersion and the fabric was dipped into this coating solution. Optionally, the coated textile was further impregnated with a resorcinol formaldehyde latex. However, during the peroxide crosslinking of the rubber macromolecules – which is based on a radical reaction – the methacrylate-group can bind chemically via the terminal double bond to the rubber polymer or the resin network. In doing so, the textile fabric is linked to the rubber or resin system by means of a covalent bonding.

Unfortunately, without the use of the additional latex layer the pull-out forces are comparatively poor but the general principle works. In this patent, another organosilane compound is presented which also improves the fiber-to-rubber adhesion. Instead of the AAMS and MAS mixture pure 2-(vinylbenzylamino)-ethyl-3-aminopropyltrimethoxy-silane is used. This multifunctional silane shows almost as good adhesion properties as the silane mixture and is therefore also a very promising bonding agent. Anyway, MAS is already used commercially (Dynasylan® MEMO, Evonik Industries [74]) in various rubber products as surface modification reagent of fillers or as additive [75].

For silicone elastomers, a wide variety of chemical coupling agents exist. However, these are not discussed in this contribution as only diene rubbers were used in this study. Readers interested in that may refer to a review of Picard *et al*, which summarized comprehensively the scientific literature and related patents [57].

2.3 Olefin metathesis meets rubber chemistry and technology

This chapter was already published in:

Olefin metathesis meets rubber chemistry and technology – S. Leimgruber, G. Trimmel *Chemical Monthly*, **2015**, 7, 1081-1097

2.3.1 Introduction

In the past half century, olefin metathesis attained great importance in organic and polymer synthesis [76-78] as well as in petrochemistry [79] due to their versatility in chemical reactions. Olefin metathesis is based on the transalkylidenation of two double bonds using metal complexes as catalysts (Figure 16).

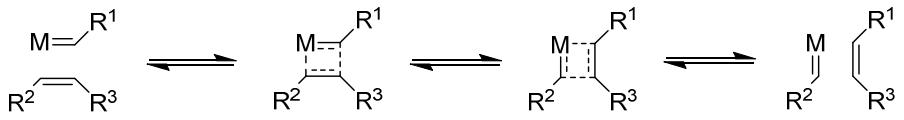

Figure 16 General mechanism of olefin-metathesis reactions.

Because of the continuous improvement of metathesis catalysts regarding their activity, stability and tolerance against functional groups and atmospheric conditions metathesis reactions were rapidly applied in industrial processes [80,81]. Olefin metathesis is today used in organic synthesis for the preparation of complex drugs using ring closure metathesis, in green chemistry by producing chemical compounds from natural resources by cross metathesis, in polymer chemistry to synthesize defined polymer architectures using either ring opening metathesis polymerization (ROMP) or acyclic diene metathesis (ADMET) polycondensation [82].

In this short review a focus is set on the different aspects olefin metathesis can contribute in rubber chemistry and technology, especially for classical sulfur-cross-linked (vulcanized) rubber systems.

2.3.2 Overview of olefin metathesis reactions in rubber technology

The core of rubber chemistry and technology is the synthesis and processing of elastomers, i.e. polymers with rubber-like elasticity, and the production of elastomeric materials for many different applications, ranging from simple rubber bands and O-ring seals to hydraulic hoses, conveyor belts, and tires. The rubber-like elasticity is based on the formation of a wide-mashed cross-linked network of soft polymer chains. Although there are several ways to crosslink rubber and alternative rubber systems, the core reaction of today´s rubber chemistry is still the vulcanization process, originally discovered by Charles Goodyear 1839 and patented 1844 [22], i.e. the cross-linking of unsaturated rubbers by sulfur under elevated temperatures and pressure, as shown in the central part of Figure 17. Originally only natural polymers like *cis*-1,4-polyisoprene (*cis*-PI) – better known as natural rubber (NR) – were used to produce rubber products but due to the increasing market and growing requirements on materials properties the demand of synthetic rubber, e.g. styrene-butadiene-rubber (SBR) and nitrile-butadiene-rubber (NBR), constantly increased.

During the last years, olefin metathesis reactions have been applied in different ways with respect to rubber chemistry. An overview is given in Figure 17.

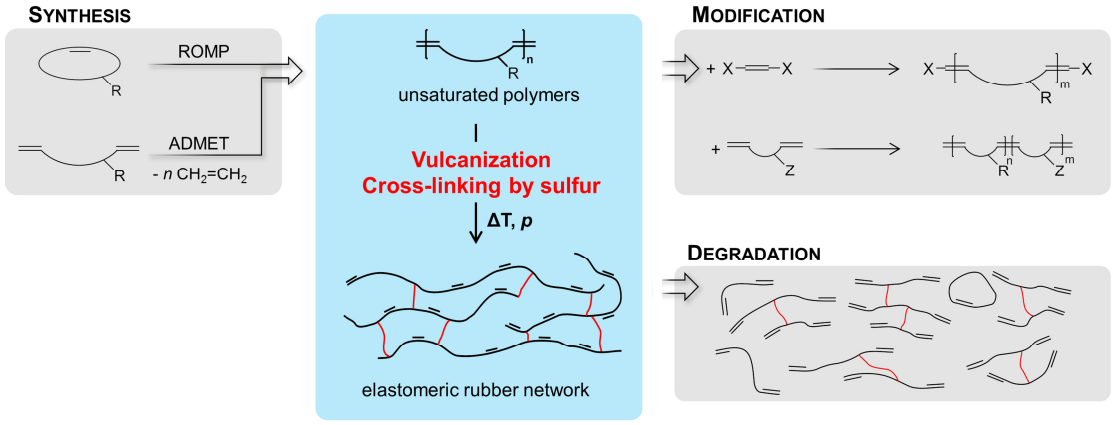

Figure 17 Overview of olefin metathesis reactions in rubber technologies and the core reaction of rubber technology - vulcanization.

First, ROMP-polymerization as well as ADMET polycondensation can be used for the synthesis of unsaturated rubbers. Secondly, metathesis reactions can be used for modifying rubber and transforming non-crosslinked rubber polymers into telechelic polymers or small functional chemicals. Thirdly, a less known application of the olefin

metathesis is the degradation of crosslinked rubber-networks containing residual double bonds in the main chain by cross metathesis. Thus, the rubber macromolecules are cleaved into small soluble compounds, which is a very useful tool for analysis and recycling of vulcanized rubbers. In the next chapters we review how olefin-metathesis reactions can contribute to these three areas in rubber chemistry.

All three approaches rely on the availability of suitable catalyst or initiator systems. Whereas in the earlier days most of the works have been performed with ill-defined initiator systems such as $WCl_6/(CH_3CH_2)_3Al$ [83], modern catalyst and initiator systems are based on transition metal carbene complexes of ruthenium, molybdenum or tungsten. A large variety of different initiators and catalysts has been introduced in the last decades and has accelerated the success of olefin metathesis reactions. Some of the most important catalysts are shown in Figure 18. Nevertheless, it is not possible to cover the whole broadness of catalyst chemistry and development within this short paper. However, there are several excellent reviews on this topic recommended for interested readers [77,84-88].

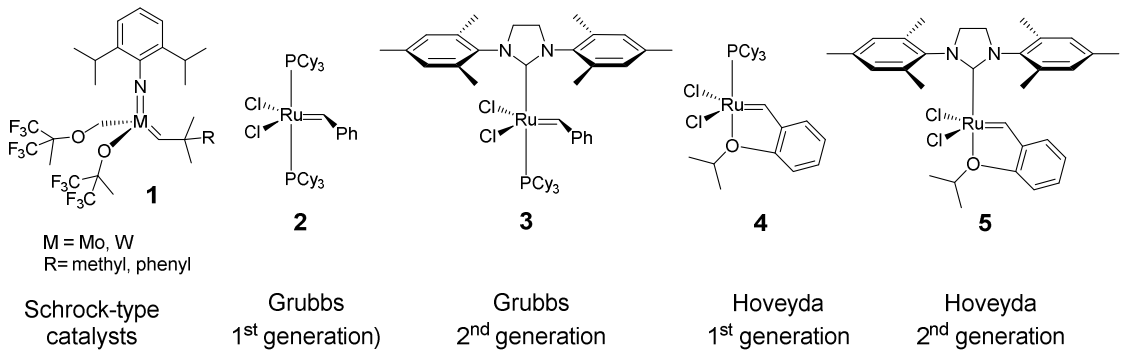

Figure 18 Chemical structures of some common organometallic catalysts used for olefin metathesis reactions related to rubber technology.

2.3.3 Rubber synthesis

First of all, olefin metathesis provides useful tools to synthesize defined macromolecules with remaining double bonds and thus yields rubber like polymers which can be crosslinked by classical vulcanization processes. ROMP of cyclic olefins is applied for the synthesis of polyalkenamers since many years [83,89-91], as shown in Figure 19.

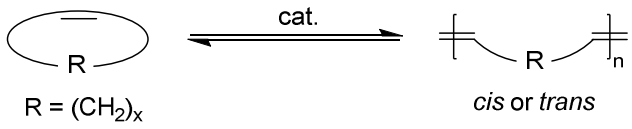

Figure 19 ROMP of cyclic olefins (x = 2, 3, 5, 6, 7, 8, 10) to polymers.

Cyclic olefins – except cyclohexene – have a relatively high ring strain because the C-C binding angle deviates from the normal value of a tetrahedron (109.5°) [92,93]. Therefore the release of the ring strain is the driving force for ROMP, whereas the polymerization of cyclohexene is not possible. ROMP of cycloalkenes leads to linear as well as to macrocyclic polymers, depending on the catalyst system and the process conditions. Also the *cis/trans*-ratio depends on the catalytic conditions [94-96]. In many cases ROMP can be carried out as a living polymerisation technique, thus also allowing the preparation of more complex polymer architectures especially block copolymers.[97]

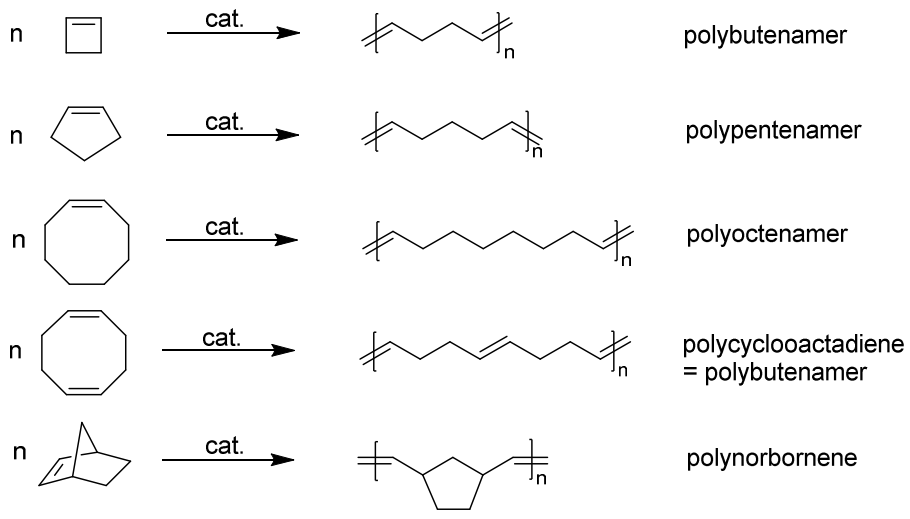

Figure 20 ROMP of various cyclic monomers to the corresponding polyalkenamers.

ROMP allows the preparation of several polyalkenamers with suitable properties to be used as rubber raw materials, as shown in Figure 20. However, the only polyalkenamers, which have gained economic importance and which are produced on a large scale are polyoctenamer and polynorbornene [80,98,99].

Polyoctenamer, also sometimes called TOR, poly-(*trans*-octenamer) rubber, is a well-established synthetic semicrystalline elastomer and is commercial available as Vestenamer® (produced by Evonik Industries), e.g. as Vestenamer 8012 with a molar mass average of approximately 90000 g/mol and 80% of *trans* double bonds [100]. At ambient temperature it is hard and has a high viscosity because of the high crystallinity. Above 60°C it displays a very low viscosity. The relatively low molar mass for a rubber, the linear structure as well as the content of macrocycles leads to a low melt viscosity. Due to the high content of double bonds, the polymer can be cross-linked using common vulcanization techniques, e.g. sulfur-accelerator systems or peroxides [76,101] Polyoctenamer is applied exclusively in blends with other rubbers, usually in a percentage of 10-30%. It is mainly used as processing auxiliary in rubber dispersions and in softener-free mixtures especially for extrusion and molding processes, as well as to increase the hardness of elastomers in tires, hoses, extruded rubber profiles, roll covers and numerous other applications due to the high crystallinity also after vulcanization.[102] New applications are as binding agent for ground rubber waste powder and as modifier in rubberized asphalt [101]. Polyoctenamer was first synthesized via ROMP by Natta *et al* in 1966 using *cis*-cyclooctene as starting reagent and $WCl_6/(C_2H_5)_3Al$ as initiator [83]. Higher activity was obtained by Calderon *et al* using $WCl_6/(C_2H_5)AlCl_2$/ethanol as catalyst.[103] However, many other strong catalyst systems were implemented in the last decades for the synthesis of polyoctenamer [e.g.104-110]. The *cis/trans* ratio as well as the formation of cyclic polymers strongly depends on the initiator system, polymers with high *cis* content exhibit a lower melting temperature as well as a lower crystallinity [111]. Consequently, Vestenamer 6213® with a content of 56% *trans*-double bonds shows a reduced melting and crystallization temperature [112].

Polynorbornene (poly-1,3-cyclopentylenevinylene) was already patented in 1955 by DuPont [113]. It was commercialized in 1976 by *CdF Chimie* under the trade name Norsorex® [114] and is now available from Astrotech. Thereby $RuCl_3$/HCl in butanol

was used as initiator system for polymerization [115]. However, also in this case many other initiator systems have been applied, e.g. based on metal complexes of tungsten [116-120], molybdenum [121-124], ruthenium [125,126], titanium [127,128], tantalum [129] and osmium [130]. During ROMP of norbornene the cyclopentenylene ring and one double bound are preserved. The double bonds have *cis/trans*-structures, depending on the used catalyst. The commercial available rubber Norsorex® has a high content (90%) of trans-double bonds and a high molar mass above $3x10^6$ g/mol. Polynorbornene can be blended with common elastomers and cross-linked by sulfur as well as by peroxide cure systems. The bulky cyclopentane-ring in the main chain restricts the segment flexibility resulting in a relative high glass transition of 35 °C, and is thus at room temperature solid (glassy) and displays rubber-like properties when plasticizers are added [101]. However, this is not a problem as a high absorption of nonpolar solvents is one of the characteristic properties of polynorbornene. This is also one of the applications of polynorbornene as absorbing materials for oil, as it can absorb typically ten times its weight of common hydrocarbons [76,101]. Another advantage of Norsorex is that high amounts of fillers can be incorporated. Norsorex based compounds can also have high friction coefficients over a large temperature range, good abrasion resistance and energy absorption properties. Thus, Norsorex is also found as vibrational damping elements e.g. for rail systems, automotive and acoustic applications, as tread compound for tires, and personal protective equipment. Often Norsorex is also used in blends with other rubbers in order to optimize their properties for special applications [101].

Generally, also other polyalkenamers prepared by ROMP have suitable properties for applications as elastomeric materials [131] such as e.g. polybutenamere and polypentenamere synthesized via the ring opening of cyclobutene and cycopentene, respectively – see Figure 20. In the case of polybutenamer, better known as butadiene rubber (BR), also different initiator systems have been applied [132-134]. Again the choice of initiator influences strongly the *cis/trans* ratio. Also perfectly *cis*-BR can be synthesized which would be needed for applications e.g. in tires. It is also worth mentioning that ROMP of 1,5-cyclooctadiene yields BR (see also Figure 20), as shown in many different works [e.g. 103,111,135,136] and BR with 99% *cis*-double bonds have been synthesized with this approach [137]. However, alternative synthetic routes

via butadiene are more economical so that both ROMP routes – via cyclobutene and 1,5-cyclooctene – are not applied for the industrial production of BR.

By using methylcyclobutene polyisoprene-like polymers can be synthesized [138]. By using Schrock type catalysts **1** Grubbs showed that "perfect natural rubber", i.e. a stereoregular polyisoprene with solely head-to-tail structures and *cis*-double bonds is accessible (Figure 21) [139]. This demonstrates the high stereoselectivity which can be obtained using tungsten or molybdenum catalysts.

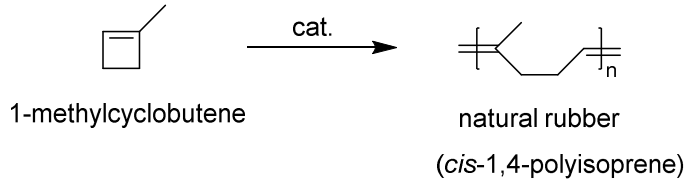

Figure 21 Synthesis of perfect natural rubber [139].

There are many reports on the synthesis of polypenteneamer via ROMP of cyclopentene [e.g. 140-146]. Polypentenamer shows also promising properties, such as high tensile strength and abrasion resistance, useful in tire applications [142]. However, the extraction of cyclopentadiene from the C_5-stream and its conversion to cyclopentene is not economical so far[147] which is also the case for the resulting polymer.

Besides ROMP, which follows a chain growth mechanism, acyclic diene metathesis (ADMET) polycondensation – following a step-growth mechanism – has shown to be a versatile method for the synthesis of rubber macromolecules. Here, diolefins with terminal double bonds (α, ω-dienes) react in the presence of a catalyst to linear polymers with double bonds in the polymer main chain by simultaneously elimination of ethene, as shown in Figure 22 [148,149].

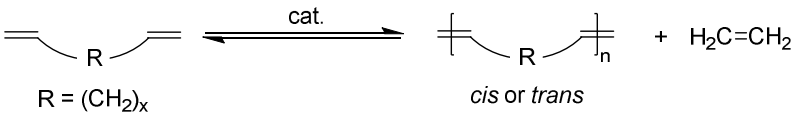

Figure 22 ADMET-polycondensation of α, ω-dienes to polymers by eliminating ethene.

In the first successful report on ADMET-polycondensation to high molar mass polymers, Wagener *et al* used a Schrock-type tungsten catalyst. Ethene was constantly removed from the reactions solution to shift the equilibrium to the polymer side [150,151]. Doing so, polyocentameres with weight number averaged molar masses of

approximately 58000 g/mol were prepared from 1,9-decadiene. Using the same procedure BR can be prepared from 1,5-hexadiene. The addition to ethene would reverse the reaction and can be used to degrade such polymers [151]. However, the synthesis of rubber macromolecules via polycondensation is not suitable for all diolefins as ring closure metathesis reaction might be more favorable, e.g. 1,7-octadiene cyclizes preferably to cyclohexene instead of building linear polymers [152,153].

Synthesis of functional polymers and co-polymers

In order to develop rubber macromolecules with specific and functional properties (gas permeability, resistance to oils or fire, photocrosslinkable rubber) several approaches can be followed. Firstly (natural) polymers are chemically modified [154], secondly, the properties can be tailored by copolymerization, and thirdly, functional groups are introduced by (co)polymerization of substituted monomers. In this field, olefin metathesis, especially ROMP but also ADMET, has impressively shown to be powerful tools to synthesize such functional (co)polymers. Regarding ROMP, a large variety of substituted monomers are accessible, such as substituted cyclobutenes [e.g. 155,156], cyclooctenes [111], and norbornenes [78]. However, many of these approaches are devoted to special applications and not related to rubber chemistry.

One first prominent example for elastomers is the synthesis of nitrile butadiene rubber (NBR)-like polymers via ROMP. NBR is used in many rubber products due to its very good oil resistance e.g. in automotive applications. A very promising approach to synthesize NBR-like elastomers was performed by the group of Nuyken. Here, *cis*-cyanocyclooct-4-ene and *cis*-1,2-dicyanocyclooct-5-ene are ROMP-polymerized using Grubbs 2nd generation catalyst **3**, as depicted in Figure 23.

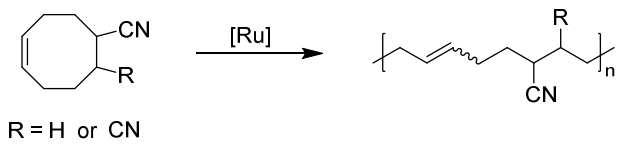

Figure 23 Synthesis of new nitrile-containing polymers [157].

The resulting polymers show in general the same structural features as the commercial available NBRs. In addition, the nitrile-containing polymers prepared by the new synthetic pathway show a more regular sequential arrangement of the structural

moieties along the polymer backbone which enables to further improve the rubber properties such as the low-temperature flexibility [157].

The copolymerization of different cylcoolefins is another approach to tune the properties of the resulting elastomers, for examples see Figure 24. As one example, a copolymer of norbornene and cyclooctene poly(COC-co-NBE) might find application as gas barrier material for pneumatic tires if used in combination with other elastomers [158]. Due to the considerable differences in ring strain, the copolymerization of these polymers often leads to a block like structure and a low content of alternating dyads, especially if the highly reactive norbornene is combined with other cyclooctenes or cylcopentenes [159]. However, by applying a large excess of cylcooctene or cyclopentene and optimizing the ligand sphere of the initiators, alternating copolymers of norbornene-cyclooctene and norbornene-cyclopentene are accessible with a high degree of alternating diades of more than 90% [160-162].

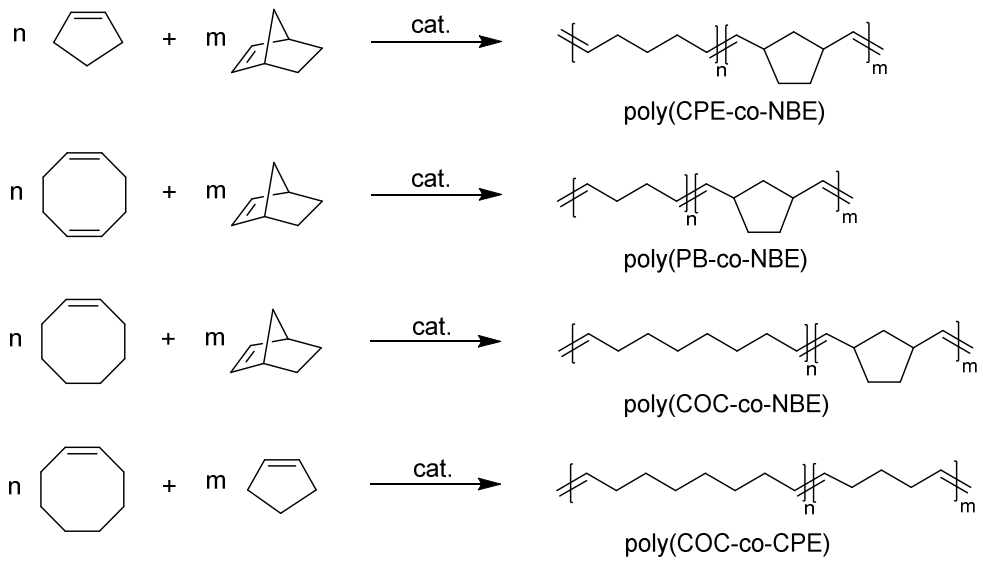

Figure 24 Synthesis of various elastomeric copolymers via ROMP.

Using electrochemically generated WCl_6-based catalysts, Cetinkaya *et al* copolymerized norbornene (NBE) with cyclopentene (CPE) to poly(CPE-co-NBE) [163] , 1,5-cyclo-octadiene with norbornene to poly(PB-co-NBE), cyclooctene (COC) with norbornene to poly(COC-co-NBE) [164] as well as cyclooctene with cyclopentene to poly(COC-co-CPE) [165] (Figure 24). Other examples are copolymers of cyclopentene and ethylidenenorbornene [144], and copolymers of cyclooctene and functionalized norbornenes [146].

As mentioned above, one major problem of the copolymerization of monomers with large differences in their reactivity is that block copolymers are obtained. However, especially in the case of unsubstituted cycloolefins, the initiator can also attack the double bonds of the main chain and via a cross metathesis mechanism this back biting can help to scramble the monomer distribution in the final polymer. However, this also means, that the same cross metathesis mechanism can be intentionally used by reacting two different polymers with a metathesis initiator to give the desired copolymer, e.g. poly(COC-co-NBE) was synthesized by interchain cross metathesis of the corresponding homopolymers (Figure 25).

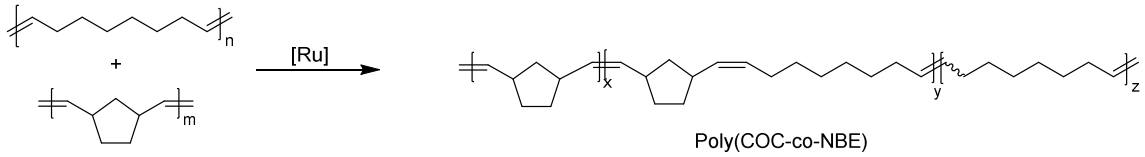

Figure 25 Norbornene-cyclooctene copolymers synthesized out of the corresponding homopolymers [166].

Using Grubbs 1st generation catalyst **2** multiblock copolymers with different average block sizes as well as almost random copolymers can be obtained depending on the reaction conditions [166].

In a similar approach by Otsuka *et al*, the reaction of polybutadiene and an unsaturated polyester gives elastomeric polyesters via the interchain cross metathesis using ruthenium catalyst **2** [167].

The structure of this polyester is very similar to polyester-polyalkenylene-copolymers prepared via ROMP from ambrettolid ((8Z)-1-oxacycloheptadec-8-en-2-one) and cycloolefins, i.e. cyclooctene, 1,5-cyclooctadiene and cyclopentene (Figure 26). For the synthesis the catalyst system $WCl_6/(CH_3CH_2)_4Sn$ was used [168].

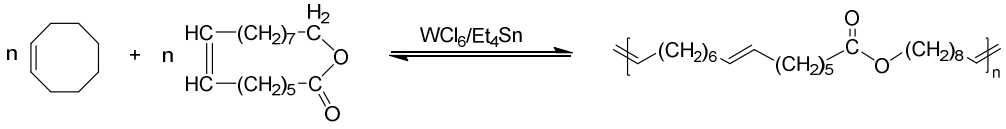

Figure 26 Synthesis of polyester-polyalkenylene-copolymers [168].

Oligomeric unsaturated polyesters have been prepared by Larock using ADMET-polycondensation of ethylene glycol dioleate, glycerine trioleate as well as of soybean

oil, opening a possible approach to prepare such polymers from renewable resources [169].

ROMP can be also used for graft polymerization, as shown e.g. for the preparation of an interesting elastomeric material based on poly(propylene oxide-*ran*-allyl glycidyl ether) prepared by anionic ring opening polymerization. In a second synthesis step, using the allylic groups of the alkylene oxide copolymer cyclooctene has been polymerized and grafted by ROMP using Grubbs 1st generation catalyst **2** (Figure 27). The authors stated that the resulting polymer has good properties for applications in hoses and fittings in contact with aggressive media [170].

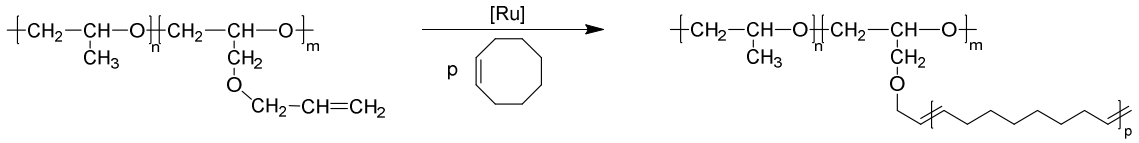

Figure 27 Grafting of cyclooctene to the allylic groups of the alkylene oxide copolymer [170].

Using ROMP and cationic polymerization in parallel, norborneneyl-modified linseed oil (Dilulin™) and a bisdecyl norbornene dicarboxylate (NBDC) were copolymerized and crosslinked by using Grubbs 2nd generation catalyst **3** as well as an initiator for cationic polymerization (Figure 28). By increasing the content of NBDC to 30wt% the glass transition temperature decreases to -17 °C, which is due to a higher content of linear polynorbornene units and thus lower amount of crosslinking sites. Likewise tensile tests showed a significant improvement of the mechanical performance - namely reduction of brittleness. Consequently, the new bio-based rubber has highly eligible properties for rubber materials [171].

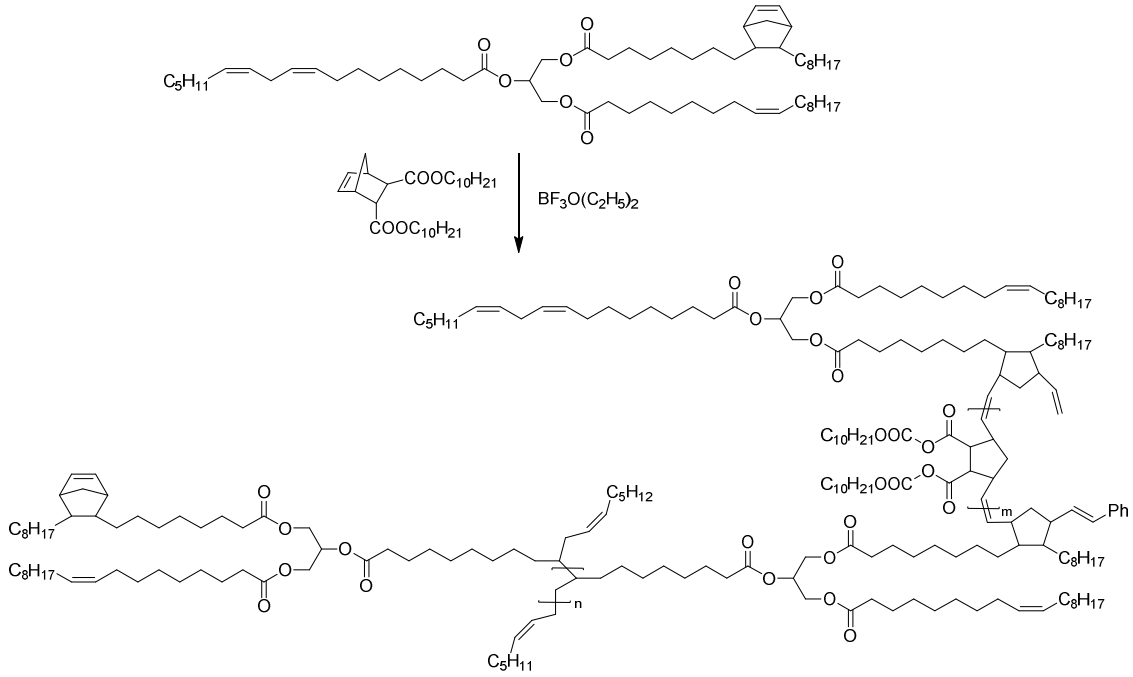

Figure 28 Dilutin™ copolymerized and cross-linked with a norbornene derivate via cationic polymerization and ROMP [171].

An interesting possible application not discussed so far, is the use of polynorbornene based coatings on different fibers – nylon, polyester, Kevlar® – as adhesion promoter to natural rubber [172]. The polymer coatings were produced using Grubbs 1st generation catalyst **2**. In a first approach, polynorbornene was coated on the fibers, whereas in a second approach the initiator was absorbed onto the fibers and the polymer coating was obtained by dipping these fibers into a monomer solution. Embedded and vulcanized in natural rubber compounds, these fibers show promising adhesion strength. However, this approach is still part of fundamental research but might help to develop new adhesion promoters for fiber-elastomer interfaces.

In the next years the range of elastomeric materials with specific functionalities is expected to grow continuously, especially for high performance products.

To date, ROMP is more often used for the synthesis of rubber macromolecules than ADMET, but both reactions provide practical synthetic pathways for new and innovative elastomers.

2.3.4 Telechelic polymers/oligomers and functional molecules

Olefin metathesis offers also interesting approaches towards functionalized telechelic polymers, oligomers and specialty chemicals. The first approach is based on a one-pot synthesis strategy via ROMP in the presence of a symmetric *bis*-functional olefin as chain transfer reagent (CTA), see Figure 29. Examples for this approach are the synthesis of hydroxy-terminated polybutadiene [173] and polyisoprene [174] using the *bis*-(tert-butyldimetylsilyl)-ether of *cis*-1,4-butenediole and *cis*-1,4-diacetoxy-2-butene, respectively, as CTA followed by hydrolysis. Other examples are the synthesis of cyano- and chloro-endgroups using the corresponding 1,4-dicyano and *bis*-1,4-dichloro-2-butenes as CTA [175] or carboxy-telechelic polyolefins using maleic acid as CTA [176]. Recently di-cyclocarbonate telechelic-polybutadiene has been reported using the asymmetric CTA (2-oxo-1,3-dioxolan-4-yl)methyl acrylate [177]. *d*-Limonene was introduced as CTA and solvent in the ROMP of cyclopentene, 1,5-cylcoctadiene, cycloheptene and norbornene [178].

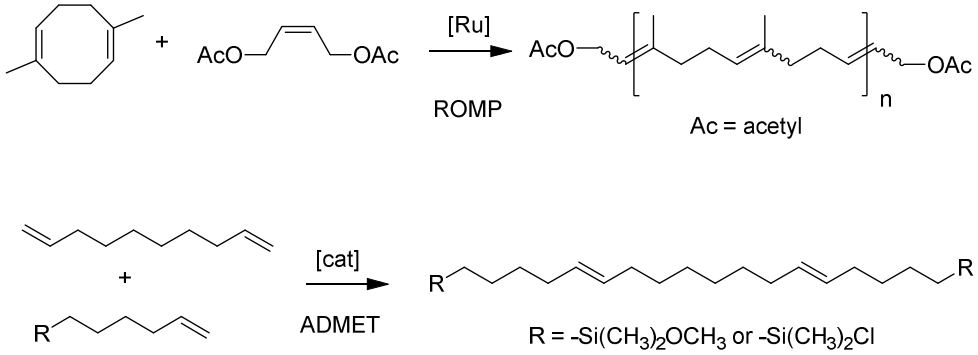

Figure 29 ROMP [174] and ADMET [179] polymerization approaches towards telechelic polymers.

Similar telechelic polymers can be synthesized by ADMET-polycondensation if a functional monoolefin is added during the polycondensations, as it was demonstrated e.g. for the preparation of silyl-telechelic polyoctenamers, also shown in Figure 29 [179]. Hydroxy- and amino-groups can be introduced using ester or phthalimide protecting groups [180-183].

However, the above described reactions are in principle reversible and thus olefin metathesis also can degrade polymers in a more or less controlled way. Depending on the used co-reagent different reactions are occurring. If a CTA is used, the formation of

acyclic α,ω-diolefins are formed, if ethene is used the reaction is named reversed ADMET (or sometimes ethenolysis) if other CTAs are used, cross metathesis. Intrachain ring-closing-metathesis (RCM) is found most frequently if no co-reagent is applied (Figure 30). In this regard, it should be added that these types of metathesis may occur in parallel, depending on the reaction conditions, on the composition of the reaction solution as well as on the catalyst system and are also side reactions in ROMP and ADMET polycondensation.

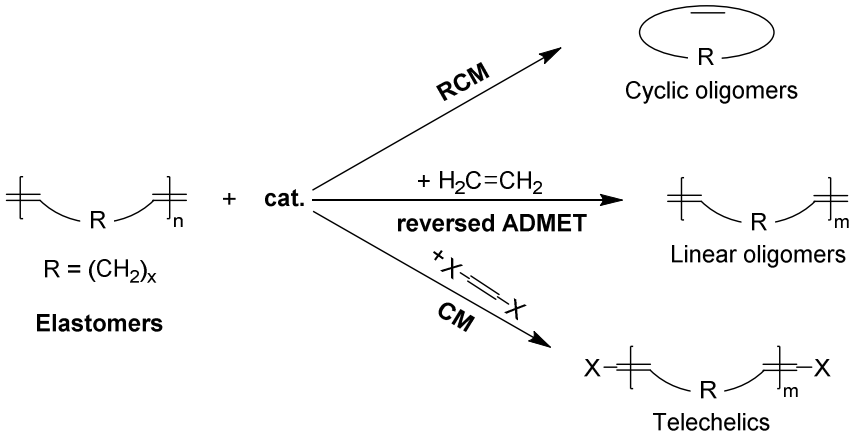

Figure 30 Degradation of unsaturated polymers to give low molecular weight cyclic or linear compounds as well as telechelics (n>>m).

The metathetic degradation of synthetic elastomers was first investigated by Ast and Hummel in 1970 on *cis*-PB in the presence of the $WCl_6/(CH_3CH_2)Al_2$ catalyst system [184]. Since 2-hexene, an unsymmetrical acyclic olefin, was used as CTA, the reaction resulted in oligomers with one and two repeating units terminated by either methyl and propyl end groups, or one of each.

However, using difunctional olefins, the same functional telechelic polymers and oligomers can be obtained as in the case of productive metathesis. Ten years later, the first telechelics with functional end groups – diester telechelic oligobutadienes – were prepared. The cross metathesis of *cis*-PB with the symmetrical dimethyl(Z)-hex-3-ene-1,6-dioate was successfully realized using $WCl_6/(CH_3)_4Sn$ (Figure 31). Most of the endgroups (92%) were terminated by ester groups [185].

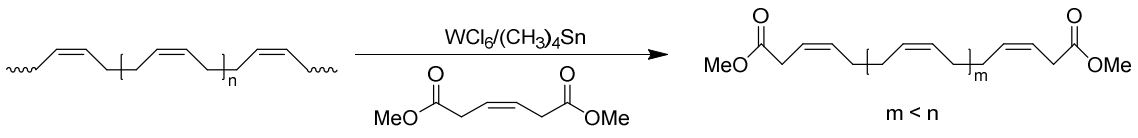

Figure 31 Cross metathesis of *cis*-PB with dimethyl (Z)-hex-3-ene-1,6-dioate [185].

The advancement of this procedure to the preparation of perfectly difunctional telechelic *cis*-PB with different functional groups was made possible by utilizing the newly developed, selective and specific metal-carbene catalysts, which are compatible with many functional groups. A large variety of functionalities has been incorporated using the corresponding difunctional monoolefins and Schrock-type catalysts. Thus, telechelic 1,4-polybutadiene-oligomers have been prepared with silyl- [186], phthalimide- and carboxylic ester [187] as well as alkyl borane end groups [188].

Cis-PI (synthetic and natural rubber) was degraded using Grubbs 1st and 2nd generation catalysts (**2, 3**) and *cis*-1,4-diacetoxy-2-butene to produce acetoxy end-functionalized telechelics in both, an organic solvent as well as in the latex phase at ambient temperature. Thus, well-defined acetoxy telechelic polyisoprene structures were obtained in a selective manner. This study showed good control of the reaction in combination with good yields (98%) [189]. Similar acetoxy telechelic SBR-oligomers were prepared by the same groups with very high end-group functionality ratios near 2 [190].

Tlenkopatchev *et al* compared three different CTAs, *cis*-1,4-dichloro-2-butene, *cis*-1,4-diacetoxy-2-butene, and dimethyl maleate for the transformation of NR via cross metathesis [191]. Using Grubbs 2nd generation catalyst **3**, the two first CTAs gave defined diallyl- and diacetoxy chloride telechelics with controlled molar masses and end-group functionality ratios near 2. Conversely, dimethyl maleate gave products with much higher molar masses, as the α-carbonyl group can coordinate to the metal center reducing the reactivity of the catalyst.

In another example, Saetung *et al* fabricated bistrithiocarbonyl telechelic *cis*-PI oligomers using the corresponding difunctionalized monoolefin as shown in Figure 32. The resulting α,ω-bistrithiocarbonyl-end functionalized telechlelic *cis*-PI was applied in a reversible addition-fragmentation chain transfer (RAFT) polymerization of *tert*-butyl acrylate (*t*-BA) to form Poly(*t*-BA)-*b*-(*cis*-PI)-*b*-P(*t*-BA) triblock co-polymers. Such polymer precursors have great potentials in numerous block copolymer applications such as for materials featuring adhesive properties [192].

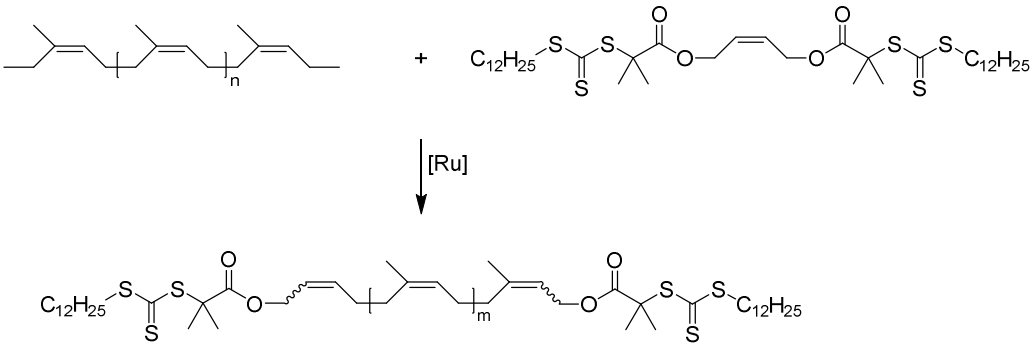

Figure 32 Synthesis of α,ω-sistrithiocarbonyl-*cis*-1,4-polyisoprene from NR and bistrithiocarbonyl-end functionalized CTA via cross metathesis [192].

The versatility of the metathetic degradation pathways was also demonstrated by various groups using asymmetric monoolefins CTA, very often natural occurring substances.

A good example represents the studies of Martinez *et al* using different citrus oils or *d*-limonene as CTA in combination with SBR as starting materials (Figure 33) [193]. Thereby, Grubbs 1st and 2nd generation catalysts, **2** and **3**, showed strong performances in the cross metathesis of SBR enabling the formation of *d*-limonene terminated butadiene oligomers. The molecular weights were reduced to around 300 g/mol with yields up to 95%. According to GC/MS analysis the yields of butadiene oligomers were 52% for mono-terminated oligomers, 23% for methylene-terminated oligomers, and 15% di-terminated oligomers, whereas the number of monomeric units varied between 1 and 4. Additionally, pure polystyrene blocks as well as trimers (10%) made out of butadiene units were detected. As observed, both catalysts showed high efficiencies and produced similar low-molecular-weight products.

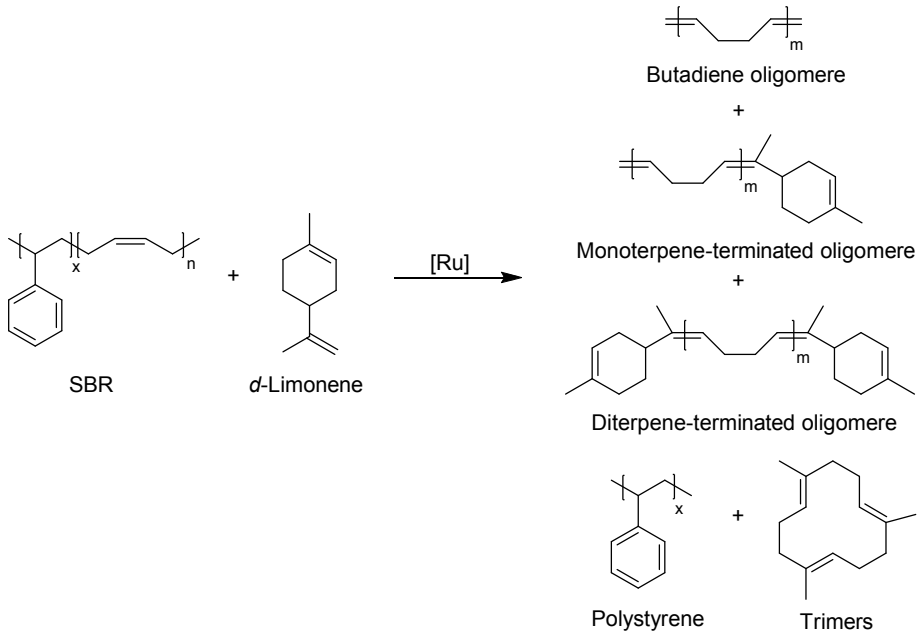

Figure 33 Butadiene oligomers obtained during the cross metathesis of SBR with *d*-limonene (n>>m) [193].

The reaction of NR with mandarin oil or *d*-limonene in the presence of the Grubbs 1st and 2nd generation catalysts, **2** and **3**, respectively yielded a different product composition [194]. For both catalysts, monoterpene-terminated isoprene oligomers were obtained as main-product. Interestingly diterpene-terminated telechelic oligomers were not detectable. These results point out that the trisubstituted double bond can only react with limonene in such a way, that the less substituted intermediate in the transition state is formed. This was also supported by simulations [195].

Grubbs 2nd generation catalyst **3** yields much smaller oligomers than the 1st generation catalysts **2**, showing its much higher reactivity towards trisubstituted double bonds. The primary products of the metathesis degradation of NR with mandarin oil were monoterpene-terminated oligomers with 2 to 4 repeating units [194]. Besides these oligomers, methylene terminated polyisoprene oligomers and a small quantity of the all-*trans* cyclic trimers (*trans-trans-trans*-1,5,9-trimethyl-1,5,9-cyclododecatriene) are detected.

In contrast to *d*-limonene, the reaction of NR with *β*-pinene as CTA and Grubbs 2nd generation catalyst **3** yields 17% of the disubstituted degradation product, as described in another study by the group of Tlenkopatchev [196]. The cross metathesis reactions were carried out under solvent free conditions using second generation Grubbs catalyst at 45°C. At these conditions *β*-pinene does not participate in self-metathesis reactions or

isomerization reactions. The main products of the cross metathesis degradation were with 42% monoterpene-terminated oligomers, 17% diterpene-terminated oligomers as well as 11% methylene terminated oligomers, see Figure 34. Further – similar to the cross metathesis with *d*-limonene - the all-*trans* cyclic trimers (*trans-trans-trans*-1,5,9-trimethyl-1,5,9-cyclododecatriene, 11%) was formed by the intramolecular cyclization reaction.

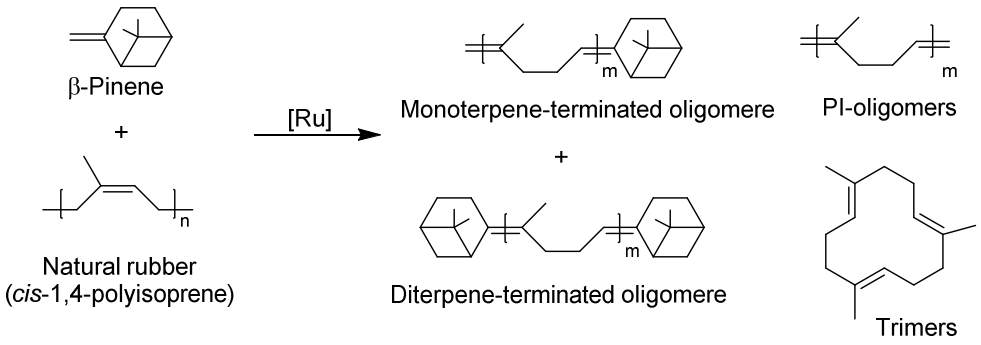

Figure 34 Metathesis degradation of NR with *β*-pinene as CTA (n>>m) [196].

The formation of thermodynamically favored all-*trans* cyclic isoprene or butadiene trimers by intramolecular metathesis degradation is based on a back-biting mechanism (Figure 35). Due to the low energy input for this cyclisation reaction these trimeric compounds appear in metathesis reactions of NR or BR [197-199]. This was also supported by computational studies on the intramolecular metathesis degradation of NR [200].

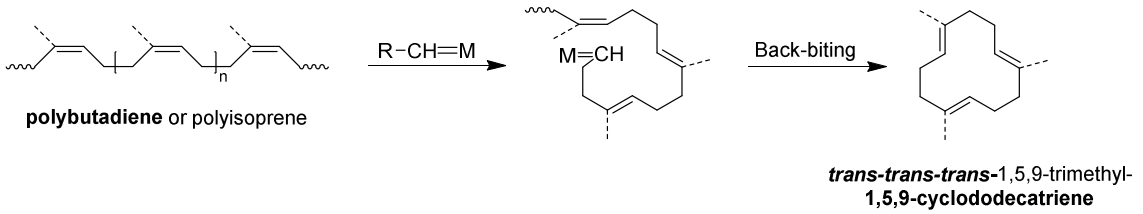

Figure 35 Metathetical back-biting cyclisation of BR and *cis*-PI (dashed lines) under the influence of a metal-carbene catalyst (M=Ru, Mo) [197].

Summing up, this approach is an elegant route towards functional telechelics and fine chemicals using common rubbers including natural rubber – a renewable resource - as starting materials. In this regard, olefin metathesis is competitive with other common methods which are investigated to transform natural products to fine chemicals and

polymers, such as ozonolysis, biodegradation, photodegradation, and degradation using ultrasonic irradiation or oxidative chemical transformations [201]. However, in most of these methods a lower control on the formed products and molar mass distribution is obtained than in olefin metathesis. Thus olefin cross metathesis might have a bright future as sustainable preparation route towards specific chemicals and polymers in different industrial areas.

2.3.5 Metathesis degradation

There is growing interest in the degradation of natural and synthetic rubber either for analytical purposes, reduction of the average molar mass or recycling of (cross-linked) rubber waste.

Reduction of molar mass

For some technological applications, not the introduction of functional end groups is of interest, but only a reduction of the average molar mass is required. The very best example, where olefin metathesis is applied already in an industrial process today, is the synthesis of hydrogenated nitrile-butadiene-rubber (HNBR). HNBR exhibits outstanding resistance to heat, chemicals and ozone, and oil. Beside very good physical and chemical properties HNBR features also excellent mechanical properties, in particular a high abrasion resistance. Therefore, HNBR has found widespread use in many applications as for seals, hoses, belts and damping elements in the automotive, ship and other mechanical engineering sectors. HNBR is synthesized via the hydrogenation of NBR, with molar masses of 200 to 500 kg/mol. However, the Mooney viscosity of these HNBRs is relatively high and in the range from 55 to 105 Mooney units, strongly restricting the processibility of HNBR for many applications. Mechanical and chemical routes to reduce the molar mass leads to wide molar mass distributions and can introduce unwanted functional groups. All these inadvertent modifications result in disadvantages in use. This can be solved by a controlled cross metathetic reduction of molar mass using mono-olefins as CTA. Thus, in a first step, the molecular weight of the nitrile-butadiene rubber-is reduced by olefin-metathesis to a Mooney viscosity of less than 30 (M_w < 70000 g/mol). In the second step, the degraded NBR is hydrogenated to achieve low molecular HNBR. The resulting HNBR was commercialized by Lanxess under the trade name Therban®. For the degradation ruthenium- and osmium-based catalysts can be used [202] but also molybdenum and tungsten catalysts like Schrock and Grubbs catalysts [203], respectively. However, it should be noted, that the metathetic degradation of NBR for analytical studies was already performed by Stelzer *et al* using 1-hexene as CTA in 1988, see also below [204].

Recently, in a similar study also SBR was degraded successfully yielding well defined lower molecular weight macromolecules [205]. Again, this illustrates the excellent controllability of the metathesis degradation under optimized reaction conditions and especially by using metal-carbene catalysts.

Analysis of the polymer microstructures

Cross metathesis with or without additional CTAs or reverse ADMET if ethene as CTA is used as well as intrachain ring closure metathesis degradation, see Figure 30, yield low molar mass fragments which are characteristic for the backbone of the degraded polymers. Thus, these reactions can be used to analyze the microstructure of macromolecules with double bonds in their main chain. For the subsequent analysis of the formed small fragments the most favorite methods are based on gas and gel permeation chromatography and on spectroscopic characterization or mass spectrometry [206]. Starting from the first reports on the degradation of BR by Ast and Hummel in 1970 [184], the investigation of the degradation products of different rubber types was initiated using the WCl_6-based catalyst systems in rather high concentrations. Thereby the cleavage of the C=C double bonds was generally possible and successful but often very unspecific and often accompanied with unwanted side reactions. The first detailed studies on the reaction products and possible reaction pathways using different monoolefins as CTA, e.g. 3-hexene [207], 4-octene [208], 7-tetradecene [209], laid the basis for the analysis of the microstructure of the polymers.

Comprehensive studies for the characterization of elastomer microstructures were performed by Thorn-Csanyi and Perner [207,210]. The microstructures of BR as well as of SBR was characterized regarding the conformation of the main chain (*cis* and *trans* double bonds), their structural units (1,4- and 1,2-links) and tacticity (syndio- or isotactic). Further the lengths of styrene-sequences have been determined. $WCl_6/(CH_3CH_2)_4Sn/(CH_3CH_2)_2O$ and 3-hexene proved to be very suitable for this application.

Using the same conditions, $WCl_6/(CH_3CH_2)_4Sn$ in combination with 3-hexene Stelzer *et al* demonstrated that NBR can be degraded which was used for the determination of the content on acrylonitrile in NBR. After adding the first portion of catalyst, the color

typical for W(VI) compounds was lost. This change in color is based on the formation of a tungsten complex and on the reduction to W(IV), respectively, due to reaction of the catalyst with the nitrile-functionalities. With higher catalyst concentrations and elevated temperatures (60°C) the degradation apparently started. Adding a second catalyst portion and further 12 h reaction time, the yield of low molecular degradation products reached its maximum for NBR samples – according to GC/MS - with an acrylonitrile content of 18 wt%. Rubber mixtures with higher nitrile contents needed a third portion of catalyst to achieve a satisfactory degree of degradation. For the different degradation products, segments with different sequences of cyanoethylene, 2-butenylene and vinylethylene units were detectable [204]. Already with these rather unspecific WCl_6-catalyst systems, the power of metathesis degradation was shown for the characterization of modified and substituted BR [211]. Examples are the analysis of partially chlorinated BR [212] or partially phenylated BR [213].

Beside the structural investigations of the main chain in polymers also the investigation of the cross-linked rubber networks is of great importance. The chemistry of the vulcanization as well as the microstructure and topology of the cross-linking points have to been known in order to produce rubber materials with specific and outstanding elastomeric properties. However, the investigation of cross-linked rubber macromolecules by spectroscopic methods – especially of real rubber products - is in many cases difficult due to their insolubility.

For peroxidic cross-linked BR Ast *et al* studied the network properties already in 1979. Thus they degraded the polymer network using $WCl_6/(CH_3CH_2)_4Sn$ in combination with a low molecular olefin and separated the cross-linked fragments using gel permeation chromatography (GPC). In doing so the experiments led to the conclusion that cross-linking of BR using this systems leads to polyfunctional cross-linking points via a cyclic polyreaction [214]. Similar studies were carried out by Kumar *et al* on the crosslinking of chlorobenzyl-functionalized BR [215].

In these works, mainly rubbers with non-sterically demanding double bonds such as BR, SBR or other unsubstituted cycloalkenamers have been studied. The trisubstituted double bond of polyisoprene shows much less reactivity to this first generation of undefined catalysts. Korshak *et al* reported the oligomerization of polyisoprene using $W(OCH(CH_2Cl)_2]Cl_4$-$Al(CH_3CH_2)_2Cl$-anisole as catalyst system [216]. However, the

obtained molar masses of the oligomers are rather high compared in similar degradation reactions of BR. Hummel *et al* proposed that Al-alkyl-containing catalysts and in particular $WCl_6/(C_2H_5)_3Al_2Cl_3$ are not degrading the isoprene double bonds but in a minor side reaction causes a double bond shift to the less substituted isomer, as shown in Figure 36 [217]. These double bonds are now accessible by the catalyst and can react. The reaction products found by GC/MS in a cross metathesis experiment of 2 methyl-2-pentene, as low molar mass model compound for NR, 7-tetradecene as CTA and $WCl_6/(C_2H_5)_3Al_2Cl_3$ can only be explained by the occurrence of such a double bond shift.

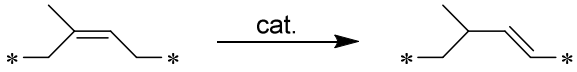

Figure 36 Double bond shift caused by catalysts containing organoaluminium compounds [217].

Alimuniar *et al* reported the degradation of NR using WCl_6-$(CH_3)_4Sn$ as catalyst, but the reaction products showed a significant loss of the double bonds, thus a lot of side reactions and/or subsequent reactions obviously occurred and the reaction pathway of the degradation is not fully clear [218].

The advancement of olefin metathesis catalyst had also a strong impact on this topic. In 1991 Wagener *et al* demonstrated the reversibility of ADMET polycondensation by using Schrock-type tungsten catalysts **1** and ethene in order to depolymerize different elastomers [219]. In this sense, inverse (or reverse) ADMET is another name for cross metathetic degradation using ethene as CTA. In the first experiments, polyoctenamer, polynorbornene and polybutadiene as starting polymers have been reacted with ethene (pressure of approx. 3.5 bar) to give low molecular weight oligomers and α,ω-alkadienes. Using this catalyst system, also *cis*-polyisoprene could be depolymerized. However, due to the above described lower reactivity of the isoprene double bond, depolymerization only occurred at elevated temperature and higher pressure (50°C, 5-6 atm). However, a relative high amount of catalyst has been used in all reactions, e.g. typically [double bonds]/[W] = 20/1 [219].

Consequently this new generation on tungsten and molybdenum initiators (cf. Figure 18) were used in detail to study the degradation products of different elastomers, e.g. for the determination of the ring-chain equilibrium of polyisoprene [198] or polybutadiene [197].

In a logical next step also the ruthenium based Grubbs catalysts were introduced and showed excellent performance in rubber degradation [220].

A comparison of Schrock type with Grubbs 1st and 2nd generation catalysts (**2** and **3**) on the degradation of the steric demanding *cis*-PI showed that Grubbs 2nd generation catalyst **3** is more efficient in ADMET depolymerization of linear and cross-linked *cis*-PI than the other two [221]. Catalyst **3** is capable to depolymerize cross-linked *cis*-PI under very mild conditions at room temperature and an ethene gauge pressure of 0.27 bar.

In block copolymers of styrene with either butadiene or isoprene, the used solvent has also a large influence on the degradation of the rubber block, and different scissions schemes were obtained when selective solvents for only one block or non-solvents are used. Also in this study Grubbs 2nd generation catalyst and no CTA was used [222].

Recently, Wolf and Plenio screened a series of new ruthenium-based complexes which are highly active and tolerant against functional groups. The key features of these complexes are NHC ligands acting as leaving groups during catalyst initiation [223]. In a first series these catalysts were applied in the ethenolysis of squalene – a naturally occurring triterpene – as a defined low molar mass analogue of polyisoprene [224]. The optimized reaction conditions were then utilized in the degradation of two types of NR. Using only a catalyst loading of 0.1% (catalyst : double bonds) well-defined oligoisoprenes with 3 to 6 repeating units and with purities up to 90% could be isolated, which might be of interest in the synthesis of natural terpene based products.

Recently, it was also shown that Grubbs and Hoveyda-catalysts (**2-5**) can degrade *trans*-1,4-polyisoprene (*trans*-PI) [225]. Grubbs 2nd generation catalyst **3** exhibited the highest activity and produced only low molar mass oligomers below 1000 g/mol using ethene as CTA at 20 °C in only two hours. The use of Grubbs 1st (**2**) and Hoveyda 1st generation catalysts (**4**) lead to a reduction of the original molar mass of a factor of 10 to 20, but in addition decomposition of the catalysts with time was observed due to the instability of the methylidene-metal species. Using 1-octene as CTA, this deactivation of the catalyst could be reduced. In contrast to highly active Grubbs 2nd generation complexes (**3**), the degradation can be much more controlled, e.g. by the concentration of catalyst and CTA, and defined polymers with reduced molar mass are accessible using the Hoveyda-type catalysts.

Degradation of cross-linked rubber networks and "real" rubber compounds

A "real" rubber compound consists of a cross-linked rubber network, thus is insoluble, and contains various additives and fillers of very different chemical nature and quantity depending on the wanted application. The rubber compound can only be swollen by a solvent to a certain degree depending on the cross-link density. Additionally, the additives may interfere with the metal center of the catalysts. Due to the difference in the used additives/fillers, it is difficult to predict if metathesis degradation can be applied successfully or not. However, as shown in this last section, there are several reports on rubber mixtures similar to industrial compounds or even real rubber compounds. Such investigations are important not only for recycling purposes but also for the analysis of the ingredients of rubber products as well as for the investigation of the metal-rubber adhesion.

Determination of Additives in Polymeric-Mixtures

The content and type of additives in cross-linked polymer networks can be determined by destroying the polymer matrix surrounding the filler particles. The selective destruction of the matrix requires differences in the properties between the polymer and the additive material so that the additives remain unchanged during the releasing procedure. Usually, the destruction of the polymers is achieved by pyrolysis, or by incineration in air (or oxygen) or using high boiling solvents. The disadvantage of these harsh methods is that also fillers, especially organic fillers, might be affected. In this sense olefin metathesis has the advantage that usually only double bonds of the rubber backbone are attacked at rather low temperatures and that organic compounds remain unchanged. This approach was mainly developed by Hummel in the early 1980´s [226].

In the first experiments, the content of different fillers in dicumylperoxide cross-linked *cis*-PB as model rubber compound were investigated via the olefin-metathesis method using $WCl_6/(CH_3)_4Sn$ and 1-octene as CTA. The used fillers were: glass beads (0,45-0,5 mm in diameter), flex fibers (5mm long, cellulose content: 85%), paper (filter for analysis), chipped wood and polyester-granulate. After the pre-swelling of the sample in chlorobenzene, the metathesis reaction was performed in an inert atmosphere and at 20°C and the amount of filler was determined gravimetrically. The experimental results show that all of these fillers can be quantitatively recovered by this method [226].

In a subsequent study, it was shown, that also the distribution of fillers can be investigated by applying cross metathesis degradation as selective etching method. As model-sample, glass beads were incorporated in a peroxide cross-linked *cis*-PB matrix. This time, the cross metathetic degradation was carried out on a non-swollen sample, again using $WCl_6/(CH_3)_4Sn$ and a mono-olefin (2-octene) as CTA. Doing so, the rubbers surface is degraded step by step, layer by layer. The swelling and degradation of the polymer is occurring at the same time starting from the surface. The glass beads are uncovered; first they poke out of the rubber mixture. The distribution can be analyzed e.g. by scanning electron microscopy. In the course of the degradation the first layer of glass bead fall out, leaving holes in the matrix. Further, the authors report, that this method was also practicable to investigate the distribution of other fillers such as carbon black, titanium dioxide, silica gels and metal powder in cross-linked polyalkenylenes [227]. The studies were extended to sulfur cross-linked rubber compounds and for the quantitative determination of carbon black, the most important fillers in rubber technology. Stelzer *et al* showed that different carbon black types can be successfully quantified in BR as well as SBR vulcanizates. The cross metathesis degradation using again $WCl_6/(CH_3)_4Sn$ as catalyst and 1-octene as CTA proved to be as good as the determination via pyrolysis [228].

By transferring this method to natural rubber difficulties arose because of the substituted double bonds of the isoprene units. Using $WCl_6/(CH_3CH_2)_4Sn$ as catalyst almost no rubber degradation was observed but, using a catalyst containing an organoaluminium compound, $WCl_6/(C_2H_5)_3Al_2Cl_3$ solved this problem. However, as it was discussed above, probably not the original isoprene double bonds are attacked, but less sterically hindered double bonds created by a double bond shift (see Figure 36) react. Subsequently, after the metathesis degradation of the rubber network the carbon black was separated by centrifugation. All experimental results confirmed the successful operation of this method since the amount of found carbon black correlates with the theoretical one. However, this method is not applicable to rubbers with high degrees in cross-linking [217].

Nowadays, using modern metathesis catalysts based on ruthenium, substituted double bonds and highly cross-linked rubber networks do not present a problem for degradation anymore, as discussed before.

Another application shown by Hummel *et al* was the determination of polyethylene (PE) [229] as well as ethylene-propylene rubber (EPR) [230] in cross-linked blends with BR. Cross-linked blends of elastomers and thermoplastics have been used frequently in technical products because of their versatile properties. In the first study, polyethylene was cross-linked with BR using dicumylperoxide [229]. Using $WCl_6/(C_2H_5)AlCl_2$ and 2-octene at room temperature, only the BR rubber is degraded and the remaining solid PE was determined gravimetrically. Low deviations from the theoretical values were obtained if the crosslinking was carried out at temperature below the melting point of PE. In the second study cross-linked blends prepared from EPR and BR were investigated by metathetic degradation of the BR component [230]. The metathesis reaction was performed with an excess of 1-octene using $WCl_6/(CH_3)_4Sn$ on compounds crosslinked either by sulfur or dicumyl peroxide. The difference between the added amount of EPR and the experimentally determined value was larger than in the above described experiments for filler quantification, but also in this case they showed that olefin metathesis can successfully be applied for this rather demanding analytical task.

Investigation of rubber-metal interfaces

In rubber technology, the rubber-metal adhesion is of great importance in many steel wire reinforced products such as tires, hoses, handrails or conveyor belts. In order to achieve a good adhesion between rubber and wires, the wires typically consist of a steel core surrounded by a thin layer of brass or zinc. In the case of brass, Cu_xS-ZnS structures are build-up during the sulfur vulcanization of rubber in which the cross-linked rubber macromolecules bind mainly mechanically on these structures. Some additional contributions via chemical bonds are believed to be of minor significance [231].

However, the investigation of the adhesion mechanism is not straight forward, because of the generally strong rubber-brass adhesion the adhesion interface is not directly accessible. Thus during the last years, we have introduced the cross metathesis degradation approach also to this analytical challenge (Figure 37). After swelling in toluene the cross-linked rubber is degraded using Grubbs 2nd generation catalyst **3** and 1-octene as CTA.

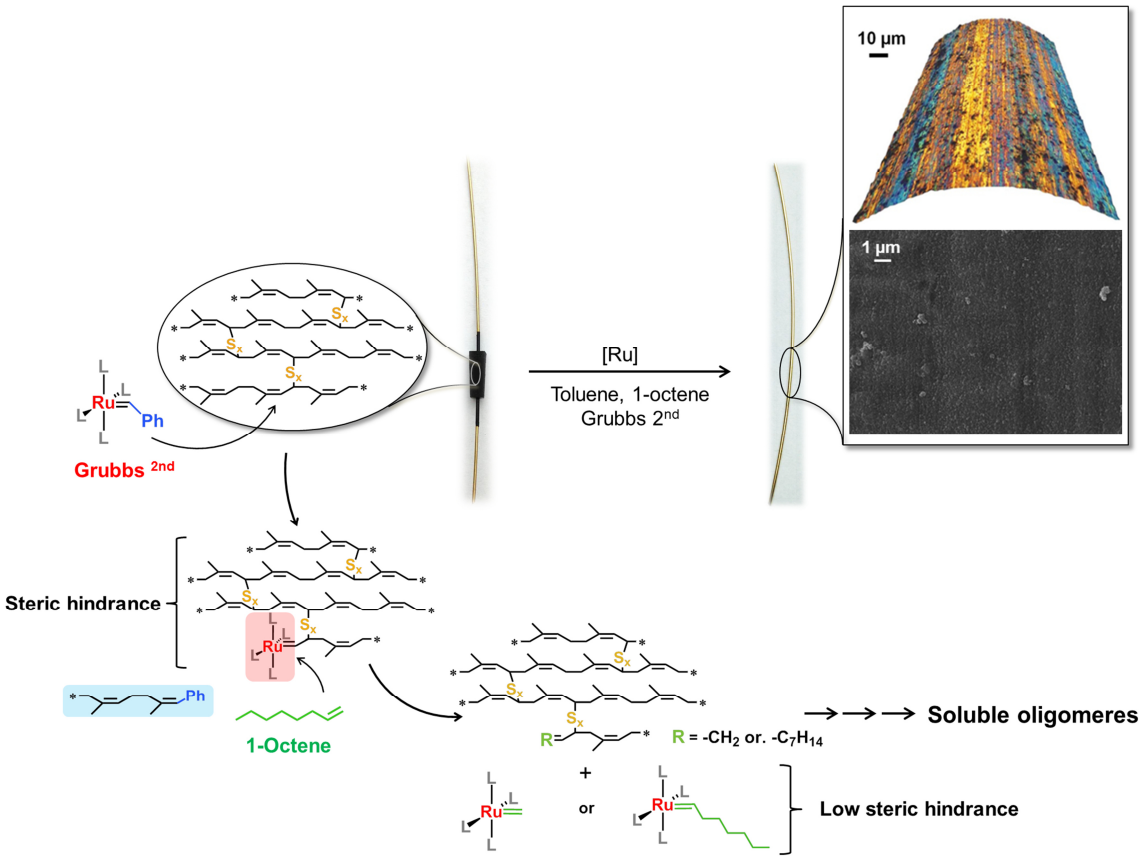

Figure 37 Principle of the olefin-metathesis method used to uncover adhesion interfaces [232].

The first studies regarding the metathetical exposure of the rubber-brass adhesion layer concentrate on the degradation of simple NR mixtures. Subsequently, these experiments were expanded to SBR and NBR. As already discussed above, the degradation depends on the type of rubber, i.e. the substitution on the double bonds. Thus NR with the tri-substituted isoprene monomeric units is sterically more demanding than butadiene units in NBR and SBR. Also in this case, the nitrile units of NBR do not interfere with the cross metathesis reaction. In all cases the rubber-brass interface was uncovered at the same high quality so that the interface is accessible for further analysis, e.g. by optical microscopy, scanning electron microscopy or X-ray photoelectron spectroscopy. It was also shown that some of the often used fillers and additives in rubber compounds, such as carbon black, silica, cobalt-stearate or a phenol-formaldehyde-resin, do not prevent a successful degradation, as in all cases the rubber-metal interfaces could be exposed in very high quality. However, it should be mentioned, that special additives or reactive fillers interacting with the metal catalyst may decelerate or even prevent the degradation [232].

Recycling

Recycling of rubber products is nowadays of substantial importance, particularly because of sustainable, environmental and economic reasons. However, the cross-linked rubber network is a challenge for an economic recycling strategy. Today, rubber products are usually recycled by physical reshaping of waste polymers (from the amount in most cases tires) into fillers and for other applications with less demanding elastomeric properties. Examples are the use of crumb rubber in rubberized asphalt, or as backfill material. However, a large quantity is burnt e.g. in the production of cement and thus recycled only energetically. Here the cross metathesis of rubber either with ethene (reversed ADMET) or other alkenes would open interesting pathways to produce soluble oligomers or even low molar mass chemicals which can be used as new raw materials in rubber chemistry as well as in chemical industry in general. Also recycling schemes for enclosed fillers could be envisaged.

As already described before, cross-linked rubber networks do not prevent the metathetic degradation per se, as already, the first WCl_6-based catalysts have been successfully exploited towards the degradation of rubber networks crosslinked by peroxides as well as by sulfur [220,233,234]. However, a controlled degradation of NR was not possible due to the inaccessibility of the isoprene double bond. However, by the introduction of the defined Schrock and especially Grubbs-carbene catalysts also this technological important rubber can be degraded, as shown by Thorn-Csanyi [220]. The rate of degradation is lower compared to the polybutadiene network, but full conversion to the small oligomers can be achieved. Additionally, real and already used tires (car and van tires) were degraded. The car tires consist mainly of BR and SBR and the van tires of NR and SBR. The GC analysis of the car tire showed the characteristic fragments of the metathetic degradation of BR and SBR for the car tire as well as the fragments of NR and SBR for the van tire [220].

In another work, the degradation of car tires was studied using Grubbs 2nd generation catalysts without a CTA. Thereby it was observed that the main degradation products of cross-linked BR are again isomers of 1,5,9-cyclododecatriene (85%), and 15% are products with higher molecular mass [235]. Beside the main products, also carbon black, sulfur and other additives were unhinged from the rubber mixture.

Recently, Wolf and Plenio investigated the reversed ADMET reaction (ethenolysis) of rubber waste in detail [236]. Old car and truck tires are very often shreddered to so-called end-of-life tires (ELT) granulates. These multicomponent materials contain – as most technical rubber products – large amounts of vulcanized elastomers (mainly natural rubber), inorganic fillers (carbon black, silica) and a number of other additives. Plenio *et al* was able to degrade these ETL granulates to organic solubles – primarily oligomeric *cis*-1,4-isoprene (as evidenced by NMR and HPLC) – using Grubbs or Hoveyda 2nd generation catalyst (**3** or **5**) in a reactor with an ethene pressure of 7 bar at 80°C for 12 hours. The so performed ethenolysis had a conversion rate of around 50%, meaning that 1.0 g of granulate led to the isolation of approximately 0.5 g of oligomeric isoprenes, which are useful starting products for the synthesis of various chemical compounds [236].

Additionally, by using functional CTA, as discussed above, functional telechelic oligomers can be directly produced from waste products, as shown in the work auf Sadaka *et al* using *cis*-1,4-diacetoxy-2-butene and waste tire rubber based on NR and BR [190].

2.3.6 Conclusion

During the last years, olefin metathesis reactions have been successfully applied in various areas of rubber chemistry and technology and will continue to contribute to this field. Especially ROMP has proven to be a valuable tool for the preparation of elastomers with high stereoselectivity as well as with functional groups. Additionally segmented block-copolymers and combination with other polymerization techniques broadens the possible use of these polymerization techniques.

Cross metathesis and reversed ADMET have been identified as further key reactions in rubber technology with a great potential in the future. First, telechelic functional oligomers and chemical specialties can be obtained from non-cross-linked NR, a natural and renewable resource. Consequently, this route provides a possible alternative to petrochemical processes.

But, secondly, also cross-linked rubber systems can be degraded which can become a recycling strategy for vulcanized rubber products. Furthermore by degrading vulcanized rubber, additives and fillers get accessible to further analysis, or in the case of metal-reinforced rubber systems, the metal surface can be uncovered, and the adhesion layer formed during vulcanization can be investigated in detail.

Summing up, olefin metathesis has generated many interesting concepts and methodologies for rubber chemistry and elastomer technology. It can be expected that this trend will continue and will lead to many more interesting applications in future.

3 AIM OF THIS THESIS

The topic of this thesis is to investigate and optimize the rubber-to-metal adhesion. It is generally known that the rubber-metal adhesion depends on many parameters, especially on the composition of the rubber compound as well as on the wires` properties. However, due to the fact that the rubber-brass bonding depends on so many parameters, it is on the one side not easy to reach a good adhesion and on the other side it is difficult to investigate how the particular parameters influence the adhesion performance.

For this reason, this thesis was divided in three following sections:

The first target was the investigation of various brass-plated steel wires. According to their manufacturer they all should have the same characteristics (brass-layer thickness, Cu-content of the brass-layer, etc.) but incomprehensibly all show different adhesion performances. Thus once we focused on the question, what are the distinctions between these wire samples.

In a second study, the influences of various compound components on the rubber-brass adhesion interface were investigated using the olefin-metathesis method. Here, the focus was set to the investigation of different rubber types as NR, NBR and SBR as well as additives and filler materials as carbon black, silica, cobalt-salts and formaldehyde resins.

The third topic of this thesis was to develop new bonding systems which are based on organic bifunctional molecules. Thereby, the rubber-metal adhesion is not achieved by mechanical interlocking of the rubber macromolecules in the brass layer but by chemical linkage. In doing so the adhesion performance is less dependent on the rubber compound composition, the wire properties and aging processes. In order to transfer the manual dip-coating procedure to a continuous process an automatic dip-coating machine had to be designed and constructed.

4 EXPERIMENTAL

4.1 Materials

4.1.1 Chemicals

Grubbs catalyst 2nd generation [$RuCl_2(H_2IMes)(PCy_3)(CHPh)$] ($H_2IMes$ = N,N-di(mesityl)-4,5-dihydroimidazolin-2-ylidene), toluene (99,9%), 2-butanone oxime (MEKO, 99%), bis[3-(triethoxysilyl)propyl]tetrasulfide (technical, ≥ 90%), bis-(trimethoxysilylpropyl)amine (technical, ≥ 90%), 3-(triethoxysilyl)propyl isocyanate (95%), diethoxyphosphinyl isocyanate (≥ 97.5%), 3-(trimethoxysilyl)propyl methacrylate (Silane A174, 98%), bromotrimethylsilane (TMSBr, ≥ 97%), triethylphosphonoacetate (98%), N,N-dimethylformamide (DMF, anhydrous 99.8%), sodium azide (NaN_3, purum p.a. ≥99%), 1,2-dicyanoethane (99%) and dodecanenitrile (99%) were all purchased from Sigma-Aldrich (Germany) and used as received.

Oxalyl chloride (purum ≥96%), 1-octene (>97%) and 4-methyl-benzonitrile (>98%) were purchased from Fluka Chemie AG (Switzerland).

Brass-coated steel wires (diam. 0.71 mm, 5 µm brass with 67% Cu and 33% Zn, Gustav Wolf Seil- und Drahtwerke GmbH & Co.), natural rubber (CV 50), styrene butadiene rubber (BUNA SB 1500), nitrile butadiene rubber (KRYNAC 2645), ethylene propylene diene monomer rubber (Dutral 4038), naphtenic oil (Gravex), paraffinic oil, dioctyladipat (DOA), zinc oxide, stearic acid, sulfur (oil content 5%), zinc salt (Dispergum L), white oil, 2,5-Dimethyl-2,5-di(tert-butylperoxy)hexane on a carrier (Trigonox 101 XL-45), silica (Silica VP3), silica-kaolinite mixture (Silitin N85), Cellobond® (phenol-formaldehyde-resin (Novolak) in combination with hexamethylenetetramine), Co-stearate (Manobond CS95, 9.3-9.8% Co), N,N-dicyclohexylbenzothiazole sulfonamide (DCBS), *N*-cyclohexyl-2-benzothiazole sulfonamide (CBS), carbon black N550 and *N*-(cyclohexylthio)phthalimide (CTP) were provided by Semperit Technische Produkte GmbH (Wimpassing, Austria) and were used without further purification.

Hulk catalyst (cis-dichloro-(κ2(C,O)-(2-iso-propylester-5-methoxybenzylidene)-(1,3-bis(2,4,6-trimethylphenyl)-4,5-dihydroimidazol-2-ylidene)-ruthenium) was provided by Eva Pump (Graz University of Technology) [237].

Nitrogen (N_2 gas, 5.0) was purchased from Messer Austria GmbH (Graz, Austria). Unless specified otherwise, solvents were used as purchased.

4.1.2 Substrates

Various brass-coated steel wires (diam. 0.71 mm, 5 µm brass) were provided by Gustav Wolf Seil- und Drahtwerke GmbH & Co. (Gütersloh, Germany) as well as by Pisec Group GmbH (Vienna, Austria). Zinc-coated steel wires and cords were provided by Metizy-94 (Zaporozhe, Ukraine).

Brass plates (25x25x0.5 mm, 63% Cu and 37% Zn) were purchased from Goodfellow Cambridge Ltd (Huntingdon, England).

4.2 Experimental methods

4.2.1 Substrate pretreatment

Brass-coated steel wires

For standard experiments regarding the rubber-metal adhesion the wires were used as received. However, for the implementation of the chemical bonding systems the brass-coated steel wires were cut into the desired size, 15 cm for the handmade coatings and 3.45 m for the experiments using the automatic coating machine. Afterwards, the brass-coated wires were washed with toluene and immediately prior to dip-coating activated by O_2-plasma (FEMTO, Diener Electronic) for 10 minutes. The plasma treatment serves as additional cleaning step and leads to an increased formation of reactive oxygen containing groups as e.g. hydroxyl groups which improve the chemical linkage of the adhesion promoter on the wire surface.

Zinc-coated steel wires

For standard experiments regarding the rubber-metal adhesion the wires were used as received. However, for the implementation of the chemical bonding systems the zinc-coated steel wires were cut into the desired size, 15 cm for the handmade coatings and 3.45 m for the experiments using the automatic coating machine. Afterwards, the zinc-coated wires were washed with toluene and immediately prior to dip-coating activated by O_2-plasma (FEMTO, Diener Electronic) for 10 minutes.

Brass plates

The brass plates could not be used as received because they had a very rough surface which would not have been suitable to simulate the brass-coated steel wire. Thus, initially, the plates were ground under watering (Struers LaboPol-25) using grinding wheel #2400 and #4000 (Struers Waterproof Silicon Carbide Papers). Afterwards, the plates were polished using first the MD-Mol polishing wheel in combination with a diamond polishing suspension (DP-S suspension, 3 µm) followed by the utilization of the MD-Chem polishing wheel combined with a corundum polishing suspension (OP-S suspension, 0.04 µm). As lubricant DP-Lubricant Red was used. In a subsequent step, the brass plates were immersed in isopropyl alcohol (puriss p.a. ≥99.8%) and treated for

15 minutes in an ultrasonic bath. Finally, the plates were rinsed again with isopropyl alcohol and dried with nitrogen. In the case of experiments regarding the adhesion of chemical bonding systems the plates were further activated for 10 minutes by O_2-plasma (FEMTO, Diener Electronic).

4.2.2 Olefin-metathesis experiments

For the olefin-metathesis experiments T-test specimens were prepared similar to ASTM D 1871. The specific compound compositions of the different samples used for the various experiments can be found in Chapter X where the results are discussed. The vulkanization was performed at 160 °C and 320 bar for 20 min with an embedment lengths of 10 mm.

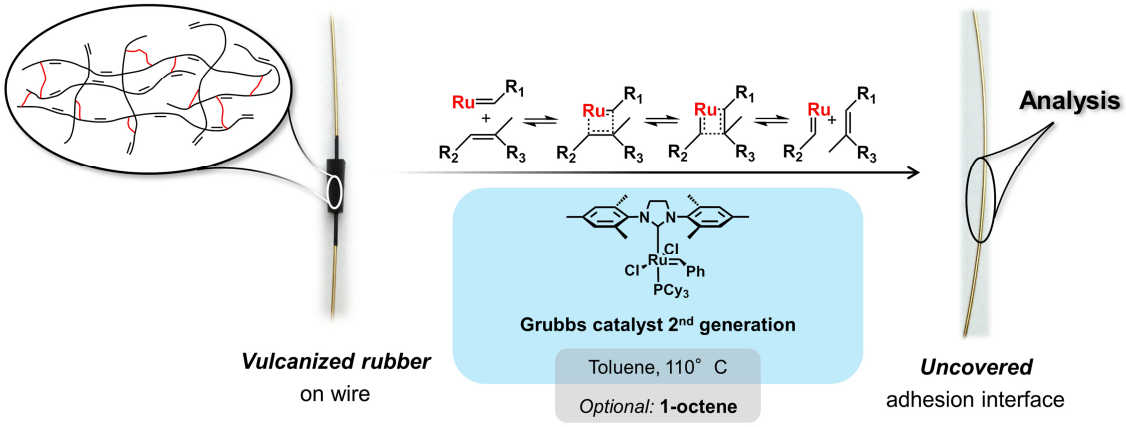

Figure 38 Scheme and mechanism of the olefin-metathesis method.

The olefin-metathesis degradation of NR, NBR and SBR was carried out under inert atmosphere. As a first step, the rubber covered areas of the wire were placed in toluene for 24 hours. Subsequently 3.5 ml of toluene was placed in a Schlenk flask and heated up in an oil bath to 110°C (Figure 38). Now, 3 mg of Grubbs catalyst 2nd generation (experiments in Chapter 5.2) and Hulk catalyst (experiments in Chapter 5.3), respectively, was added followed by the immersion of the rubber wire specimen. To accelerate as well as to improve the rubber degradation 100 µL of 1-octene was added. After one hour the reaction was stopped with ethyl vinyl ether. Subsequently, the wires were removed, rinsed with toluene and dried. In case of rubber residues on the wire the procedure was repeated until a clean surface was obtained. Finally, the uncovered wires were stored in vials filled with inert gas (N_2).

4.2.3 Synthesis of chemical adhesion promoter

Synthesis of MEKO blocked 3-(triethoxysilyl)propyl isocyanate

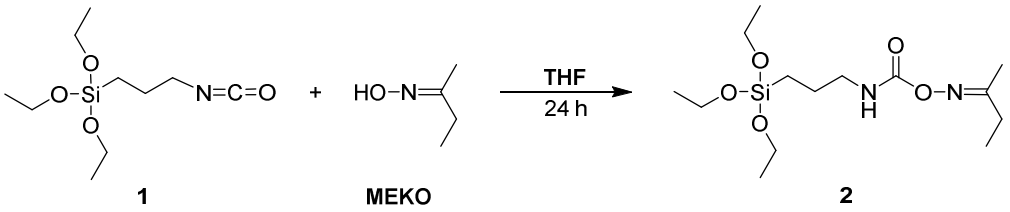

Figure 39 Synthesis of MEKO blocked 3-(triethoxysilyl)propyl isocyanate.

In a 250 ml three-necked flask filled with inert gas (N_2), 2 g (8.1 mmol, 1 eq) 3-(triethoxysilyl)propyl isocyanate (1) were dissolved in 20 ml of THF absolute . After addition of 0.78 g (9 mmol, 1.1 eq) 2-butanoneoxime (MEKO) drop by drop, the solution was stirred at room temperature for 24 hours. Now, in the IR-spectrum the isocyanate-peak (2275-2250 cm^{-1}) completely disappeared and the urethane-peak (1740-1690 cm^{-1}) appeared, which provides proof of a complete blocking reaction of the isocyanat-group with MEKO. Finally, the solvent was evaporated in a rotary evaporator and the resulting colorless liquid was dried applying an oil pump vacuum at 50°C. By this way the excess of MEKO could be removed entirely.

Yield: 2,7 g (8 mmol, 99%), colorless liquid

^{1}H-NMR (300 MHz, $CDCl_3$) δ: 6.38 (bs, 1H, -CH_2-N**H**-C-), 3.77-3.84 (q, $^3J_{HH}$=7.0 Hz, 6H, CH_3-C**H_2**-O-), 3.24-3.30 (q, $^3J_{HH}$=7.0 Hz, 2H, -CH_2-C**H_2**-NH-), 2.98 (s, 3H, C**H_3**-C-), 2.24-2.32 (q, $^3J_{HH}$=7.5 Hz, 2H, CH_3-C**H_2**-C-), 1.61-1.71 (m, $^3J_{HH}$=8.0 Hz, 2H, -CH_2-C**H_2**-CH_2-), 1.18-1.23 (t, $^3J_{HH}$=7.0 Hz, 9H, C**H_3**-CH_2-O-), 1.08-1.14 (t, $^3J_{HH}$=7.5 Hz, 2H, C**H_3**-CH_2-C-) 0.60-0.66 (t, $^3J_{HH}$=8.2 Hz, 2H, -Si-C**H_2**-CH_2-) ppm

ATR-IR: ν_{max} (cm^{-1}) 3425 (w, N-H), 2972 (m, CH_3-, -CH_2-), 2865 (m, CH_3-, -CH_2-), 1740 (m, -O-CO-N-), 1500 (m, CH_3-, -CH_2-), 1432 (w, C=O), 1066 (s, N-H), 906 (s, C-H), 770 (m, N-H)

Synthesis of MEKO blocked isocyanate phosphonic acid

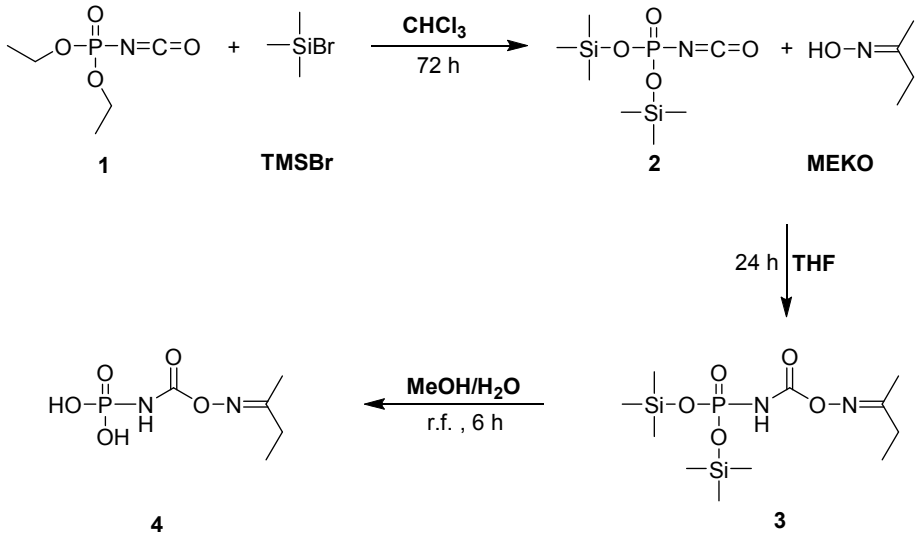

Figure 40 Synthesis of MEKO blocked isocyanate phosphonic acid.

A 250 ml three-necked flask was filled with inert gas (N_2) and equipped with a magnetic stir bar. There, 2.45 g (14 mmol, 1 eq) of diethoxyphosphinyl isocyanate (1) were mixed with 8.6 g (56 mmol, 4 eq) bromotrimethylsilane in dichlormethane absolute and stirred for 72 hours. Now, the solvent as well as the excess of TMSBr were removed by applying an oil pump vacuum at 80°C. The isocyanate-peak (2275-2250 cm^{-1}) was still visible in the IR-spectrum, which means the isocyanate-group was not involved in any side reaction. Now, 3.7 g (13,8 mmol, 1 eq) of **2** stirred together with 1.65 g (0.019 mmol, 1.38 eq) of MEKO for 24 h in THF absolute and in an inert atmosphere. After a complete conversion, which was followed by IR-spectroscopy - the isocyanate-peak (2275-2250 cm^{-1}) completely disappeared and the urethane-peak (1740-1690 cm^{-1}) appeared - the solvent and the remained MEKO was evaporated in a rotary evaporator and dried on the oil pump at room temperature. The colorless oily residue was heated with 20 ml MeOH and 2 ml dest H_2O for 6 hours under reflux. After evaporation of the solvent on the rotary evaporator and drying using the oil pump, 4.8 g of a yellowish oil was received. The raw product was purified by column chromatography, in which cyclohexane mixed with ethylacetate in the ratio 1 to 3 was used as the first eluent and pure methanol as the second one.

Yield: 2.42g (11.5 mmol, 82.3%), white solid

^{1}H-NMR (300 MHz, CD_3OD) δ: 1.24 (t, $^3J_{HH}$=7.2 Hz, 3H, C**H$_3$**-CH_2-C-), 2.06-2.14 (q, $^3J_{HH}$=7.5 Hz, 2H, -CH_2-C**H$_2$**-C-), 3.16 (s, 3H, C**H$_3$**-C-), 6.17 (bs, 2H, **H**O-P-), 7.24 (bs, 1H, -P-N**H**-C-) ppm

ATR-IR: ν_{max} (cm^{-1}) 3282 (m, -P-OH), 2951 (m, CH_3-, -CH_2-), 2862 (m, CH_3-, -CH_2-), 2352 (w, -P-OH in hydrogen bonds), 1708 (s, C=O), 1475 (m, CH_3-, -CH_2-), 1454 (m, C=O), 1187 (s, P=O), 1005 (s, N-H), 939 (s, -P-O-), 859 (s, N-H), 782 (s, -CH_2-), 476 (s, -OH)

Synthesis of acyl azide phosphonic acid

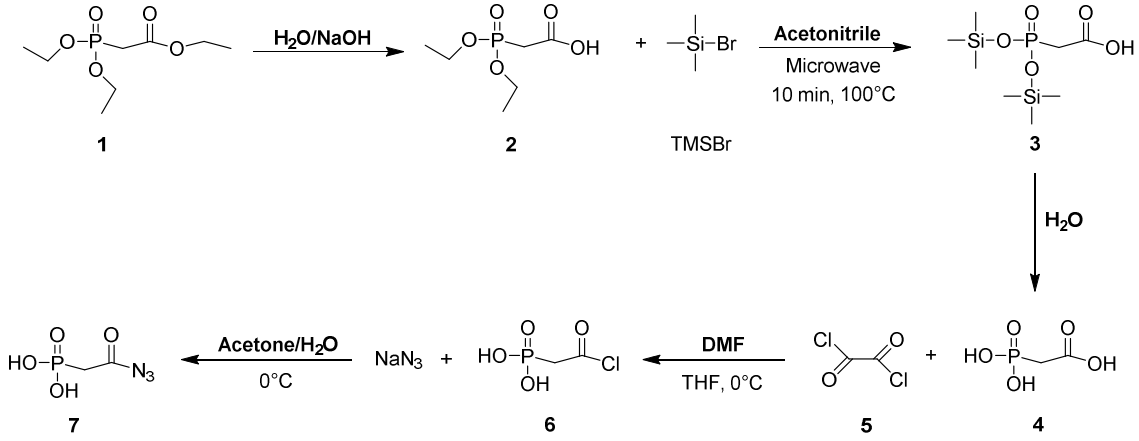

Figure 41 Synthesis of acyl azide phosphonic acid.

10 g (44.6 mmol, 1 eq) of triethylphosphonoacetate (**1**) were dissolved in 50 ml of a solution made out of 1.8 g NaOH in H_2O:MeOH=1:1. This mixture was stirred for 2 hours at room temperature followed by two extraction steps with ethylacetate. The aqueous phase was set to pH 1.5 and again extracted three times using ethylacetate. The collected organic phases were dried by Na_2SO_4, filtered and concentrated. Thus, 8.6 g (43,8 mmol, 1 eq) of **2** were received and solved in 30 ml MeCN absolute under protective gas (N_2). Now, the solution is put together with 13.43 g (87,6 mmol, 2 eq) of TMSBr in a vial, which was already filled with protective gas. After closing the vial with a septum it was treated for 10 minutes at 100°C with microwaves (Biotage Initiator 2.5). The mixture was now quenched for 30 minutes in dest H_2O, which was subsequently evaporated with MeCN using the oil pump. The amount of starting product **2** was converted to product **4** in four single rounds because the microwave

equipment is limited to a reaction volume of 20 ml. After evaporation, the oily liquid was precipitated first in chloroform, than dissolved in acetone and again precipitated in diethyl ether. In a next step, 3.4 g (24.3 mmol, 1 eq) of **4** were solved in 20 ml THF absolute in an inert atmosphere. Under vigorous stirring, 6.17 g (48.6 mmol, 2 eq) oxalyl chloride (**5**) were added drop by drop within 30 minutes alt 0°C. Further, 10 droplets of DMF (catalytic amounts) were added. Thus, the formation of carbon monoxide and carbon dioxide was observed (blistering). After 90 minutes stirring at room temperature, the excess of oxalyl chloride was removed on the rotary evaporator at 30°C. In a final step, 2.08 g (13.1 mmol, 1 eq) of the orange product **6** were solved in 10 ml acetone and added in drops and under vigorous stirring to an ice cooled solution, which consisted of 1.70 g sodium azide (26.2 mmol, 2 eq) in 10 ml dest H_2O. This solution was stirred for 30 minutes at 0°C. Now, the solvents evaporated under reduced pressure and the remaining 2.18 g of the final raw product (**7**) were purified by column chromatography, in which cyclohexane mixed with ethylacetate in the ratio 1 to 3 was used as the first eluent and pure methanol as the second one.

Yield: 1.13 g (6.9 mmol, 15.8%), brown-orange solid

^{1}H-NMR (300 MHz, CD_3OD) δ: 2.52 (s, 2H, -P-C**H_2**-C), 7.93 (s, 2H, **H**O-P-) ppm

ATR-IR: ν_{max} (cm^{-1}) 2923 (m, -P-OH), 2793 (m, -CH_2-), 2312 (w, -P-OH in hydrogen bonds), 2151 (s, -N_3), 1703 (s, C=O), 1468 (m, -CH_2-), 1414 (m, C=O), 1113 (s, P=O), 928 (s, P-O), 594 (m, -OH)

4.2.4 Preparation of Sol-Gel adhesion systems

Preparation of polysulfide silane adhesion systems

For the preparation of the silane based coating solution, bis[3-(triethoxysilyl)propyl]tetrasulfide (S_4-Si) was mixed with bis-(trimethoxysilylpropyl)amine (A) in the ratio 3:1 and subsequently stirred for 10 minutes at room temperature in a Duran glass flask.

Manual coating

To determine the adhesion performance of the bis[3-(triethoxysilyl)propyl]tetrasulfide adhesion system, the silane-mixture was deposited on a pretreated wire (see Chapter 4.2.1) via dip-coating. Thus the wires were dipped manually for 10 seconds into the silane-mixture and then set up vertically for 30 minutes. Thereby the excess of silane solution was able to run off so that thin layers were achieved. Afterwards the coated wires were dried and cross-linked for 40 minutes at 160°C in a heating chamber.

Automated coating

In order to enhance the reproducibility and to reduce the standard deviations of the pull-out tests the manual dip-coat process was automated. Therefore an automated coating machine was designed as well as constructed (Figure 42). Thus, initially, the wire was manually rolled up on the feed reel and threaded through the open air plasma system (Ahlbrandt, Germany) with a slot length of 20 cm. Afterwards, the wire was threaded around the return pulley (here the wire runs through the coating solution) as well as the tube furnace and finally fixed on the take-up reel. The wire was moved by a step motor through the coating machine by rotating the take-up reel. The coating parameters were set using a microcontroller. The driving rate was varied between 6 and 12 mm/min (controls the time of plasma activation, dip-coating and drying) and the temperature of the tube furnace was set to 160°C. The plasma system operated with an air-pressure of 1.5 bar and a power of 200 watt. The interior space of the coating solution reservoir was filled with inert gas (N_2) to protect the coating solutions from reacting with atmospheric oxygen or moisture. Further, by blowing an N_2-gas jet on the solutions surface thin layers could be produced. All running processes could be stopped automatically.

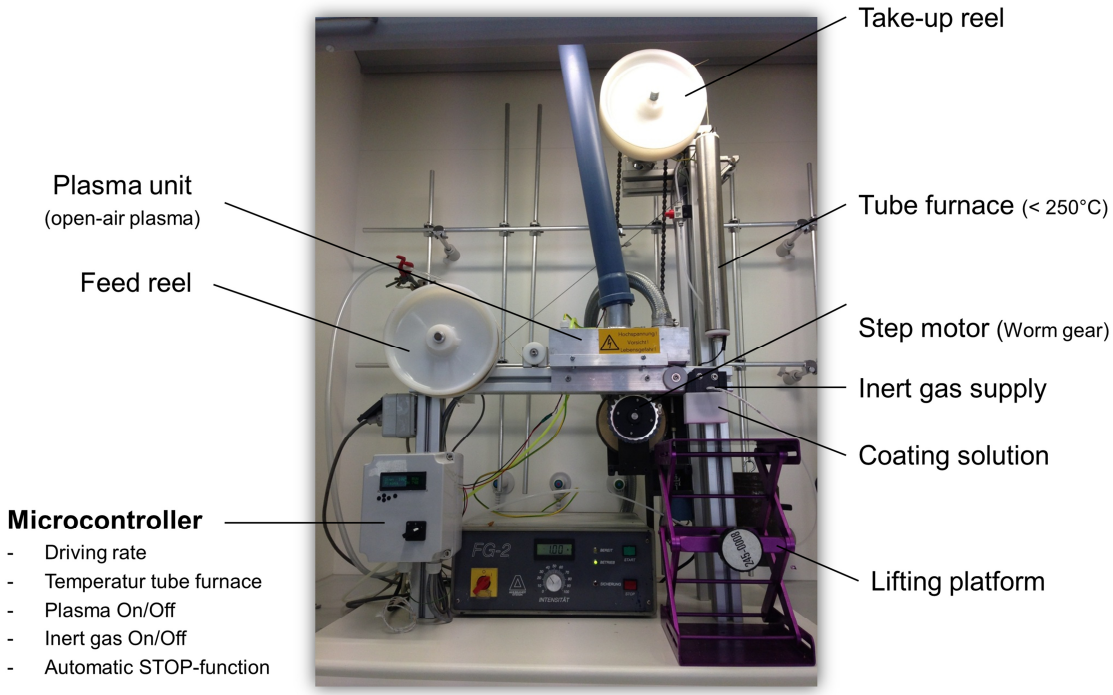

Figure 42 Image of the in-house constructed automated wire-coating machine.

Preparation of MEKO blocked isocyanatesilane adhesion systems

For both, the manual and the automated coating process, the MEKO blocked 3-(triethoxysilyl)propyl isocyanate (Iso) was mixed with bis-(trimethoxysilylpropyl)amine in the ratio 3:1 and subsequently stirred for 10 minutes at room temperature in a Duran glass flask.

Manual coating

To determine the adhesion performance of the MEKO blocked 3-(triethoxysilyl)propyl isocyanate adhesion system, the silane-mixture was deposited on a pretreated wire (see Chapter 4.2.1) via the dip-coat process. Thus the wires were dipped manually for 10 seconds into the silane-mixture and then set up vertically for 30 minutes. Thereby the excess of silane solution was able to run off so that thin layers were achieved. Afterwards the coated wires were dried and cross-linked for 1 hour at 100°C in a heating chamber.

Automated coating

The automated coating process of the MEKO blocked 3-(triethoxysilyl)propyl isocyanate adhesion systems was performed identically to the polysulfide silane adhesion system. However, the temperature of the tube furnace was set to 100°C instead of 160°C.

Preparation methacrylatesilane adhesion systems

Adhesion systems used for peroxide cross-linked rubber compounds, 3-(trimethoxysilyl)propyl methacrylate (MAS) was mixed with bis-(trimethoxysilylpropyl)amine in the ratio 3:1 and subsequently stirred for 10 minutes at room temperature in a Duran glass flask. As a next step, the silane-mixture was deposited on a pretreated wire (see Chapter 4.2.1) via dip-coating. Thus the wires were dipped manually for 10 seconds into the silane-mixture and then set up vertically for 30 minutes. Thereby the excess of silane solution was able to run off so that thin layers were achieved. Afterwards the coated wires were dried and cross-linked, respectively, for 1 hour at 100°C or for 40 minutes at 160°C in a heating chamber. Even though 3-(trimethoxysilyl)propyl methacrylate is highly moisture-sensitive, the coating preparation process was not done under atmospheric conditions.

4.2.5 Preparation of self-assembled monolayer adhesion systems

Preparation of MEKO blocked isocyanate phosphonic acid adhesion systems

In order to prepare adhesion systems based on self-assembled monolayers 50 mg of MEKO blocked isocyanate phosphonic acid were dissolved in 10 ml MeOH and stirred for 1 hour at room temperature in a Duran glass flask.

For the investigation of the adhesion properties of the MEKO blocked isocyanate phosphonic acid adhesion system the pretreated wires (see Chapter 4.2.1) were dipped in the coating solution. The dipping-time was set to 2 hours at ambient temperature. Here, an exact and clean working technique was indispensable for the formation of perfect self-assembled monolayers since particles of dirt and dust prevent the adhesion of the phosphonic acid groups. After the dip-coating procedure the wires were placed in isopropanol and treated with ultrasound for 20 minutes. Finally, the wires were rinsed with isopropanol, dried with nitrogen and in some cases tempered for 1 hour at 90°C in a drying chamber.

Preparation of azyl azide phosphonic acid adhesion systems

For the self-assembled monolayers based on Azyl azide phosphonic acid a solution with 5 mg/ml in dest H_2O was prepared and stirred for 1 hour at room temperature in a Duran glass flask.

To investigate the adhesion characteristics of the azyl azide phosphonic acid adhesion system the pretreated wires (see Chapter 4.2.1) were dip-coated in the coating solution. The dipping-time was set to 2 hours at ambient temperature. Also here, an exact and clean working technique was indispensable for the formation of perfect self-assembled monolayers since particles of dirt and dust prevent the adhesion of the phosphonic acid groups. After the dip-coat procedure the wires were placed in isopropanol and treated with ultrasound for 20 minutes. Finally, the wires were rinsed with isopropanol and dried with nitrogen. In this case, the final coating was not tempered because azides are supposed to be explosive and therefore an additional heating step was renounced.

4.3 Methods of analysis

4.3.1 Optical microscopy

Optical microscopy was done using an Olympus BX60 microscope coupled with an Olympus E-520 camera. Images were captured at maximum light intensity. The wires were aligned as good as possible horizontally in the viewing direction of the operator.

4.3.2 Focusvariation microscopy

3D information and true color images with full depth of field were recorded by focusvariation microscopy. The image acquisition was performed with the infinite focus microscope from Alicona Imaging GmbH. The wires were aligned perfectly in line of sight of the operator. An area of 110 µm x145 µm was captured and the resulting image was stretched four-fold in z-direction to improve the visibility of the surface morphology.

4.3.3 Scanning electron microscopy - energy dispersive X-ray spectroscopy (SEM-EDX)

The investigation of the microstructure was performed by using a Tescan Vega3 scanning electron microscope coupled with an energy dispersive X-ray spectrometer (Oxford Instruments, INCAx-act). Thereby, the electron energy was set to 20 keV and for a better comparison the atom% of the elements were normalized proportional to Cu (100 atom%). The decision was taken for Cu because it is the only element which does not change its content on the rubber-metal interface during vulcanization.

In addition very detailed and highly resolved microanalyses were performed by Peter Pölt and Angelika Reichmann from the Austrian Centre for Electron Microscopy and Nanoanalysis (FELMI-ZFE) using a Zeiss Ultra 55 scanning electron microscope (Carl Zeiss NTS, Oberkochen, Germany) coupled with an energy dispersive X-ray spectrometer (Genesis, EDAX Inc., Mahwah, NJ, USA). Depending on the attention to detail, the electron energy used for the analysis was adjusted between 7 and 15 keV. For a better comparison all values were normalized proportional to Cu and the Cu value was set to 100 atom%. To investigate the wires` cross section they were first embedded into an epoxy resin and in a next step grinded as well as polished.

4.3.4 X-ray diffraction (XRD)

X-Ray diffraction measurements were carried out by Franz-Andreas Mautner from the Graz University of Technology. The X-ray characterization was done with a Bruker D8 Advance Pert, planar sample, Bragg-Brentano 6 – Experimental 114 geometry, Cu-Kα radiation. The samples were measured from 20 to 90 °2θ, step size 0.02 °2 θ, measuring time 20 s/step.

The Rietveld calculation was done by Brigitte Bitschnau from the Graz University of Technology using the software FULLPROF [238] as well as X'PertHighScorePlus by Panalytical. The starting geometries were obtained from the Inorganic Crystal Structure Database (ICSD), FIZ Karlsruhe [239].

4.3.5 Nuclear magnetic resonance spectroscopy (NMR)

Nuclear magnetic resonance spectra (^{1}H, ^{13}C) were recorded on a Bruker Avance III 300 MHz spectrometer. Deuterated solvents such as $CDCl_3$, CD_3OD were obtained from Cambridge Isotope Laboratories Inc. and remaining peaks as well as peaks originating from the solvents were referenced according to literature [240]. The following abbreviations were taken to indicate different peak shapes: s (singlet), d (doublet), t (triplet), q (quadruplet), m (multiplet), bs (broad singlet).

4.3.6 Infrared spectroscopy (IR)

For FT-IR spectroscopy a Bruker ALPHA FT-IR Spectrometer was used. The measurements were performed in ATR mode. The number of scans was set to 48 with a resolution of 1 cm^{-1}. The range of measurements was between 400 and 4000 cm^{-1}.

4.3.7 Contact angle

Measurement of the contact angle as well as the surface energy was performed with a Drop Shape Analysis System DSA100 (Krüss GmbH, Hamburg, Germany) with a T1E CCD video camera (25 fps) and the DSA1 v 1.90 software. The measurements were carried out using 3 µl droplets of Milli-Q water and diiodomethane as test liquids in the sessile drop modus at 25 °C. The dispense rate was adjusted to 400 µl/min and the time before the image was captured was 2 seconds. The contact angle calculations were performed using the Young-Laplace equation.

4.3.8 Stylus profilometry

To measure the film thickness of the silane coatings on the wire`s surface a DEKTAK 150 Stylus Profiler from Veeco was used. The scan length was set to 100 µm over the time duration of 3 seconds. The diamond stylus had a radius of 12.5 µm and the force was 3 mg with a resolution of 0.133 µm/sample and a measurement range of 6.5 µm. The profile was set to Hills and Valleys. A scratch in the silane layer was used to calculate the thickness of the coating.

4.3.9 Thermal gravimetric analysis (TGA)

Thermal gravimetric analysis was performed using a Netzsch 449C apparatus. As purge gas helium was used. Thermogravimetric losses were monitored in the range of 20°C to 550°C applying a heating rate of 10°C/min.

4.3.10 Atom absorption spectroscopy (AAS)

Atom absorption spectroscopy was performed with a contrAA 300 apparatus and an AS autosampler from Analytik Jena. The samples were acidified (mixture of concentrated HCl : H_2O_2-35% = 1:1) and after the addition of a Cs/La-buffer filled-up to 50 ml. Afterwards, these solutions were analyzed for the elements copper and zinc. Flame type: acetylene/air.

4.3.11 Vulcanization

The sulfur as well as the peroxide vulcanization was carried out on a KV141.1 vulcanization press of Bucks Maschinenbau GmbH (Germany). Unless otherwise specified, the vulcanization was performed at 160°C and 320 bar for 20 minutes with an embedment lengths of 10 mm. Cure rate data of the rubber compounds as the scorch time t_{05} were determined according to DIN 53529/3.

4.3.12 Pull-out testing

Pull-out testing was done on a Zwick/Roell Z2.5 universal testing machine. T-test specimens were prepared similar to ASTM D 1871. In order to evaluate the adhesion performance, the wires were pulled out from the T-test specimens at constant rate (=100 mm/min) with an applied preload of 50 N. Rubber coverage was assessed from 0 to 3 (0 = 0%, 1 = 1-49%, 2 = 50-99%, 3 = 100% rubber coverage). The adhesion was also determined after a thermal aging treatment (7 days at 70°C).

4.3.13 Rubber properties testing

Elongation at break and tensile strength were measured in compliance with DIN 53504 and tear strength was specified using the procedure described in ISO 34-2.

5 RESULTS

5.1 Comparison of brass-coated steel wires

Beside the composition of the rubber mixture as well as the vulcanization conditions also the properties of the brass-plated steel wires have a strong influence on the rubber-metal adhesion performance. Most likely, the wire characteristics vary in terms of Cu-content of the brass composition, brass film thickness, zinc oxide layer thickness, reminder of drawing additives and surface roughness [14,15]. Therefore, seven different wires – all having different adhesion performances – were investigated by different characterization methods. Using optical characterization methods such as optical microscopy and scanning electron microscopy a first impression of the wire surfaces was received whereas energy dispersive X-ray spectroscopy as well as X-ray diffraction was applied to determine the chemical composition of the wires. According to the wires` manufacturer, all wire samples are supposed to have the same specifications in terms of diameter (0.71 mm), brass-coating thickness, and Cu-content of the brass layer (67.5 wt%). However, incomprehensibly, each of these wires shows different adhesion properties. Therefore, the aim of this study was to find the reason for these different adhesion behaviors.

5.1.1 Comparison of optical and structural characteristics

In Figure 43 the optical microscopy and SEM images of the different brass-plated steel wires are shown. Both, the optical as well as the scanning electron microscopy images, respectively, do not differ significantly from each other. All wires feature drawing lines, which derive from the wires manufacturing process and which are the reason for an irregular brass-coating thickness. Further, all samples show some small scratches and defects. However, these are more or less homogeneously distributed over the surface of all samples. Thus, one can conclude that in visual and morphological terms the wires are very similar and no correlation between optical appearance and adhesion performance (compare Table I) is observable.

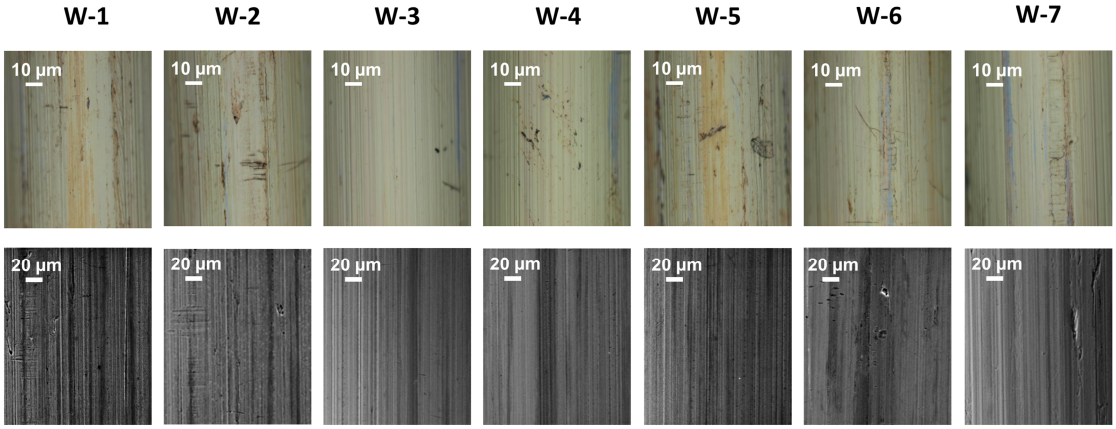

Figure 43 Optical microscopy (up) and SEM (below) images of the different wire samples.

5.1.2 Comparison elemental composition

Because of the very small differences in the optical appearance of the wire samples, the brass composition was investigated by EDX and XRD (Table I).

Table I Cu-content of the wire samples measured by EDX and XRD including the corresponding pull-out forces of the SBR compound.

	Cu-content of CuZn [wt%]		Pull-out force [N] (Adhesion to SBR)	Rubber coverage
	EDX 20 keV	*XRD*		
W-1	66 ± 1	67 ± 1	269 ± 81	2
W-2	62 ± 0	66 ± 1	210 ± 42	2
W-3	62 ± 1	65 ± 1	180 ± 18	1
W-4	67 ± 1	66 ±1	147 ± 37	1
W-5	66 ± 1	66 ± 1	143 ± 59	2
W-6	66 ± 1	69 ± 1	122 ± 15	1
W-7	66 ± 1	72 ± 0	74 ± 19	1

According to literature [15] the optimal copper content of the brass-plating has to be between 60 and 70 wt%, which is the case for each wire sample except W-7 (72±0 wt%) in the XRD measurements. Though, most of the Cu levels significantly deviate from the expected values of 67.5 wt% Cu. This variance stems from the fact, that the surface is not flat and therefore, the calculated concentrations are rather roughly approximated values than accurate results. However, all wires have the same diameter and are measured using the same set-up, for which reason the values can be qualitatively evaluated in comparison to each other to find a general trend. As one can clearly see, in most of the cases the results vary also significantly depending on the used measurement method. The EDX measurements are performed on a small area of the wire sample and due to the curved shape of the wire as well as the inhomogeneous brass-coating thickness (see Figure 44) the measured values using EDX are estimates and may not reflect the real copper content.

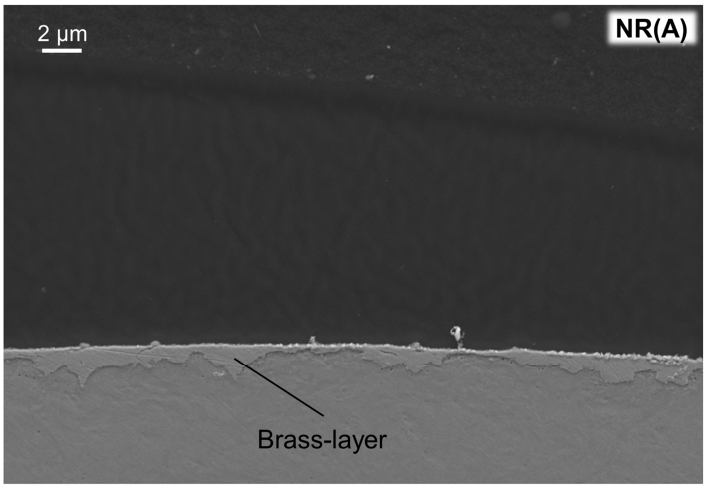

Figure 44 Cross section of a brass-plated steel wire after vulcanizing in a natural rubber compound (NR(A)) captured by SEM after grinding and polishing the wire (image was taken by FELMI-ZFE Graz).

In contrast, for the XRD measurements several small pieces of a particular wire were arranged next to each other and placed into the XRD chamber so that the X-ray beam is parallel to the wires. Thus, the wires are analyzed despite their curved surface and the obtained results are an average of several pieces of the same wire sample. Nevertheless, no correlation between the copper content of the brass-coating and the adhesion performance is observable, whether for the XRD values neither for the EDX one. Since W-7 is the worst adhering wire (Table I) one may assume that a Cu-content out of the optimum (60-70 wt%) has truly a bad impact on the adhesion performance. Also sample W-6 is with 69±1 wt% close to be out of this region and shows a rather poorly adhesion to rubber. Consequently it was confirmed that if the Cu-content of the brass layer is in the range between 60 and 70%, the adhesion performance is mostly satisfying to very good. Conversely, if the Cu level deviates from the optimal range this may be related to poor adhesion properties.

5.1.3 Correlation between XRD pattern and adhesion performance

The X-ray diffractograms are shown in Figure 45. In the XRD pattern mostly aluminium (Al, 38°), α-brass (α-CuZn, 42° and 49°) and iron (Fe, 45° and 65°) are detectable. Aluminium originates from the specimen mount and iron from the steel core of the wire. In the case of W-7, an additional weak reflection at 63° can be seen. This reflection can be assigned to β-brass (β-CuZn, 43°, 63°), in which the second reflection at 43° is hidden behind the α-brass reflection. For rubber reinforcing devices β-brass is absolutely undesirable [241]. This is associated with the fact that β-brass is quite brittle and consequently may detach easily from the wire surface. For this reason, only the worst adhering wire W-7 shows a β-brass phase.

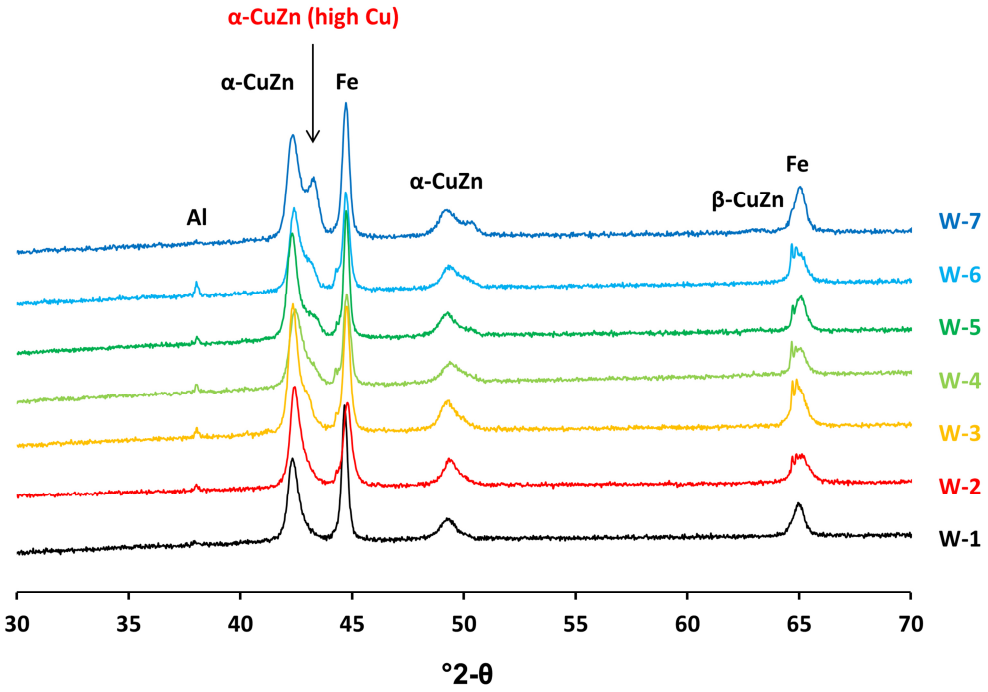

Figure 45 X-Ray diffraction patterns of W-1 to W-7.

Furthermore, with decreasing pull-out forces a second α-brass reflection is detectable. This peak corresponds to the Cu rich phase (43°) of α-brass. A high peak for the Cu rich phase indicates an incomplete mixing of the copper and zinc during the manufacturing process of the wire. To establish a correlation between the Cu rich phase (43°) of α-brass and the pull-out forces of the wires to SBR (composition see Table II), the reflections of the Cu rich peaks were quantified. With the help of the lattice parameters of these reflections (determined by a Rietveld calculation) the amount of Cu rich phase in α-brass was calculated and plotted against the corresponding pull-out forces, as

depicted in Figure 46. Thus, a trend is clearly observable, namely the adhesion performance increases with decreasing the amount of Cu rich phase in α-brass and thus with improving the homogeneity of the brass coating. W-5 deviates most from the regression line, but this wire sample generally showed fluctuating adhesion properties.

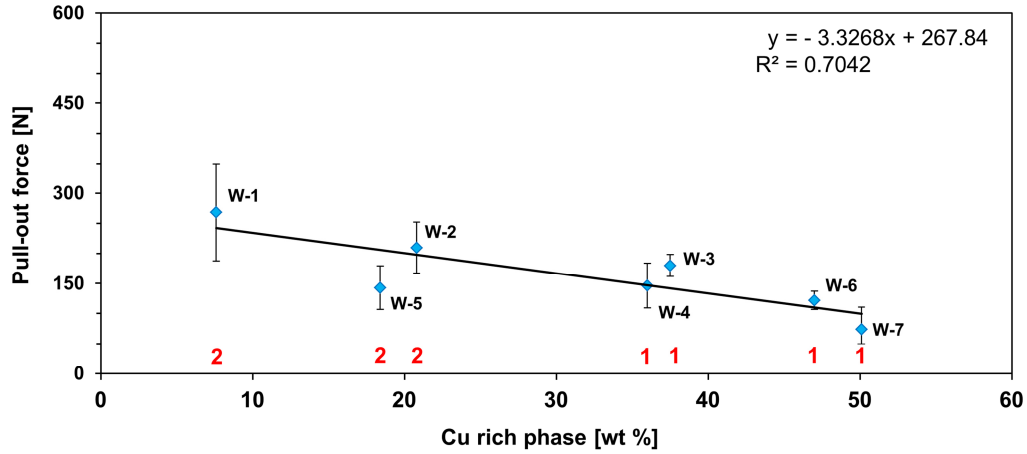

Figure 46 Percentage of the Cu rich phase in α-brass of the different wire samples against the corresponding pull-out forces measured between the wires and SBR. The numbers in red represent the rubber coverage after the pull-out tests.

The same trend was detected using NR(B-SiO_2) (composition see Table IV) as rubber compound for the pull-out force measurements (Figure 47). By using NR(B-SiO_2) the slope of the regression line is with -3.3 absolutely identical to the slop of the SBR mixture. Therefore, the amount of Cu rich phase in α-brass and thus the homogeneity can be seen as relevant wire property which has a high impact on the rubber-brass adhesion performance.

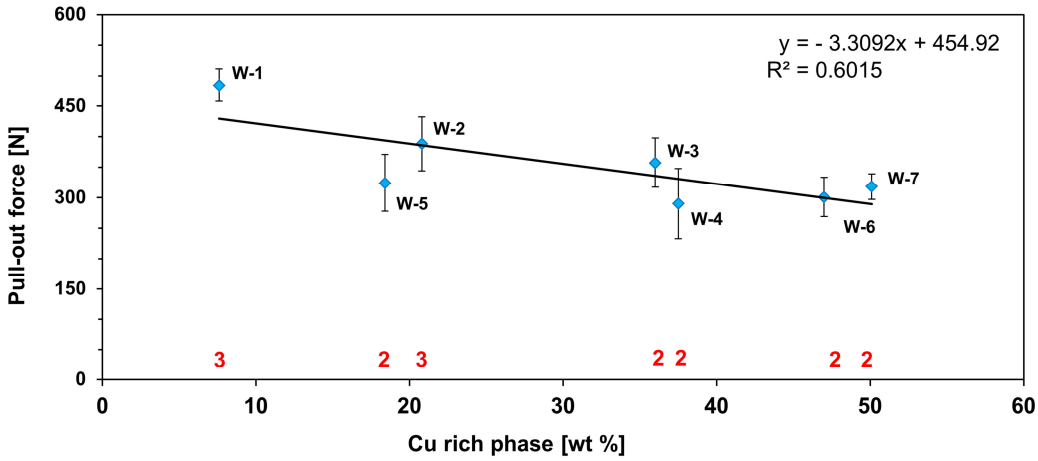

Figure 47 Percentage of the Cu rich phase in α-brass of the different wire samples against the corresponding pull-out forces measured between the wires and NR(B-SiO_2). The numbers in red represent the rubber coverage after the pull-out tests.

Now the question may arise, how does the Cu rich phase of the α-brass influence the rubber-brass adhesion performance? One possible explanation could be the Kirkendall effect [242]. To understand the influence of this effect on the adhesion performance one has to know initially how the wire samples are produced. As depicted in Figure 48, first of all a pure steel wire is coated with a layer of copper followed by a layer of zinc.

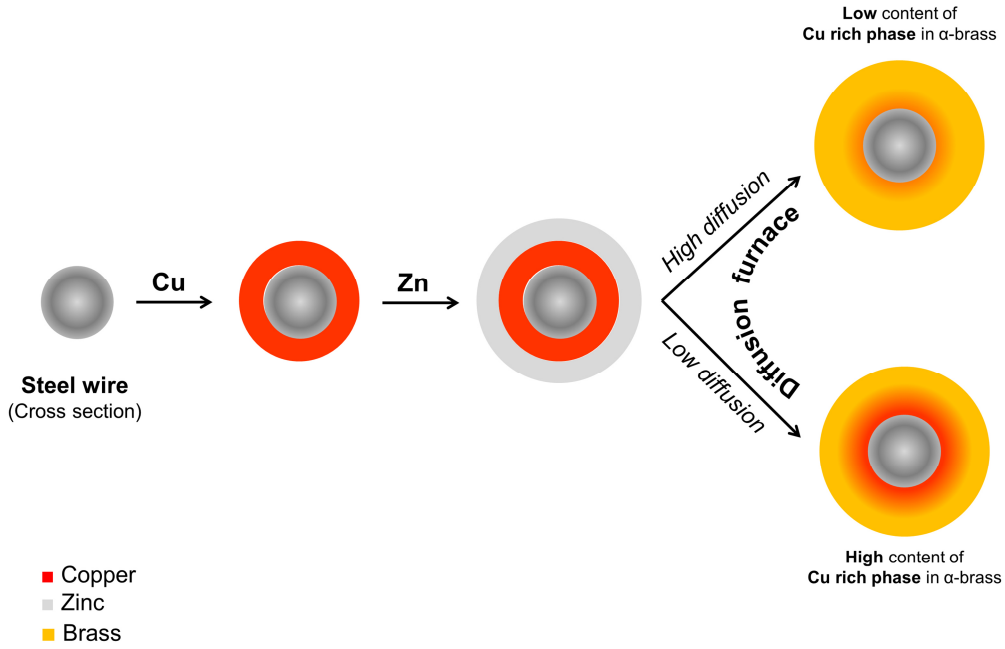

Figure 48 Scheme of the manufacturing process of the brass-plated steel wires.

Now, the wire is given into the diffusion furnace at elevated temperatures for a specific period of time. During this procedure the brass layer is formed by diffusion processes of the copper and zinc atoms. The Kirkendall effect states that by forming an alloy out of two metal species – in this case brass out of copper and zinc – the alloy grows in the direction of the faster moving species zinc. The reason for this effect is that all elements have different diffusion coefficients and consequently that zinc diffuses faster into copper as copper into zinc. This means for the brass-coating that zinc diffuses faster from the brass-phase into the copper-phase as copper into the brass-phase. As a consequence, inhomogeneous brass layers are formed unless the process parameters are optimally selected. Additionally, differences in the diffusion coefficients result in holes and vacancies in the brass-phase, so called Kirkendall voids and porosities. Since the formation of the adhesion layer is influenced by the composition of the entire brass layer, inhomogeneities and material defects may negatively influence the build-up of a well-defined rubber-brass adhesion interface by disturbing the diffusion of copper and

zinc ions as well as electrons to the brass surface (compare Chapter X). Hence, the wires with a high percentage of Cu rich phase in the α-brass were not heated for a sufficient period of time or at too low temperatures during the manufacturing process so that homogeneous brass layers could be produced.

5.1.4 Conclusion

Seven wire samples were analyzed in order to understand why they show different adhesion performances although they all have – according to their manufacturer – the same specifications. By watching the optical appearance of the wire surfaces no significant differences were observed. Therefore, the specimens were investigated regarding their elemental composition by EDX and XRD. Thus, no correlation between the brass composition and the pull-out forces was detected. However, it was shown that if the Cu level of the brass layer is over 70 wt% the adhesion fails. Additionally, it could be shown that the appearance of β-brass has a negative impact on the rubber-brass adhesion because it is rather brittle and consequently detaches easily from the wire surface. Further, on closer inspection, a Cu rich phase in α-brass was detected using XRD. Here, another dependence was observed, namely the adhesion performance increases with decreasing amount of the Cu rich phase in α-brass. This could be attributed to the Kirkendall effect, which says that the homogeneity of an alloy depends on the diffusion coefficients of the single components as well as on the process parameters. This means for the brass-coating, that zinc diffuses faster from the brass-phase into the copper-phase as copper into the brass-phase. As a consequence, the brass layer is inhomogeneously formed and may get so called Kirkendall voids. This inhomogeneous brass layer could be the reason for a faulty build-up of the rubber-brass adhesion interface since the formation of the Cu_xS-structures strongly depends on the diffusion behavior of the copper and zinc ions in the brass layer. Hence, the wires with high percentages of Cu rich phase in the brass layer were highly probable not heated for a sufficient period of time or at to low temperatures which leads in consequence to poor adhesion properties. Thus one can conclude that the wires may have on the first view the same specifications, but on a closer look they differ in the brass-phase-composition, which is very likely caused by ill-defined parameter control during the wires manufacturing process.

Based on these results, **W-1** was used for all further studies.

5.2 Investigation of the rubber-brass adhesion

This chapter was already published in:

Investigation of the Rubber-Brass Adhesion Layer Using the Olefin-Metathesis Method – S. Leimgruber, W. Kern, R. Hochenauer, M. Melmer, A. Holzner, G. Trimmel *Rubber Chemistry and Technology*, **2015**, 88, 219-233

5.2.1 Introduction

In many technical products made out of rubber, such as tires, hydraulic hoses, and handrails, brass-coated steel wires are incorporated to enhance their strength, dimensional stability, and persistence. To attain the highest standard of mechanical properties, an excellent and long-lasting adhesion between rubber and metal is required. This adhesion is accomplished by the formation of a rough interface, created during the sulfur vulcanization of the rubber [12,14,15,46,243]. According to the mechanism postulated by van Ooij in 1977, dendritic structures made out of nonstoichiometric copper sulfides (Cu_xS) and zinc sulfides (ZnS) are built up during the vulcanization [244]. Thus, adhesion is obtained by a mechanical interlocking of the rubber with the rough Cu_xS layer [243]. Covalent binding between brass and rubber is considered to be only a minor factor. The adhesion properties are influenced by various factors involving the rubber mixture [38,40,43,245-247] and the brass surface [21,248,249]. For good adhesion, the CuS layer must form in an optimal thickness. If the interface is too thin, no effective bonding occurs; if it is too thick, it gets brittle and may detach from the brass layer. In both cases, the adhesion strength would be rather low [4]. Hence the investigation of the influence of the compound ingredients on the adhesion layer is a key issue to control the adhesion in rubber products.

For a thorough investigation of the rubber–brass interface, a method is needed wherein the built-up interface can be uncovered without seriously damaging the adhesion layer. However, due to the generally strong adhesive strength of the rubber to the wire, it is difficult to uncover the adhesion interface.

There are several methods typically applied to investigate the adhesion interface. The easiest method is to analyze areas that are uncovered after the pull-out tests. However, in these parts of the interface the adhesion failed; consequently, only the poorly adhering areas can be characterized [250].

An improved method uses extreme coldness to expose the adhesion layer. In a first step, the rubber part is frozen using liquid nitrogen, and afterward it is removed with a sledge [251-254]. This approach has the advantage that the entire adhesion interface of real rubber products can be investigated. At the same time, however, it has to be considered that it is a very rough method wherein the adhesion interface can be easily destroyed [50]. Also the ‘‘solvent swelling method’’ is applicable on actual rubber products. Here the test sample is swollen in ortho-dichlorobenzene for a specific time and afterward is wiped off immediately [52]. During the wiping process, this procedure also leads to eventual mechanical damage of the adhesion interface and is consequently less appropriate for detailed investigations.

Another often-applied method is the so-called squalene method, wherein squalene is used as a low-molecular-weight analog of natural rubber [9,20,38,40,245,246,255-257]. This method has the advantage that it is a liquid and therefore can be easily removed after the reaction; thus, the brass layer can usually be directly investigated. However, it is a model system wherein not all aspects of a vulcanization reaction, for example, the applied pressure and the viscosity of the rubber compound and thus the diffusion coefficients of the reactant, can be simulated. The obtained results should be consideredwith care and not be overinterpreted.Another method is the so-called filter paper method. This method has been widely used to study rubber–brass adhesion [8,52,258-260].

The filter paper method uses a real rubber compound, but a filter paper is inserted in between the rubber and the wires before the vulcanization. The filter paper enables the active sulfidizing species (e.g., sulfur, accelerator, activator) to get through, whereas other components, such as rubber molecules and carbon black, are retained [15]. After the vulcanization process, the wire can be easily separated from the rubber and can be subjected to further analysis. However, the diffusion processes are significantly changed, and the filter paper may react with aggressive compound additives.

The ‘‘metathesis method’’ discussed herein is a relatively new approach to investigate the rubber–brass adhesion interface [261]. The olefin-metathesis reaction has been applied to study other aspects of rubber products. For example, it has been used to study nitrile–butadiene copolymers [204], to determine fillers in natural rubber [217], to investigate polymer structures [211], and to address similar analytical questions

[224,262-264]. Initially, WCl_6 catalyst systems were mostly used for the metathesis reactions, whereas in recent years ruthenium-based catalysts have increased in popularity due to their lower sensibility to moisture and air.
During the metathesis reaction, the metal catalyst attacks the double bonds and cleaves the cross-linked rubber molecules into small soluble fragments via the olefin-metathesis reaction.

Thus, the metathesis method has the advantage that a real rubber system can be directly investigated. In principle, samples from ‘‘real’’ rubber products, such as tires or handrails, can be analyzed as well. For these reasons, the olefin-metathesis method is a very promising method for future studies of the rubber–brass adhesion mechanism.

Our first studies were limited to natural rubber (NR) [261]. Herein, we elaborate the potentials and limitations of this method by using NR, styrene–butadiene rubber (SBR), and acrylonitrile–butadiene rubber (NBR). For NBR, an interaction of the nitrile groups of the NBR with the metal center might hinder or change the degradation. Experimentally, brass-plated steel wires were incorporated into the different rubber mixtures. After vulcanization, the rubber was degraded by the metathesis reaction using Grubbs catalyst 2^{nd} generation. The characterization of the adhesion layers was done by optical microscopy, focusvariation microscopy, and scanning electron microscopy (SEM) coupled with energy dispersive X-ray (EDX) analysis. Adhesion force was measured by pull-out testing of the t-test specimens.

5.2.2 Olefin-metathesis of natural rubber (NR) with and without 1-octene

First, for the optimisation of the metathesis reaction, the olefin-metathesis is performed with and without 1-octene on samples of the NR(A) compound (Table II).

Table II Mixture compositions of the different rubber types for the olefin-metathesis experiments in phr.

	NR(A)	NBR	SBR
NR	100	-	-
NBR	-	100	-
SBR	-	-	100
Carbon black	70	70	70
ZnO	4.74	4.74	4.74
Stearic acid	1.05	1.05	1.05
Sulfur	3	3	3
CBS	1.84	1.84	1.84
Paraffinic oil	9	-	9
DOA	-	9	-

After the degradation, the revealed brass surfaces are compared to the original wire surface, as shown in Figure 49. The optical microscopy pictures as well as the focusvariation microscopy images have a gray-beige color for the untreated wire (first row) but appear blue and yellowish for the samples after the vulcanization and metathesis degradation (rows B and C). In addition, black spots are detected especially on the sample degraded without 1-octene. The SEM picture of the blank wire shows a very smooth surface without any specific structures except drawing lines. The surface of the adhesion layer after the metathesis reaction without 1-octene (middle row of Figure 49) shows a high surface coverage with organic residues – rubber and carbon black – preventing the investigation of the underlying adhesion layer. In contrast to this, adding 1-octene to the metathesis reaction leads to an almost complete removal of the organics and the adhesion layer is now uncovered. The brass surface is rougher than the original wire with a quite homogeneous microstructure. It has to be noted, that also in this case, it might be necessary to repeat the metathesis reaction a few times to achieve a complete removal of the carbon residues.

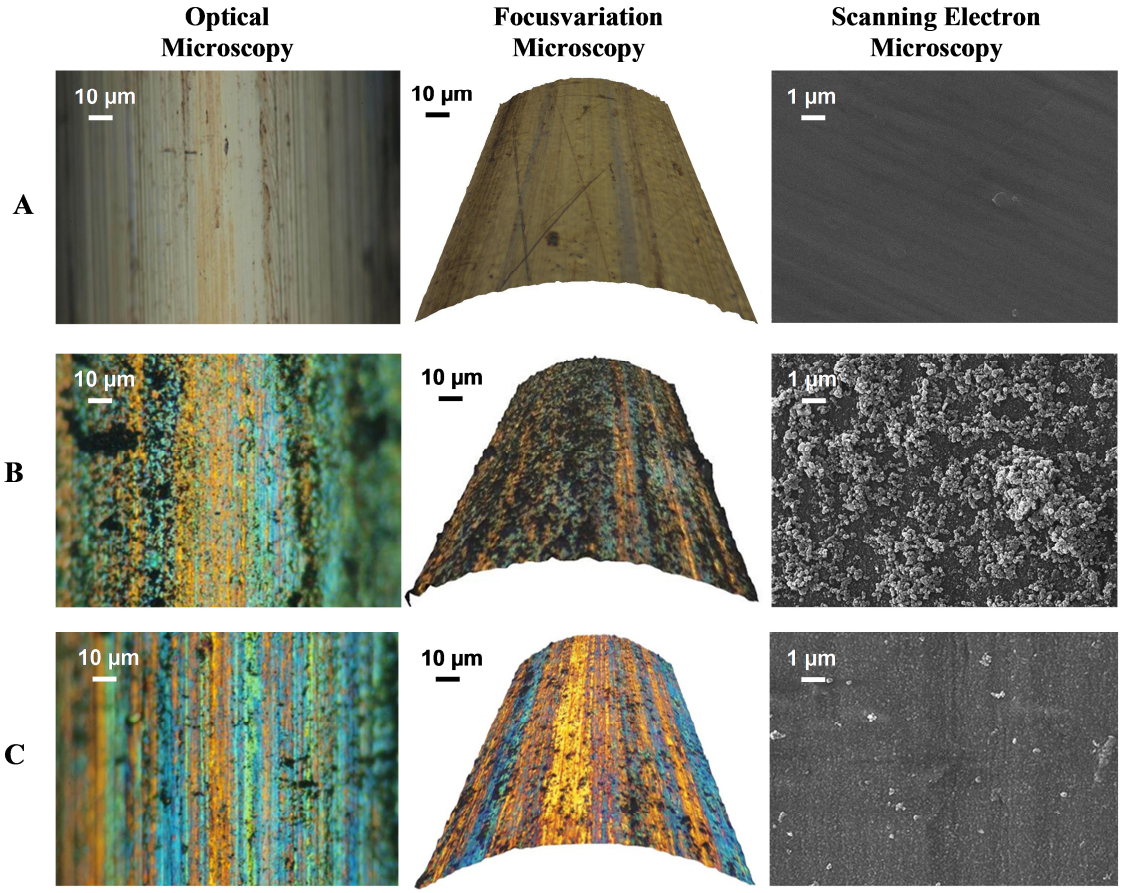

Figure 49 Optical microscopy images (left) focus variation microscopy pictures (middle) and SEM pictures (right) of an untreated wire surface (A) and wires uncovered from natural rubber (NR(A)) by metathesis degradation without (B) and with (C) 1-octene.

Figure 50 shows the results of the corresponding EDX measurements. For the pristine brass-coated steel wire the highest element concentrations were detected for copper, zinc, and iron. The iron as well as the small amounts of carbon and oxygen originate from the steel wire. Copper forms together with zinc the brass layer. For a better comparison all values were normalized to copper and the copper value was set to 100 atom%. After the vulcanization process sulfur is clearly detectable which is due to the formation of Cu_xS-dendrites. In the sample where the metathesis is performed without 1-octene the carbon peak is much higher than for the sample where 1-octene is used for the metathesis (at similar percentages of the other elements). The higher carbon level derives from the increased rubber residues.

Thus, the metathesis reaction is drastically improved by 1-octene but also accelerated as the overall degradation time is reduced by approximately 50 to 70%.

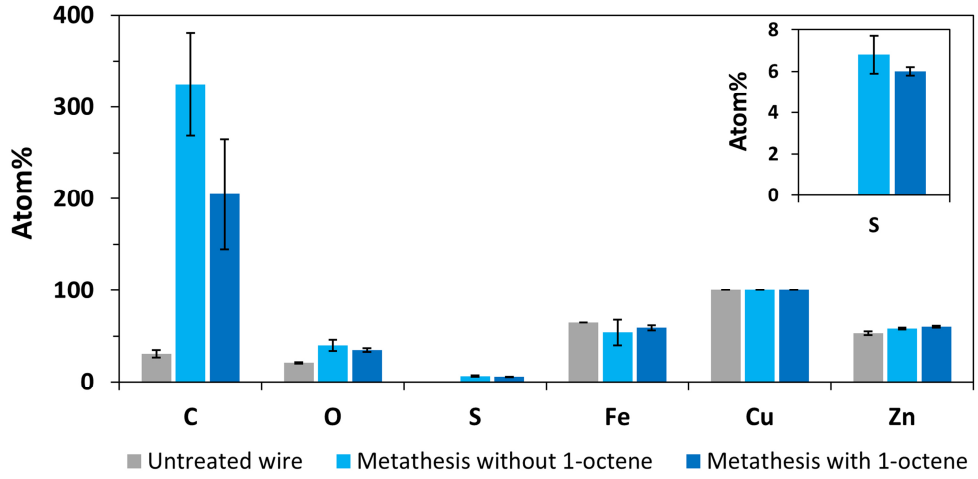

Figure 50 EDX values of untreated wire (gray) and wires after sulfur vulcanization followed by metathesis degradation without (light blue) and with (dark blue) 1-octene. All values relative to Cu (=100 atom%), *20keV*.

The reason for this higher reactivity and faster degradation of rubber in the presensence of 1-octene probably comes from the fact, that the cross-linked rubber network is not easyly accessible due to steric as well as diffusion effects. As illustrated in Figure 51, at the beginning of the metathesis reaction the metathesis catalyst react with the double bonds of the cross-linked rubber. Thereupon the carbon-carbon bond of the polymer is cleaved due to the rearrangement of the double bonds (cross metathesis). In doing so, the metal center remains bound to the rubber, a rubber particle or a rubber polymer. However in this stages, it is hardly available for the olefin-metathesis because of its steric hindrance as the next double bond has to be coordinated. 1-Octene is able to diffuse easily to the steric hindered metal center and can react according to the cross metathesis. Now, the catalyst has “recycled” and can continue with the olefin-metathesis-degradation of the rubber network.

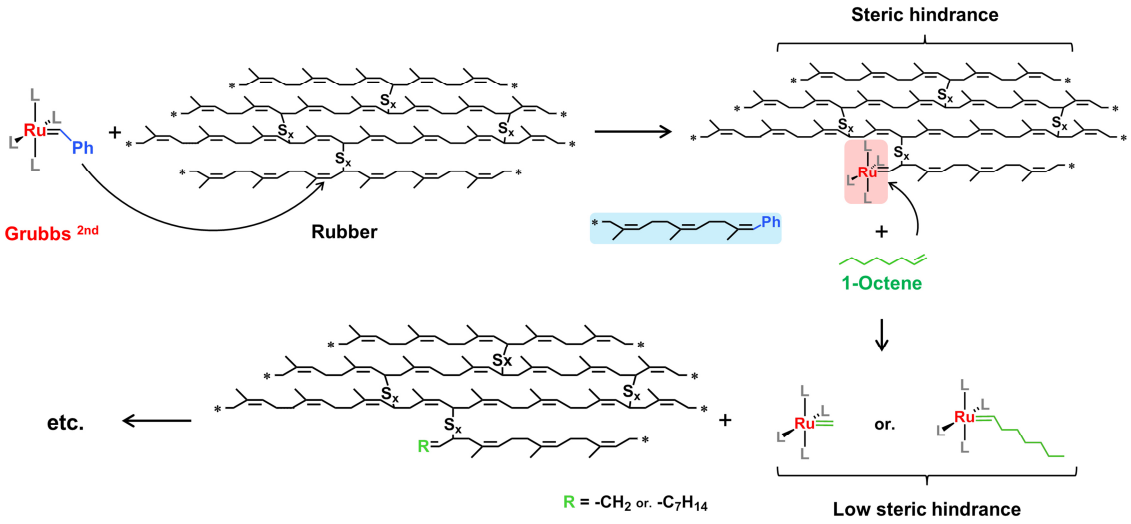

Figure 51 Influence of 1-octene on the olefin-metathesis.

It can be concluded, that the adhesion layer of brass-rubber systems can be revealed by the olefin-metathesis reaction and subsequently investigated by common surface analysis methods. It has been shown that 1-octene drastically decreases the reaction time of the olefin-metathesis by acting as co-reagent [211,265]. In addition, also less accessible double bonds of the rubber network can react leading to a more uncovered brass surface.

5.2.3 Control experiments

In order to preclude influences of the metathesis reaction on the adhesion interface, two control experiments were carried out. First, the influence of the metathesis reagents on the bare brass surface was investigated. Therefore, an untreated brass-coated steel wire was exposed to a toluene solution containing the same amounts of Grubbs catalyst, 2nd generation, and 1-octene as in the metathesis experiments using the same reaction conditions. As shown in Figure 52, the microstructure of the brass layer remains unchanged. Both, the optical microscopy images as well as the scanning electron microscopy pictures, show a smooth surface with some drawing lines which derive from the manufacturing process of the wire.

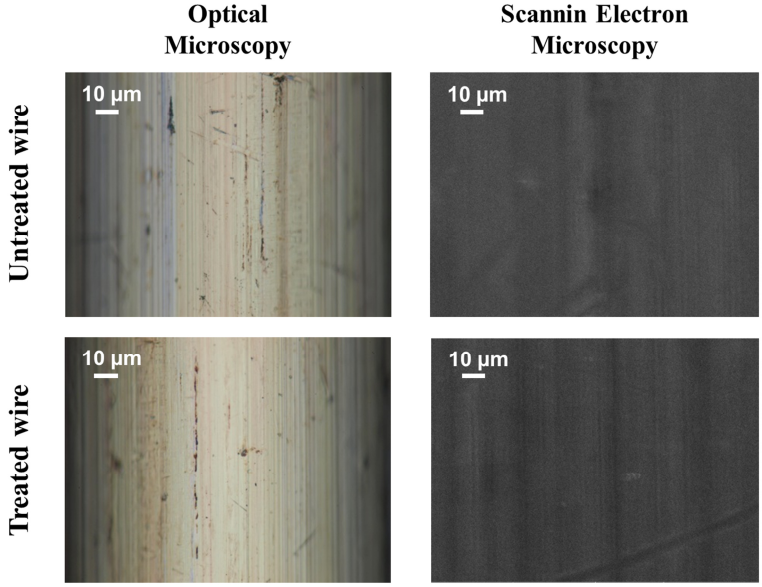

Figure 52 Optical microscopy pictures (left) and SEM pictures (right) of an untreated wire surface and its surface after treating in a toluene solution containing Grubbs catalyst 2nd generation and 1-octene.

In a second control experiment, the influence of the metathesis reaction on the metal-sulfide structures of the adhesion layers was studied. For this experiment, we used a wire after the pull-out test with a negligible coverage but with significant surface structures. This wire was also treated the same way, putting it into a solution of toluene, Grubbs catalyst 2nd generation and 1-octene. A comparison of the SEM images is presented in Figure 53. Both the surfaces structures as well as the EDX values are almost identically.

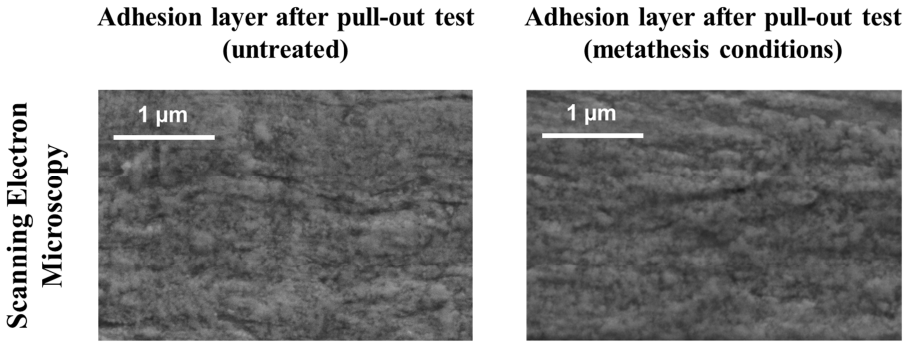

Figure 53 SEM pictures of an untreated adhesion layer after the pull-out test (*EDX* C:194, O:17, S:12, Fe:50, Zn:68, Cu:100) and its surface after treating in a toluene solution containing Grubbs catalyst 2nd generation and 1-octene (*EDX* C:196, O:18, S:12, Fe:51, Zn:69, Cu:100). The images were taken by FELMI-ZFE Graz.

It may therefore be assumed that the olefin-metathesis degradation of the rubber network does not influence the adhesion interface, both the bare brass surface and the metal sulfide structure are unchanged.

5.2.4 Rubber-brass adhesion layer of different rubber types

In the next part, we explore the possiblities to use the metathesis method also on other rubber systems than NR (Table II). Thus, rubber compounds from SBR and NBR were degraded by olefin-metathesis and the adhesion layers are compared with the results obtained on NR samples. First the pull-out forces, the coverage of the wire surface as well as the necessary reaction time for the olefin-metathesis are summarized in Table III.

Table III Pull-out forces of the T-tests and rubber coverage of the brass-coated steel wires after the T-tests; required reaction time for the olefin-metathesis (with 1-octene) to uncover the adhesion layers.

	Pull-out force, N	Coverage	Reaction time, h
NR(A)	159 ± 38	1	6
NBR	23 ± 6	0	4
SBR	233 ± 30	1	1

Regarding the pull-out forces, it is obvious that SBR and NR(A) show relatively good adhesion properties with pull-out forces of 233 N and 159 N, respectively, whereas NBR has (without furhter adhesion promoters) only a very low pull-out force of 23 N. However, the rubber-brass adhesion does not only depend on the adhesion interface but also on the physical properties of the rubber. In the case of sample NR(A) and SBR a coverage of 1 was observed, meaning a rubber coverage on the wire of less than 50% after the T-test. It can be concluded, that the adhesion values obtained were partly affected by the rubber properties as the adhesive strength exceeded the cohesive strength of the rubber on 1-49% of the adhesion interface. The NBR sample has a coverage of 0. This means that the adhesion completely failed. Therefore the pull-out force can be seen as real adhesion value.

Now, the question may arise why NBR shows no adhesion to the brass coated steel wire. Thus all three samples are subjected to the metathesis reaction. First, it is interesting to note that the time to uncover the adhesion layer via the olefin-metathesis varies depending on the type of rubber, namely 6 hours for NR(A), 4 hours for NBR and only 1 hour for SBR. In the case of NR(A), the reason is caused by the steric hindrance at the double bond. It is generally known that quaternary carbon atoms in double bonds deteriorate the attachment of Ru-based catalysts. The reaction time for the NBR sample was significantly faster as that one of NR(A). The reason for this is that

the double bonds of the butadiene unit are sterically less demanding and thus can react faster. However, the nitrile-groups are able to coordinate to the Ruthenium center of the catalyst and block the reactive center decelerating the olefin-metathesis. Conversely, the adhesion interface of the styrene butadiene rubber was uncovered in 1 hour. This is on the one hand due to the accessibility of the butadien unit and on the other hand the styrene group does not coordinate to the metal center and consequently does not interfere with the metathesis reaction.

All three samples are investigated by optical, focusvariation and scanning electron microscopy as can be seen in Figure 54.

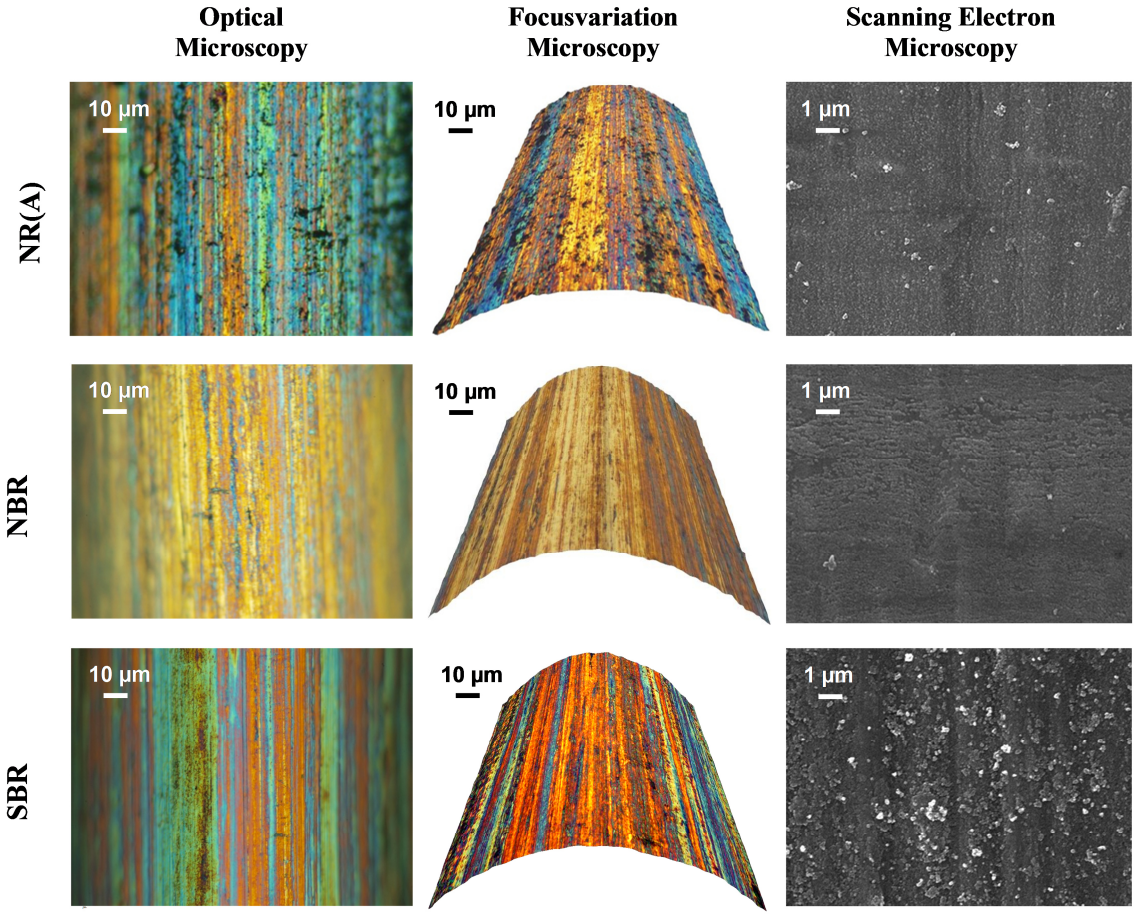

Figure 54 Optical microscopy pictures (left) focusvariation microscopy pictures (middle) and SEM pictures (right) of the NR(A), NBR and SBR adhesion layer after olefin-metathesis with 1-octene.

The color of the optical microscopy and focusvariation microscopy pictures changes depending on the rubber type. Sample NR(A) has an orange-blueish color, sample NBR is colored gold-yellowish and sample SBR shows a orange-greenish interface. These differences might be related to different degrees of sulfurization as shown by E. Ziegler

et al [261] in squalene experiments. Accordingly, the adhesion layer of the NBR sample contains lower amounts of sulfur compared to samples NR(A) and SBR. This correlates with the EDX data shown in Figure 55. The NBR sample has a relatively low sulfur value of 3 atom% compared to sample NR(A) and SBR with 6 and 7 atom%, respectively. However, it should be noted, that the EDX values are giving only a qualitative trend and not absolute values due the uncertainties of the EDX analysis – especially on curved surfaces. One can further see that variations in color occur along the wire caused by differences in sulfidation. The origin of this effect is due to the drawing lines and thus varying thicknesses of the brass layer. But not only the color of the wire surfaces differ but also the surface microstructures. As discussed in the previous chapter, the SEM image of sample NR(A) shows well defined small structures which correspond to the Cu_xS-dendrites. In contrast the NBR sample depicts no regular pattern but a smooth adhesion layer with undefined flakes. Here, from the EDX results it is indicated that also copper sulfide is formed but in lower amounts. The typical rough surface structures can not be observed and therefore its absence is – in accordance with the above discussed mechanism of the rubber-brass bonding – the reason for the weak adhesion strength. In the SEM picture of the SBR sample, however, these structures of different sizes are observed, again. These microstructures appear not as periodically as those of the NR(A) sample. However, their average size is bigger and the surface is somehow rougher than on the NR sample. Also the EDX data correlate well with the microstructures of the SEM pictures. The more distinctive the Cu_xS-structures, the higher the sulfur content of the rubber-brass adhesion layer.

Finally, the EDX analysis show that the NR(A) and SBR samples have still a significant amount of carbon at the surface, whereas the NBR sample has approximately the same amount of carbon as the untreated steel wire (compare Figure 50). If the adhesion layer is very strong the accessibility of the surface-near region of the rubber for the ruthenium catalyst might be reduced and/or a good interface might trap organic residues (polymer fragments and carbon black) within the CuxS-structures. However, a differentiation of these two effects was not possible.

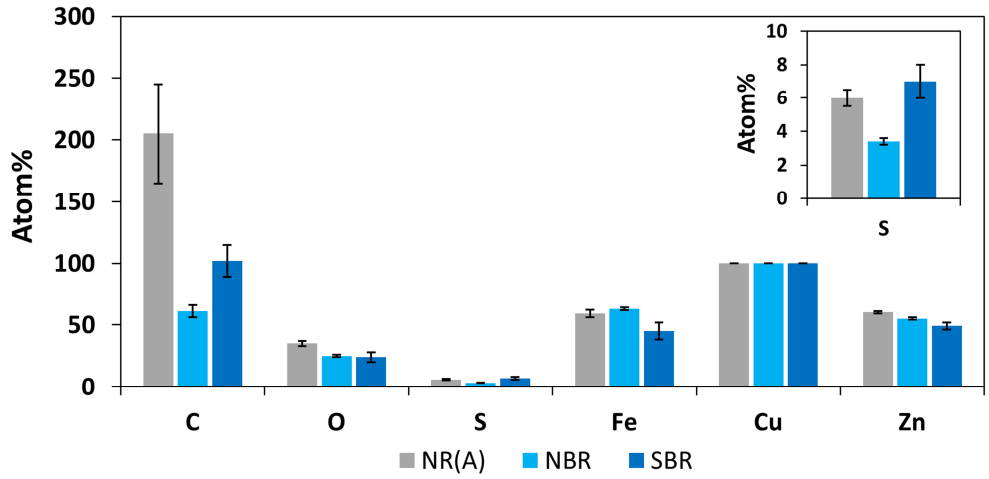

Figure 55 EDX values of the NR(A) (gray), NBR (light blue) and SBR (dark blue) adhesion layer after olefin-metathesis with 1-octene. All values relative to Cu (=100 atom%), *20keV*.

Why shows the NBR no adhesion to the brass coated steel wire? It is well known that nitrile-groups adsorb on copper surfaces in two ways: either by σ-bonding via the free electron pair of the nitrogen atom or by π-bonding via the π-system of the nitrile-group. Thereby the nitrile-groups of the NBR probably adsorb on the brass surface and thus prevent the sulfur to react with the brass. In doing so the adhesion interface is insufficiently sulfurized which leads to incomplete build-up of Cu_xS-structures and consequently the adhesion fails.

In conclusion one can say that the olefin-metathesis method is well applicable to different rubber types. Investigations of the various adhesion layers show clear optical as well as structural differences and are in agreement with the corresponding elemental composition measurements. Due to steric and blocking effects of some rubber-types the olefin-metathesis degradation time varies considerably.

5.2.5 Rubber-brass adhesion layers of NR mixtures with different additives

However, not only the difference in the polymer structure may influence the metathesis reaction, also typical additives and fillers used in rubber chemistry can influence the olefin-metathesis. Thus in a second series we compare NR-compounds with different additives (Table IV).

Table IV NR mixture compositions in phr.

	NR(B)	NR(B-Co)	NR(B-SiO_2)	NR(B-resin)
NR	100	100	100	100
Carbon black	50	50	50	50
ZnO	7	7	7	7
Stearic acid	1	1	1	1
Sulfur	6.25	6.25	6.25	6.25
DCBS	0.7	0.7	0.7	0.7
Naphthenic oil	6	6	6	6
Co-Stearate	-	2	-	-
Silica	-	-	50	-
Cellobond	-	-	-	5

NR(B) is comparable with NR(A) but with DCBS and a higher content of sulfur. The other 3 samples contain only one additional component, NR(B-Co) 2 phr Co-stearate as co-adhesion promoter, NR(B-SiO_2) 50 phr of silica, NR(B-resin) 5 phr of Cellobond – a phenol-formaldehyde-resin in combination with hexamethylenetetramine – as adhesion resin. In this context, on one side chemicals changing the adhesion layer (Co-stearate, resins) may change the accessibility of the rubber-network close or at the interface and thus influence the metathesis reaction. On the other side, the high surface area as well as the reactive Si-OH bond also might interact and deactivate the Ruthenium catalyst.

First, the reaction times for the metathesis degradation as well as the pull-out forces for these four samples are summarized in Table V. The pull-out force of the sample NR(B) is with a value of 168 N in the same range and exhibit the same low coverage below 49% than as the before discussed sample NR(A). All other samples show a large increase of the adhesion strength. For the sample NR(B-SiO_2) a pull out force of 369 N by the same coverage (1) is observed. However, by sample NR(B-Co) and NR(B-resin) extremely high values of 505 N and 596 N at full coverage (3) are found. This means that in these two cases, the cohesive strength of the rubber is less than the adhesive

strength between rubber and brass, with other words, the rubber breaks and not the interface. On all samples, the rubber was degraded by olefin-metathesis. All four samples show similar reaction times of 6 h, thus these additives seem to have no negative influence on the reaction mechanism.

Table V NR-samples with different additives: Pull-out forces of the T-tests, rubber coverage of the brass-coated steel wires after the T-tests; required reaction time for the olefin-metathesis to uncover the adhesion layers.

	Pull-out force, N	Coverage	Reaction time, h
NR(B)	168 ± 34	1	6
NR(B-Co)	505 ± 39	3	6
NR(B-SiO_2)	369 ± 49	1	6
NR(B-resin)	596 ± 44	3	6

The adhesion layer was again investigated by optical, focusvariation and scanning electron microscopy, as depicted in Figure 56. The corresponding EDX analysis is summarized in Figure 57. Again, the optical and focusvariaton micrographs are significantly different for all samples. Sample NR(B) has a more blueish appearance as the above discussed sample NR(A) due to its different recipe and the microstructures observed by SEM also show besides small Cu_xS-dendrites also flake-like structures. Both samples NR(B-Co) and NR(B-SiO_2) are colored orange-greenish, whereby NR(B-SiO_2) features more drawing lines. It is noticeable that NR(B-resin) shows a very homogeneous green appearing surface. Also the drawing lines are less visible. Comparing the SEM pictures of these NR samples with different additives, one can see that all sample differ in their microstructures. However, all interfaces show a structured and partially well-defined surface morphology typically observed in such adhesion layers. Also the EDX-values for sulfur between 6 to 8% are pointing towards Cu_xS-structures, cf. Figure 57. However, how can the large difference in pull-out forces be explained comparing the microstructures. Especially, as in the samples NR(B-Co) with a value of approx. 500 N and NR(B-resin) with a value of approx. 600 N the adhesion layer did not fail, but the rupture happened in the rubber phase (full coverage of the wire surface after the pull-out test in both cases). From the SEM images, these two samples have several agglomerates and some large surface structures in range up to µm but the underlying surface topography with structures between 100 and 200 nm are homogenous over the whole surface. These two samples have also the highest sulfur

levels in the EDX analysis. Together with the fact that the structures of the drawing lines appear weaker than in the other two samples, it seems that the most homogenous and thickest Cu_xS layer is formed and partially overgrows the drawing lines. This is also what would be expected from literature. For NR(B-Co), cobalt ions are incorporated into the adhesion interface where they change the relative diffusion rates of zinc and copper ions [15]. As reported by Fulton *et al* [266] as well as Chandra *et al* [17] cobalt ions are incorporated into the ZnO layer (~40 nm thick layer of ZnO onto the brass coating) during the vulcanization reaction but before the sulfidation of the brass layer get started. Cobalt ions reduce the diffusion rate of Zn^{2+} ions. Consequently, the formation of ZnS at the surface is reduced and Cu_xS formation increased. Since the adhesion strength increases with higher amounts of copper sulfide cobalt ions improve the rubber-brass adhesion properties. Cobalt salts are also very popular because they influence the durability of the adhesion [15]. In the course of the ageing process, the adhesion interface continues to grow, becomes brittle and will therefore break more easily. Through the addition of cobalt salts this process is slowed down [48] and as a result less dendritic structures are build-up. This lower crystallinity and thus less brittleness (predominantly amorphous character) might be responsible for the high pull-out force. Similar effects might also be the reason for sample NR(B-resin) as similar structures are observed. For sample NR(B-SiO_2) the SEM images show that the structures are relatively small and inhomogeneously distributed. Generally, silica is a frequently used filler in rubber compounds. With increasing silica content of the mixture the adhesion strength increases [41,42], which holds also true for this series, as the pull-out force is higher than for NR(B). However, as described by Waddell *et al* [43] and illustrated in Figure 57, silica in the rubber compound decreases the total amount of sulfur in the adhesion interface. This mediating effect of silica results in a thinner copper sulfide layer which might be the reason, why the adhesion strength is lower than in the samples NR(B-Co) and NR(B-resin).

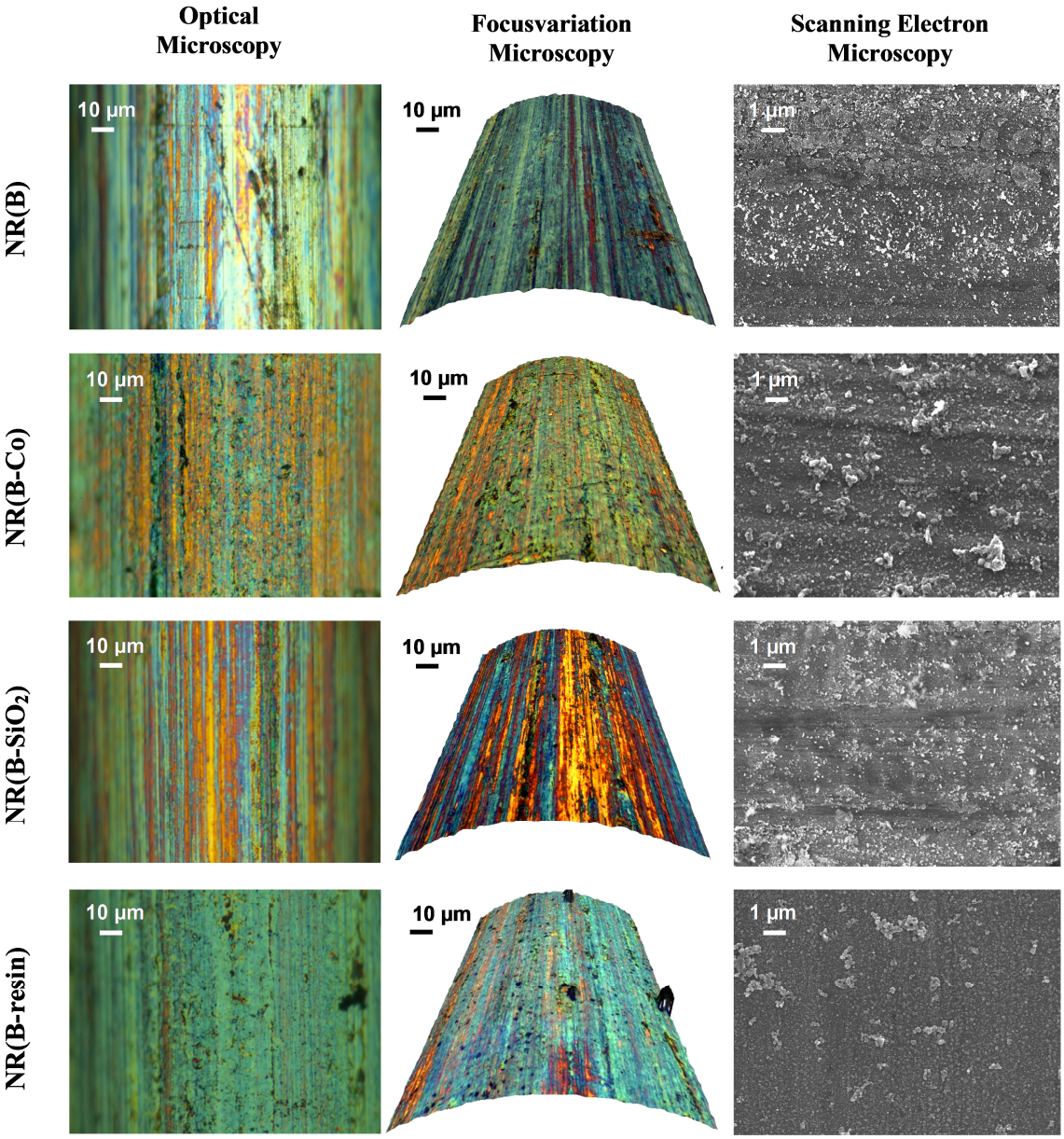

Figure 56 Optical microscopy pictures (left) focusvariation microscopy pictures (middle) and SEM pictures (right) of the NR(B) (A), NR with Co-stearate (B), NR with silica (C) and NR with resins (D) adhesion layer after olefin-metathesis with 1-octene.

However, these interpretations are first indications. For a more detailed analysis, more detailed SEM-analysis as well as XPS or TOF-SIMS are necessary to analyze the differences in surface structure more precisely. Furthermore, the addition of auxiliaries to a rubber system not only affects the adhesion interface but also the rubbers physical and rheological properties [48,54]. These properties in turn influence the adhesion performance. Therefore, for a comprehensive and detailed analysis of the adhesion influencing factors these characteristics have to be considered.

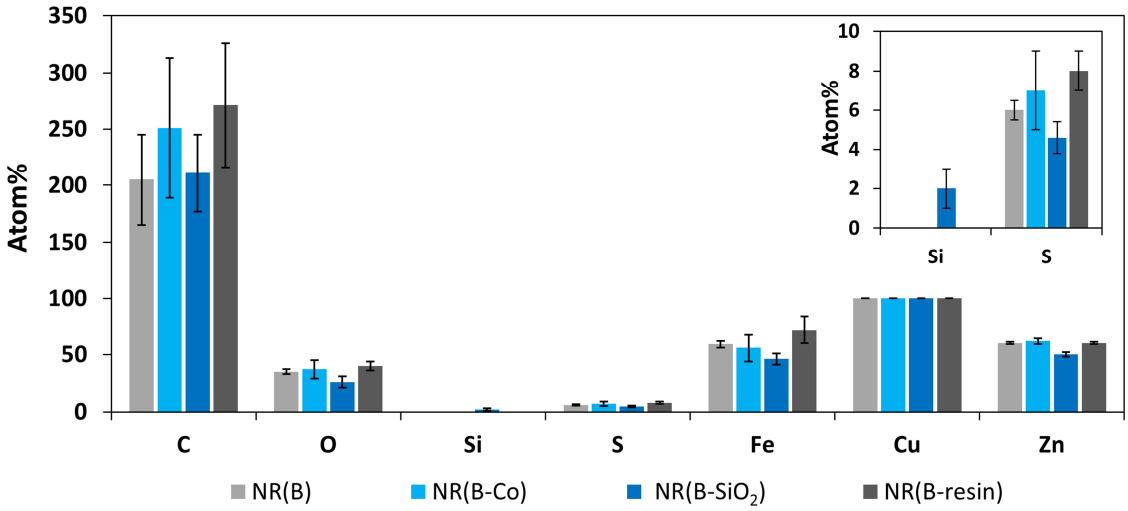

Figure 57 EDX values of a NR(B) (gray), NR with Co-stearate (light blue), NR with silica (dark blue) and NR with resins (purple) adhesion layers after olefin-metathesis with 1-octene. All values relative to Cu (=100 atom%), *20keV*.

Overall, regarding the subject of these investigations it can be concluded that the quality and velocity of the olefin-metathesis is not influenced by investigated fillers and adhesion promoters.

5.2.6 Conclusion

The olefin-metathesis is a versatile method to uncover metal-elastomer adhesion layers. This procedure is applicable to all rubber systems with double bonds in the main chain. It is a very gentle procedure at which no structures are mechanically destroyed. It was shown that the reaction of sulfur with the brass layer leads mostly to the build-up of a well-defined and structured adhesion interface. These microstructures can be perfectly investigated by most common surface analysis methods after the olefin-metathesis. It has been demonstrated that 1-octene improves the quality of the rubber degradation while drastically reducing the reaction time of the olefin-metathesis.

The olefin-metathesis method can be applied to different rubber types. Due to steric and blocking effects of various functional groups on the rubber macromolecules the olefin-metathesis degradation time varies considerably. Furthermore, commonly applied fillers, adhesion promoters or other auxiliaries do not interfere with this method. However, it should be mentioned, that some special additives or reactive fillers interacting with the metal catalyst may decelerate or even prevent the degradation. Thus, it was possible to show that the olefin-metathesis method can be widely applied for the investigation of the rubber-brass adhesion. As a next step investigations will focus on the application of this method to investigate rubber-brass interfaces of real rubber products.

5.3 Investigation of the nitrile rubber (NBR)-brass adhesion

In Chapter 5.2.4 the rubber-brass adhesion layer of different rubber types was investigated using the olefin-metathesis method. Thus it was observed that compared to the adhesion layers of NR and SBR the interface of NBR shows no Cu_xS-structures, which are usually build-up during the vulcanization reaction and which are mainly responsible for the rubber-to-brass adhesion. Also the sulfur content of only 1-3 atom% compared to commonly amounts of 6 to 7 atom% for well-adherent interfaces is unusual. These anomalies may also be responsible for the very low pull-out force of 23 N of the NBR sample. However, adding silica (SiO_2) to the NBR compound Cu_xS-structures can be found on the adhesion interface and the adhesion strength increases with increasing silica content in the rubber mixture. Thus, pull-out forces up to 334 N can be reached. As a consequence of these observations the question was opened what happens to the interface of the NBR sample during the sulfur vulcanization compared to NR and SBR?

In order to investigate the NBR adhesion interface in detail conventional analytical methods as e.g. optical microscopy and SEM-EDX were used. Beside this, NBR model systems were established so that further information about the NBR-to-brass adhesion could be obtained. The model systems are based on low molecular nitrile compounds, which are coated on the wire samples prior of moulding in NR compounds to simulate the nitrile groups of the nitrile butadiene rubber.

5.3.1 Influence of NBR content in NR-NBR blends

In a first step, the influence of the amount of nitrile groups in a rubber mixtures was investigated. Therefore, NR compounds containing different portions of NBR (0-100 phr) were prepared according to Table VI. In these elastomer mixtures all components were kept constant except the amount of the two rubber types as well as the composition of the plasticizer (paraffinic oil, DOA/MILLAN).

Table VI Composition of the different NR-NBR blends in phr.

	NBR-0	NBR-20	NBR-40	NBR-60	NBR-80	NBR-100
***NR** (CV 50)*	100	80	60	40	20	-
***NBR** (KRYANAC 2645)*	-	20	40	60	80	100
Carbon black	70	70	70	70	70	70
ZnO	4.74	4.74	4.74	4.74	4.74	4.74
Stearic acid	1.05	1.05	1.05	1.05	1.05	1.05
Sulfur	3	3	3	3	3	3
CBS	1.84	1.84	1.84	1.84	1.84	1,84
Paraffinic oil	9	7,2	5,4	3,6	1,8	-
DOA/MILLAN	-	1.8	3.6	5.4	7.2	9

up of the adhesion interface.

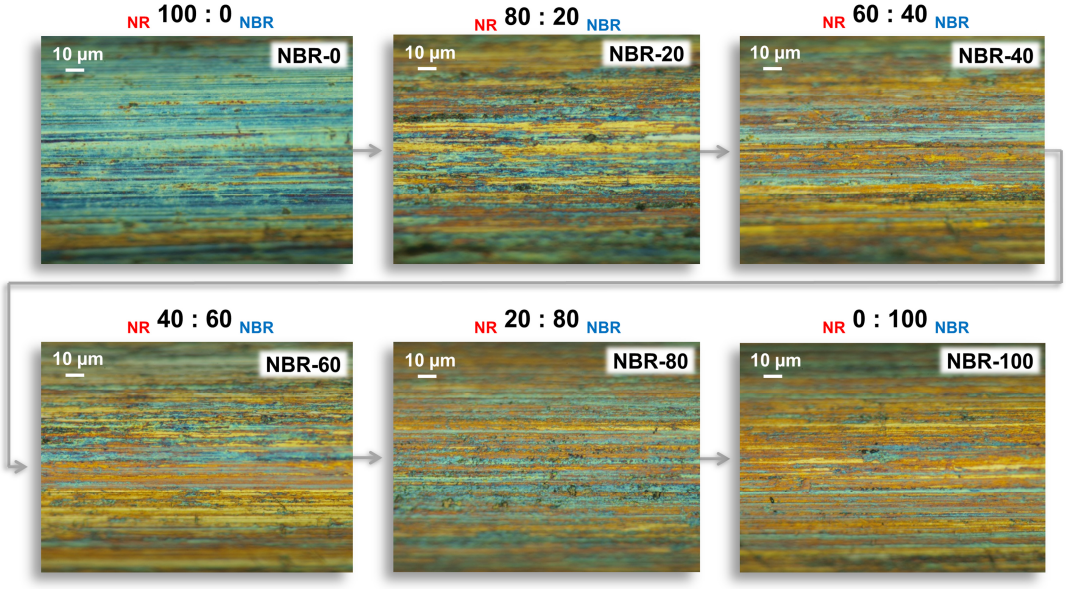

Figure 58 depicts the optical microscopy images of the different NR-NBR blends. It can be clearly seen that with increasing content of NBR in the rubber mixtures the interfaces change their color from bluish (NBR-0) to gold and yellowish (NBR-100). Since the color of the optical microscopy images indicates the degree of sulfidation [261], one can assume that the samples vary in the build-up of the adhesion interface.

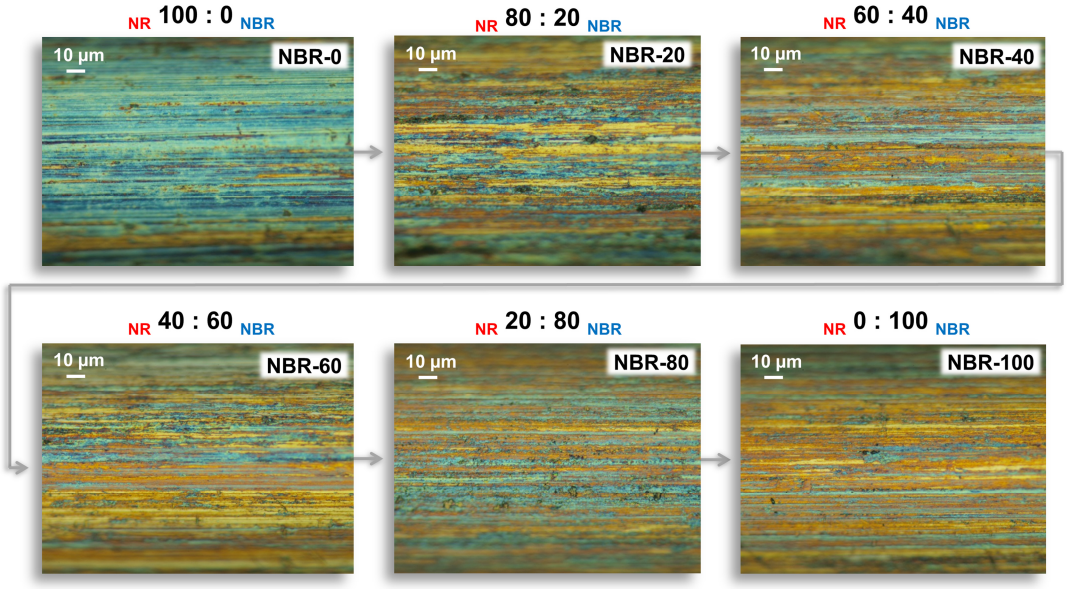

Figure 58 Optical microscopy images of the different NR-NBR blends starting from 0 phr NBR (top left) to 100 phr NBR (bottom right).

The microstructures of the NR-NBR rubber compounds investigated by SEM are shown in Figure 59. The sample **NBR-0**, which does not contain any NBR, shows homogeneous microstructures, which correspond to the Cu_xS-structure. These structures are formed during the vulcanization reaction and are mainly responsible for the rubber-to-brass adhesion. With increasing the content of NBR in the elastomer compound the granular texture disappears and ends in a smooth surface with some flaky like structures for the sample where NBR is the only rubber component (**NBR-100**). These observations indicate that the nitrile groups of the NBR prevent the build-up of the sulfuric structures and cause thereby just a little deformation of the brass surface.

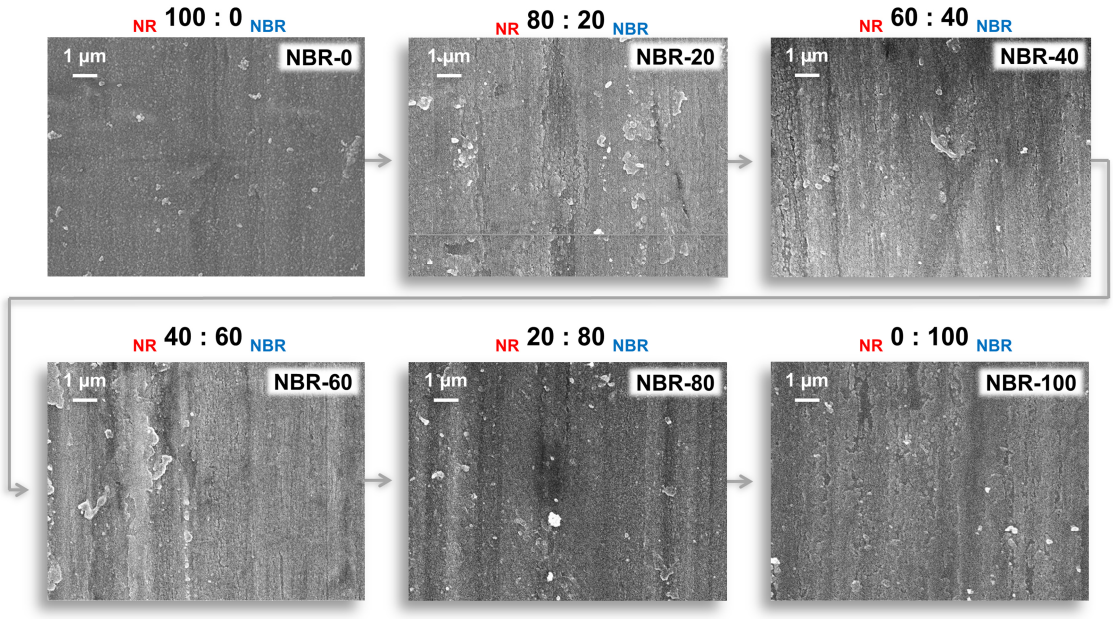

Figure 59 Scanning electron microscopy images of the different NR-NBR blends starting from 0 phr NBR (top left) to 100 phr NBR (bottom right).

The shape of these microstructures agrees excellently with the corresponding pull-out forces (Figure 60). The more distinctive the Cu_xS-structures, the higher the adhesion strength, and in this case also the higher the sulfur content of the interface. Thus it seems that the nitrile groups of NBR prevent the sulfidation of the brass surface, which as a consequence leads to the absence of well-defined microstructures.

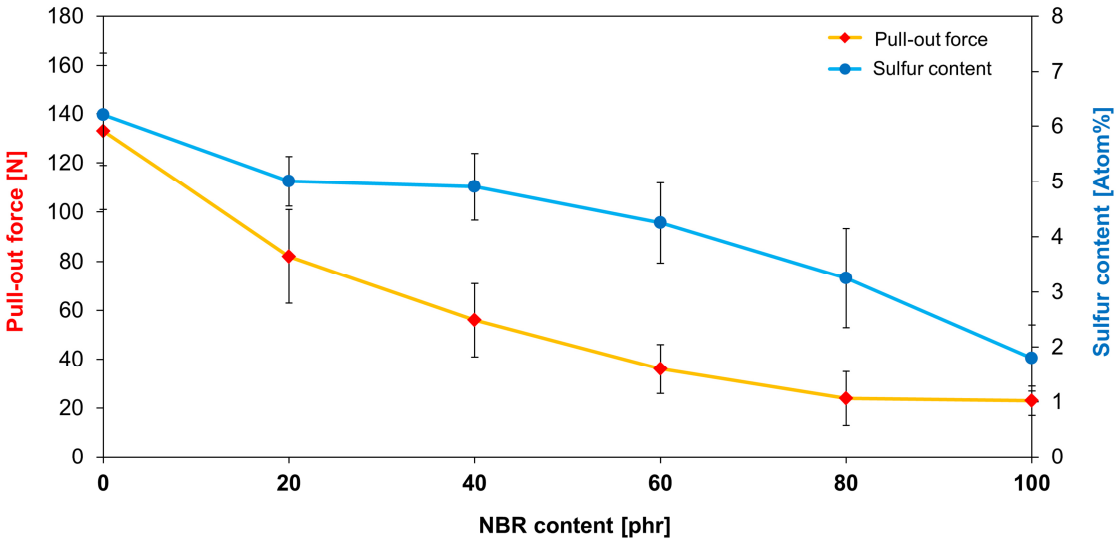

Figure 60 Pull-out forces (red) and sulfur contents (blue) of the different NR-NBR blends.

Consequently, it might be assumed that the nitrile groups absorb or interact with the brass surface preventing the sulfur to form sulfuric copper as well as zinc structures and

layers, respectively. However, the nitrile groups may also interfere the vulcanization reaction and influence the rubbers' physical properties. Therefore, in order to make precise conclusions, additional experiments have to be performed.

5.3.2 Influence of silica on NBR-brass adhesion

Silica is already used in real NBR mixtures as filler material and well-known to improve the NBR-brass adhesion performance. However, it is not known why silica does increase the bonding strength between NBR and brass and how does it change the appearance as well as the chemical composition of the adhesion layer.

In Table VII the silica filled NBR compound compositions are summarized. Here, all components are kept constant except silica and carbon black. With increasing silica contents the amount of carbon black was reduced in order to compensate the amount of total filler materials.

Table VII Composition of NBR compounds with different contents of silica in phr.

NBR	SiO_2-0	SiO_2-10	SiO_2-20	SiO_2-30	SiO_2-40	SiO_2-50
NBR (KRYANAC 2645)	100	100	100	100	100	100
Carbon black	70	60	50	40	30	20
ZnO	4.74	4.74	4.74	4.74	4.74	4.74
Stearic acid	1.05	1.05	1.05	1.05	1.05	1.05
Sulfur	3	3	3	3	3	3
CBS	1.84	1.84	1.84	1.84	1.84	1.84
DOA/MILLAN	9	9	9	9	9	9
Silica	0	10	20	30	40	50

As can be seen in Figure 61, the color of the different NBR-silica interfaces changes with increasing silica content from gold-yellowish to blue-greenish. This was also observed in the previous experiment of the NR-NBR blends. There the color changed in the same way with decreasing NBR content in the rubber mixture. So one may assume again that the level of sulfidation changes depending on the amount of silica in the NBR compounds.

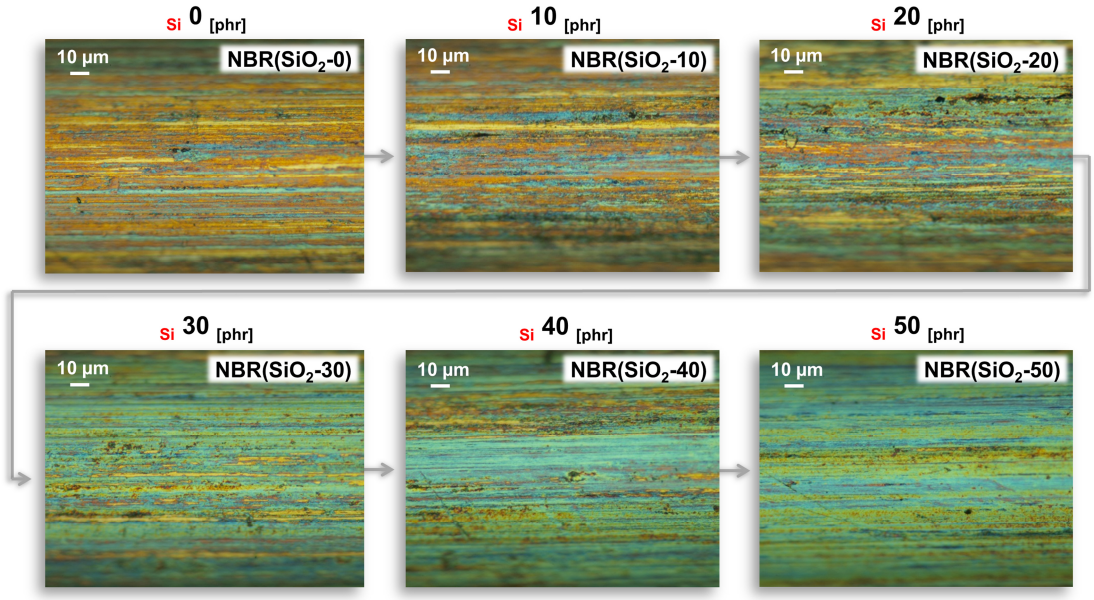

Figure 61 Optical microscopy images of the different NBR compounds starting from 0 phr silica (top left) to 50 phr silica (bottom right).

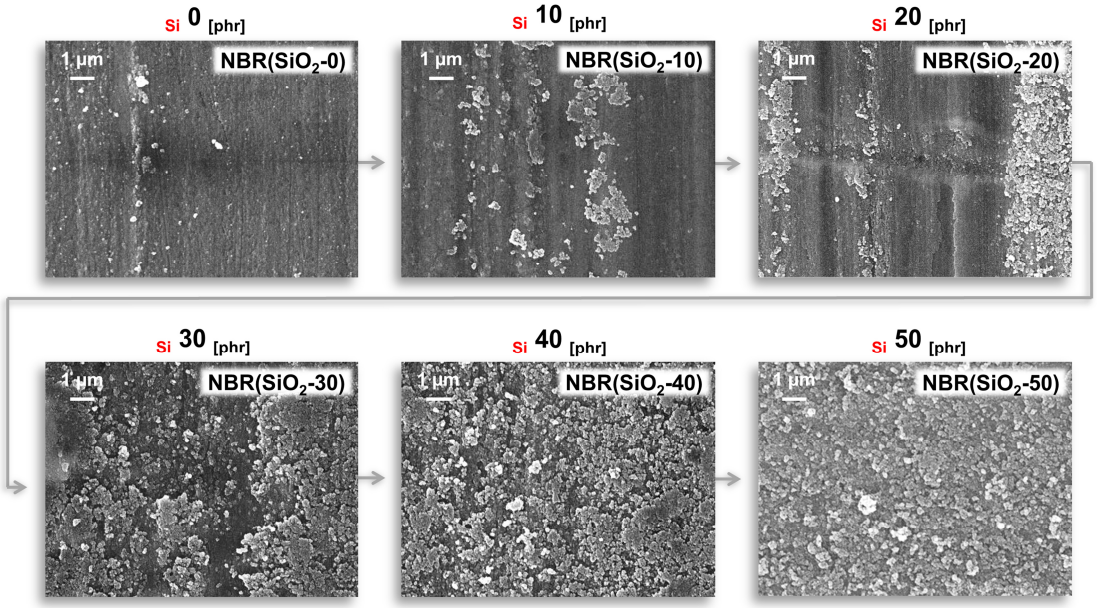

Figure 62 depicts the corresponding microstructures captured using scanning electron microscopy. The sample NBR(SiO_2-0) – which contains no silica – has a slightly rough surface without any specific structures. However, with increasing silica content of the rubber compound the accumulation of Cu_xS-structures on the adhesion interface increases as well. Thus, at 50 phr silica (NBR(SiO_2-50)) well-defined microstructures are formed which should lead to good adhesion performances due to the excellent opportunity for the rubber polymers to interlock mechanically into these structures.

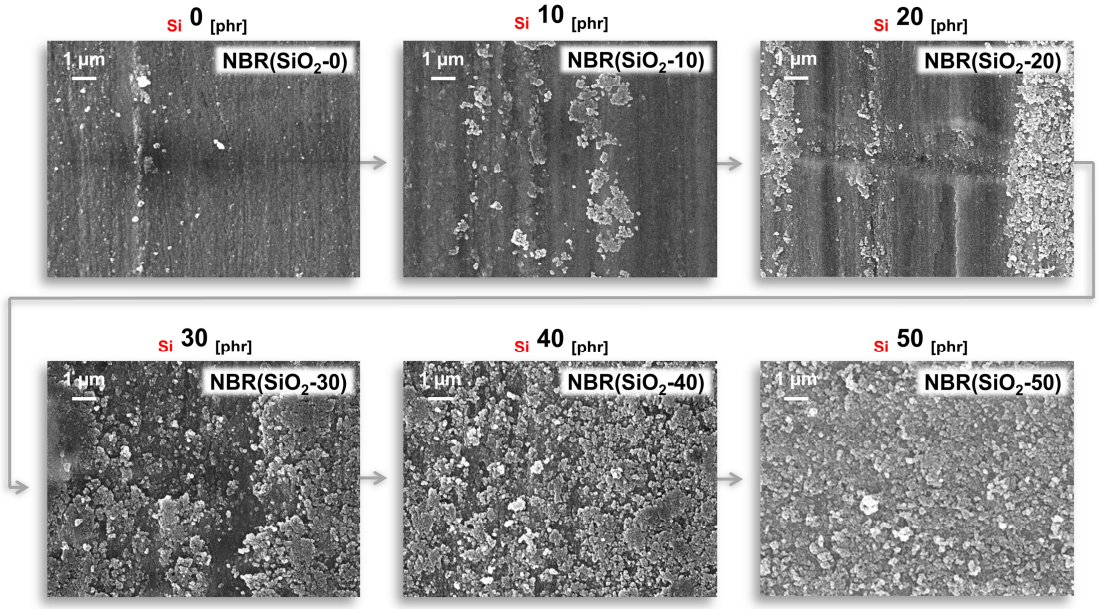

Figure 62 Scanning electron microscopy images of the different NBR compounds starting from 0 phr silica (top left) to 50 phr silica (bottom right).

This assumption was confirmed by pull-out tests (Figure 63). The higher the silica content of the NBR mixture the higher the sulfur content of the adhesion interface as well as the better the adhesion strength. These observations strengthen the theory that the nitrile groups interact with the brass surface preventing the build-up of well-defined Cu_xS-structures. Adding silica to the NBR mixture leads to pull-out forces of 334 N in the case of 50 phr silica, which is an enormous improvement compared to 23 N without silica. Also the degree of coverage increases with the amount of used silica, namely up to 1 for 30 phr silica and 2 for 40 and 50 phr silica. By comparing the microstructures and the pull-out forces of the different NBR compounds one can clearly see a silica content between 20 and 30 phr is necessary for a significant adhesion. Thus, the sulfuric structures are formed on the entire surface and the pull-out forces exceed the 100 N mark. Consequently, one can conclude that a critical silica content is mandatory so that the build-up of the adhesion interface occurs.

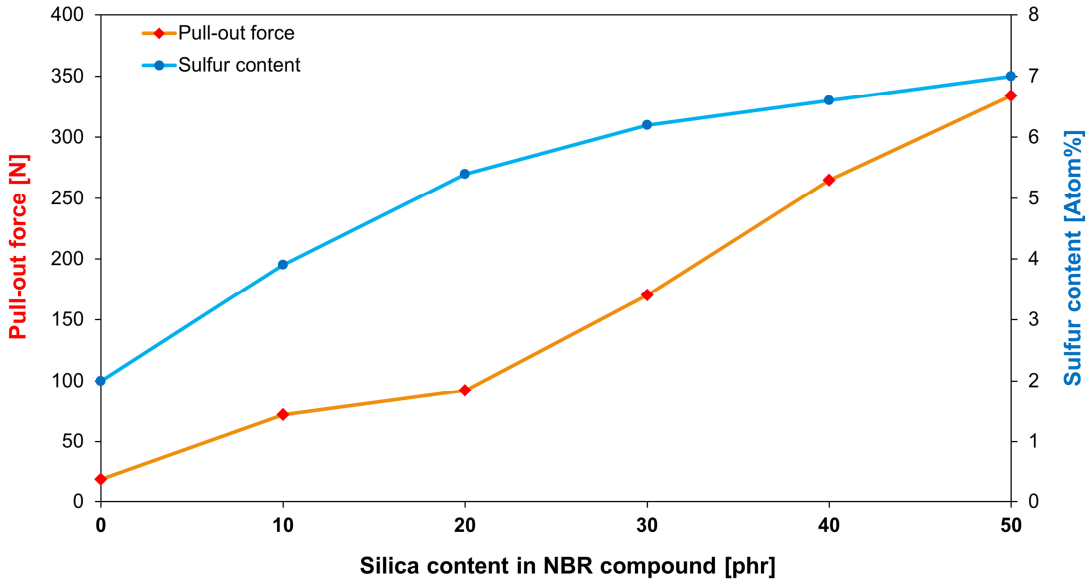

Figure 63 Pull-out forces (red) and sulfur contents (blue) of the NBR compounds with different silica contents.

Now the question may arise, how does silica influence the NBR-brass interaction? It is generally known that nitrile groups are able to adsorb on copper surfaces via two possible mechanisms (Figure 64) [267,268]. First, nitrile groups can bind to the copper surface by means of a σ-bonding via the free electron pair of the nitrogen atom. Alternatively, π-bindings can cause the adsorption of nitrile groups on copper surfaces.

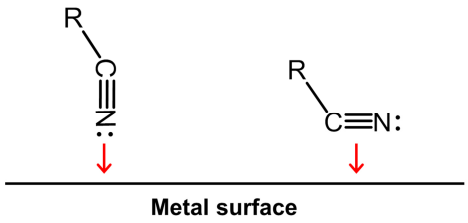

Figure 64 Possible bonding mechanisms of nitrile groups on metal surfaces: σ-bonding (left) and π-bonding (right).

Thus, the adsorbed nitrile groups may prevent that sulfur diffuses to the brass surface forming Cu_xS-structures. Further, nitrile groups are well known to form complexes with e.g. copper [269,270], which could also be the reason for the lack of sulfuric structures on the adhesion layer of simple NBR compounds. In this case, the brass layer would be degraded instead of transformed to copper and zinc sulfide structures. Nevertheless, in both cases the nitrile groups are the reason for the failed build-up of a bonding layer and in both cases the protection of the nitrile groups using silica enables the formation of an adhesion layer.

So how does silica protect the nitrile groups from interacting with the brass surface? One possible explanation would be, as illustrated in Figure 65, the formation of hydrogen bonds between the polar nitrile groups (alkaline character) and the hydroxyl groups of the silica (silanol-groups). The interaction between the nitrile groups of NBR and silica is already used technologically. In order to improve the dispersion of polar silica particles in nonpolar NR compounds small amounts of NBR are added. Thus, the polar nitrile groups interact with the silica particles resulting in a well-dispersed rubber mixture [271,272].

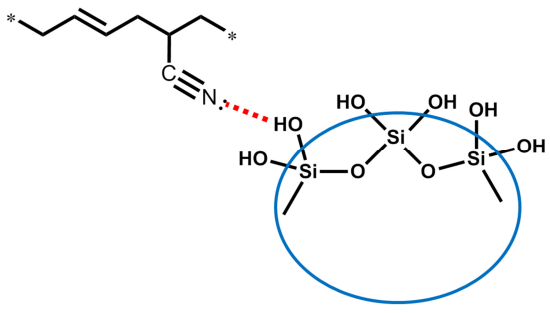

Figure 65 Hydrogen bonds between silica particles and the nitrile groups of NBR.

However, since with increasing silica content in the NBR compounds also the scorch-time increases – from 11.3 min (NBR(SiO_2-0) to 48.6 (NBR(SiO_2-100) – it had to be investigated if the NBR-brass adhesion is improved due to the increased scorch-time. Therefore, the scorch-time of an unfilled NBR mixture was increased using the rubber anti-scorch retarder *N*-(cyclohexylthio)phthalimide (CPT) (Table VIII).

Table VIII NBR-100 compound compositions with different retarder amounts in phr.

	NBR-100	NBR-100(R-I)	NBR-100(R-II)	NBR-100(R-III)
NBR (KRYANAC 2645)	100	100	100	100
Carbon black	70	70	70	70
ZnO	4.74	4.74	4.74	4.74
Stearic acid	1.05	1.05	1.05	1.05
Sulfur	3	3	3	3
CBS	1.84	1.84	1.84	1.84
DOA/MILLAN	9	9	9	9
CTP (Retarder)	0	0.2	0.4	0.6

Thus it can be clearly seen that the scorch-time increases with increasing the retarder concentration (Figure 66). However, thereby, the adhesion performance is not improved but steadily decreases with increasing scorch-time.

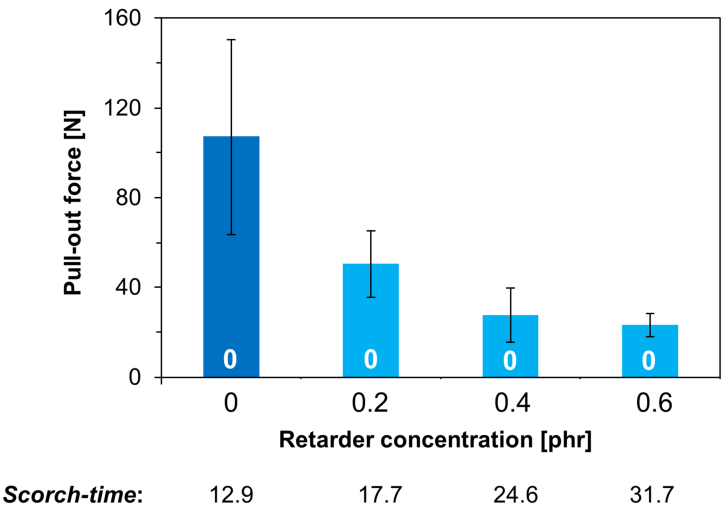

Figure 66 Pull-out forces of the untreated brass-plated steel wires and NBR-100 compounds with increasing retarder concentration (R-I to R-III) as well as the corresponding scorch-times in minutes. The numbers in the lower part of the columns correspond to the degree of coverage after the T-test experiments.

Now, in summary one can conclude that the scorch-time has no positive influence on the NBR-to-brass adhesion strength but on the other side it can also not confirmed yet that the nitrile-silica interactions are the reason for the increased bonding strength.

Therefore, further information about the mechanism of the NBR-to-brass adhesion have to be gathered. This is achieved by means of low-molecular-weight nitrile compounds.

5.3.3 NBR-model systems

Since the interactions between the ingredients of the rubber compounds are very complex and versatile, certain mechanisms and influences have to be investigated using model systems.

First of all, the adsorption behavior of the nitrile groups on the brass surface was investigated. Therefore, low molecular nitrile compounds – in this case succinonitriles – were adsorbed on the metal surface. First, planar brass platelets were used instead of the brass-coated steel wires in order to follow the change of contact angle of H_2O as a result of the succinonitrile adsorption (Figure 67). After 2 hours of dipping the brass platelets in the acetone-succinonitrile solution (1:2) the contact angle decreased below 60°, which indicates according to literature [267,273] that the entire wire surface is covered with succinonitrile compounds. Dip-coating of the untreated platelets in a simple acetone solution for different time-periods leads to a decrease in the H_2O contact angle.

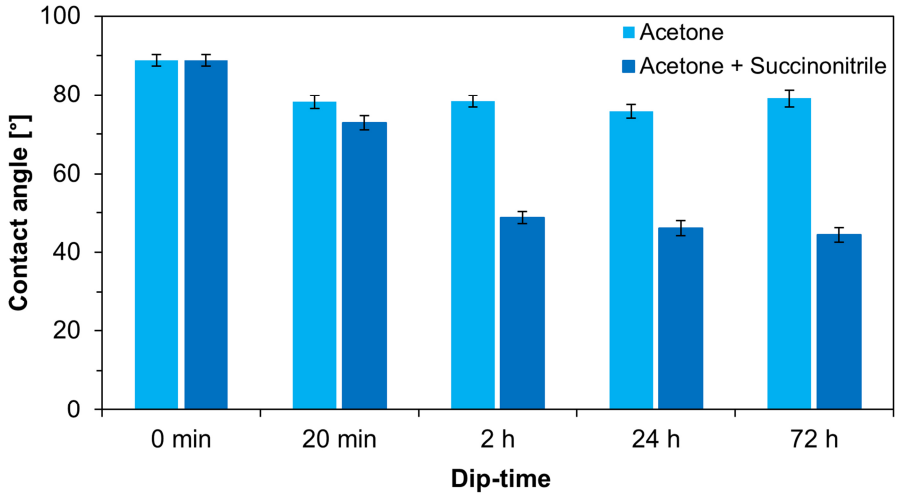

Figure 67 H_2O contact angles of brass platelets after dip-coated in pure acetone (reference) and in an acetone-succinonitrile (1:2) solution for different times.

Based on these results, brass-plated steel wires were dip-coated in the acetone-succinonitrile solution (1:2) for up to 2 hours and the adhesion strength to a simple natural rubber compound (NR(A)) was tested. Figure 68 depicts the pull-out forces of the brass-plated wires coated with the acetone-succinonitrile solution as well as of wires dipped in pure acetone as reference. Thus it can be clearly seen, that the adhesion strength decreases with increasing dipping-time of the wires in the succinonitrile solution whereas the wires treated with pure acetone increase only slightly. Therefore, the reduction of the pull-out forces has to be dependent on the succinonitrile-coating.

These results correlate very well with the observations in Chapter 5.3.1, where the bonding performance of the NR-NBR blend deteriorated with a higher NBR content. Due to the fact that the untreated wire shows with 228 N a relatively good adhesion performance to NR whereas after dipping in the succinonitrile solution for 2 hours the pull-out force reaches only 45 N, one can assume that the nitrile groups of the succinonitrile-coating prevent the formation of an adhesion interface.

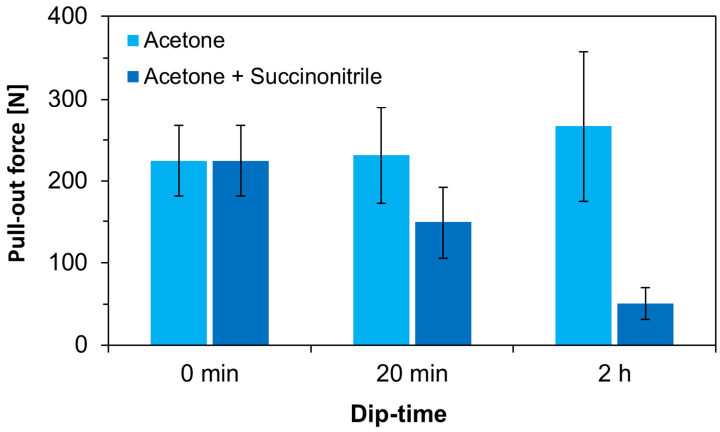

Figure 68 Pull-out forces of untreated wires and wires after dip coating whether in pure acetone (reference) or in an acetone-succinonitrile solution (1:2). The adhesion performance was tested to NR(A). The numbers in the lower part of the columns correspond to the degree of coverage after the T-test experiments.

In a next step, the dip-coated wires were investigated using SEM-EDX. Figure 69 depicts the adhesion interface of the NR(A) sample after olefin-metathesis. Here, the well-defined Cu_xS-structures can be clearly seen, which are mainly responsible for the rubber-to-brass adhesion. However, for the adhesion layer of the NR(A)-SCN sample - where the wire was dip-coated in the succinonitrile-solution and afterwards vulcanized in a natural rubber compound - these sulfuric structures cannot be seen after the olefin-metathesis degradation of the rubber. The surface shows only some irregularly distributed flakey-like structures. These are similar characteristics, which are observed on the "bonding" layer of the NBR-100 sample. By analyzing the wire sample after dip-coating in the succinonitrile solution (SCN) without further vulcanizing in a rubber compound, these flaky like structures are very pronounced. In order to exclude that these structures are caused only by succinonitrile, also the influence of p-tolunitrile solutions on the brass surface was investigated. Thus it was observed that p-tolunitrile (p-TCN) affects the brass layer in the same way as succinonitrile but to a lower extend. Conversely, the NBR sample containing 50 phr silica (NBR(SiO_2-50)) shows again

homogeneous microstructures, wherefore the adhesion performance is of reasonable quality.

Now the question may arise, whether these flakey-like structures are formed as a result of an incomplete build-up of the sulfuric adhesion interface or by a partly removal of the brass layer? By comparing the corresponding EDX-values further hints are provided (Figure 69). The NR(A) sample shows with a S-value of 5 atom% and a Fe-value of 83 atom% standard values for a well adhering bonding layer. NBR(SiO_2-50) shows comparable results for the EDX-measurements as NR(A). However, all adhesion systems where nitrile groups were applied on the brass surface without silica – real (NBR-100) and model (SCN, p-TCN, NR(A)-SCN) systems – show no or very low sulfur values but increased Fe-values. The high Fe-content can be explained only by thinning of the brass layer, which would confirm that the nitrile groups dissolve the brass layer. In case of the real NBR-100 sample, the Fe-value is not that high as for the model systems, which is highly probable because the nitrile-groups in the succinonitrile solution can diffuse more easily to the brass surface so that the decomposition of the brass-coating is promoted.

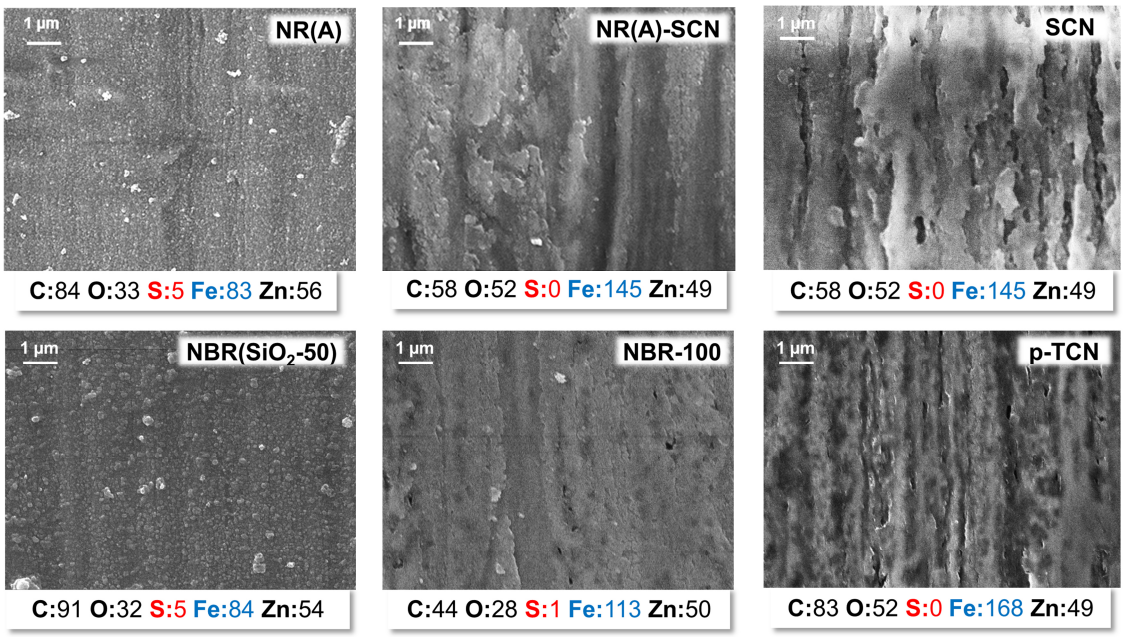

Figure 69 SEM pictures of the interfaces of a NR compound (NR(A)), a NBR compound with 50 phr silica (NBR(SiO_2-50)), a succinonitrile coated wire sample vulcanized into a NR compound (NR(A)-SCN), a simple NBR mixture (NBR-100) and wires simply dipped for 2 hours in a acetone-succinonitrile solution (1:2) and acetone-p-tolunitrile solution (1:2) for 2 hours. Below the pictures the corresponding EDX-values are shown.

By comparing the cross-sections of the NR(A) and NBR-100 samples, one can clearly see their fundamental differences (Figure 70). The adhesion interface of NR(A) is perfectly divided in four areas: in the sequence from bottom to top first the steel wire can be seen followed by the brass layer and the Cu_xS-structures. On the very top the rubber compound is presented. In comparison to this, the adhesion layer of the NBR-100 sample does not show any sulfuric structures but a very rough surface which seems to be partially degraded. Also rubber cannot be seen because without an adhesion interface the rubber is not able to stick to the wire sample.

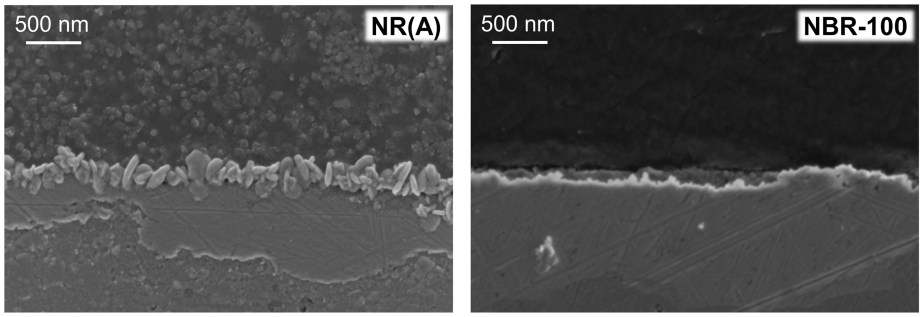

Figure 70 SEM images of the cross-section of the adhesion interface between a NR mixture (NR(A)) as well as a NBR compound (NBR-100) to brass-coated steel wires. The samples were first embedded in an epoxy-resin followed by grinding and polishing (images were taken by FELMI-ZFE Graz).

Well, if the brass layer is degraded by the nitrile groups of NBR and succinonitrile, they should be detectable either on the interface of the NBR(100) vulcanisate (where the adhesion failed) or in the succinonitrile solution. Therefore, in a first step the rubber was analyzed by EDX in order to find copper or zinc residues. Unfortunately, the used EDX set-up did not allow detecting very small concentrations. Consequently, very low detection limits are required. Since the rubber area facing to the brass surface is very small, the investigation of the succinonitrile solution after dip-coating was found to be the more promising option. The investigation of the succinonitrile solution was performed using atom absorption spectroscopy at which 55 ppm copper and 24 ppm zinc were detected. These observations provide the evidence that nitrile groups degrade the brass-layer of the steel wires even though it is not known by which mechanism. However, these results correlate well with the observations of Lin *et al* [274]. They observed the presence of copper and zinc on the vulcanizate surface after sulfur vulcanization of brass-coated steel wires in a simple NBR compound. In order to detect the brass components on the rubber interface they analyzed the ash of the vulcanizate using polarography techniques.

5.3.4 Conclusion

Since good adhesion properties between NBR and brass can just be achieved by high filler loadings, the reason for the bonding failure of simple NBR compounds was studied. Initial experiments with real rubber compounds demonstrated already the dependence of the adhesion performance from the amount of nitrile groups in the rubber compound as well as the influence of silica. The more silica and the less nitrile groups are presented in the rubber mixture the better the NBR-brass bonding characteristics. However, further experiments using model systems, which were based on low molecular nitrile compounds led to the assumption that the nitrile groups prevent the formation of well-defined Cu_xS-structures by adsorbing on the brass surface and subsequently dissolving the brass-coating of the steel wire. These observations contribute to understand the general rubber-to-metal adhesion mechanism and pave the way to further improve the NBR-to-brass adhesion.

Such detailed investigations of the NBR-brass adhesion interface are found rarely in literature for which the observations found in this thesis are valuable contributions to understand the rubber-to-brass bonding.

5.4 Adhesion promoter for chemical rubber-to-brass bonding

The quality of the rubber-brass adhesion based on the mechanical interlocking mechanism depends on many parameters. In particular, the adhesion performance depends on the vulcanization conditions, on the composition and properties of the rubber compounds as well as on the wires properties. Therefore, one has always to compromise in order to achieve good adhesion properties and simultaneously good mechanical rubber properties. To circumvent such compromises new bonding systems were developed which are based on organic bifunctional molecules. Thereby, the rubber-metal adhesion is achieved by a chemical linkage between the rubber polymers and the metal wires (brass- and zinc-plated steel wires). Here, the principles of the bifunctional adhesion promoter for sulfur (NR, NBR and SBR) and peroxide (EPDM) cross-linked rubber systems are presented as well as the corresponding results obtained by using optimized process parameters before and after thermal aging. The used mixture compositions for the pull-out tests are given in Table II and Table IX. Further, the coating process was automated using an in-house designed and constructed wire-coating machine.

5.4.1 Polysulfide silane

The bifunctional organosilane bis[3-(triethoxysilyl)propyl] tetrasulfide – also known as polysulfide silane – has already been used for years in rubber compounds containing silica to facilitate the distribution of the filler [67] and was explored first by Jayaseelan and van Ooij [66] in 2003 as alternative rubber-metal adhesion system. In this study the adhesion performance of the polysulfide silane was tested for the first time between brass- or zinc-plated steel wires and NR, NBR as well as SBR mixtures.

Principle

The mechanism of the chemical bonding system based on polysulfide silanes is explained well in Chapter 2.2.3 and depicted again in Figure 71. First, the polysulfide silane is linked to the plasma-activated wire surface via manual or automated dip-coating (see Chapter 4.2.4). Afterwards the coated metal wire is incorporated into the rubber compound and placed in a heating press. Now, during the vulcanization reaction of the rubber compound, free sulfur is integrated into the polysulfide chain of the multifunctional silane. Thus, the silane is activated and can react with the rubber macromolecules. In doing so a chemical bonding between the cured rubber polymers and the wire surface is achieved.

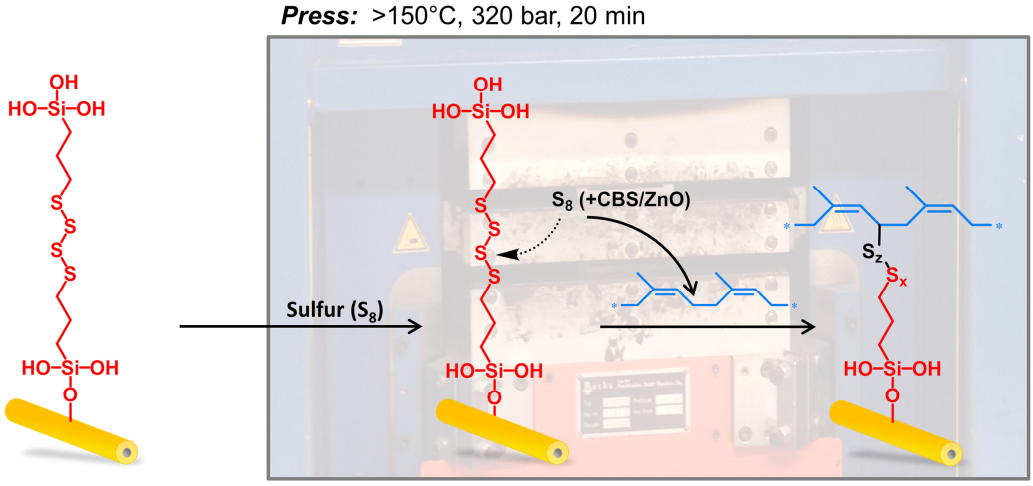

Figure 71 Principle of the polysulfide silane adhesion system.

Optimization of the process parameters

Optimizations of the process parameters for the polysulfide silane adhesion system have shown that a mixture ratio of 75 parts polysulfide silane by volume and 25 parts aminosilane by volume (3:1), a crosslinking time of 40 minutes, a crosslinking and drying temperature of 140 to 160 °C, and a layer thickness of 6 µm lead to very good adhesion properties (Figure 72). These parameters correlate very well with the optimized process parameters of Jayaseelan and van Ooij [66]. Interestingly, these parameters were found to be most suitable for all tested rubber types, namely NR, NBR as well as SBR.

Figure 72 Optimized parameters for the adhesion system based on a mixture of polysulfide silanes (S_4-Si) and aminosilanes (A) obtained via manual dip-coating.

In a next step, the optimized parameters from the manual dip-coating procedure were transferred to the automated dip-coating process. Thus, it was observed that again the same parameters lead to reputable adhesion strengths (Figure 73). In order to achieve a crosslinking and drying time of 40 minutes, the driving rate of the automated dip-coating machine was set to 10 mm/min.

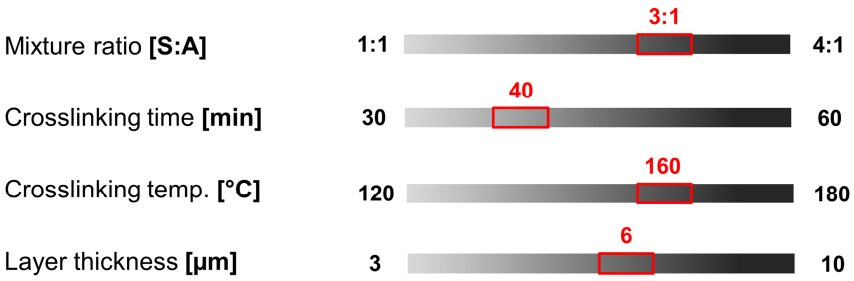

Figure 73 Optimized parameters for the adhesion system based on a mixture of polysulfide silanes (S_4-Si) and aminosilanes (A) obtained via automated dip-coating.

Here one has to mention that especially the layer thickness of the organofunctional silane coatings was found to play a crucial role for the rubber-metal adhesion. Very thin coatings (<3 µm) showed absolutely no improvements of the adhesion – most probably because of bond failure – whereas comparatively thick coatings (8-10 µm) resulted in moderate adhesion performances, maybe because of film delamination or cracking during moulding or drying [44]. As mentioned above, the highest pull-out strength could be measured at a layer thickness of 6 µm. Therefore, to obtain this exact thickness, the manually coated wire samples had to be fixed vertically for 30 minutes subsequently after dip-coating. In case of the automated coating procedure N_2-gas was injected into the coating solution to reduce its surface tension which enabled to adjust the desired coating thickness by varying the gas flow.

Results

First of all, the pull-out tests lead to the conclusion that the adhesion performance is significantly improved using polysulfide silanes as adhesion promoters. As depicted in Figure 74, untreated brass-plated steel wires show with 23 N no adhesion to NBR samples and with 124 N and 159 N very low adhesion strengths to SBR and NR(A), respectively.

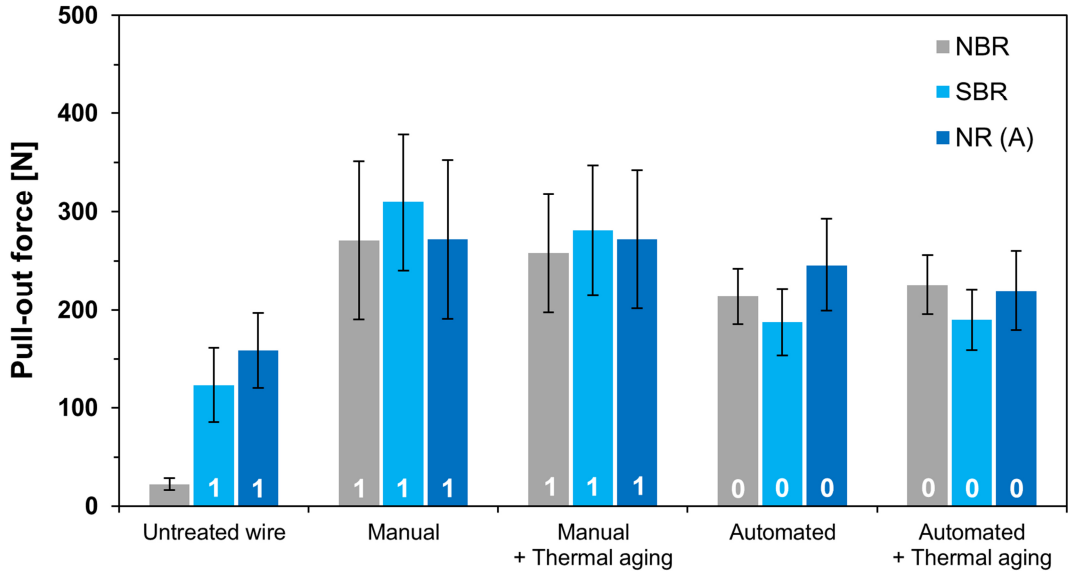

Figure 74 Adhesion strengths of NBR, SBR, and NR(A) to untreated brass-plated steel wires as well as to wires coated with polysulfide silanes (S_4-Si:A=3:1, 40 min @ 160°C) whether by manual or automated dip-coating as well as after thermal aging for 7 days at 70°C. The numbers in the lower part of the columns correspond to the degree of coverage after the T-test experiments, whereas columns showing no number correspond to a coverage of 0.

However, by coating the brass-plated steel wires with the polysulfide coupling agent the adhesion performance is enhanced to pull-out forces between 272 and 310 N, depending on the type of rubber. But due to the high standard deviations of the measured pull-out forces – which are caused most likely by several impurities during the preparation of the T-test specimens – one can say that in average they all reach the same final adhesion strength but differ in their relative increase. This means that the pull-out force of the NBR sample increases by a factor of approximately twelve whereas the pull-out strengths of SBR and NR(A) increase only by a factor of 2.5 and 1.5, respectively. Consequently, the greatest improvement of the adhesion performance was achieved for the NBR sample. Another remarkable feature of this adhesion system is that the chemical bonding strength between the rubber macromolecules and the wire surface is preserved after thermal aging for 7 days at 70 °C. Since adhesion failure due to increased temperatures is a considerable problem in many rubber products this is a very beneficial characteristic of the polysulfide silane coupling agent. By using the automated wire-coating machine the pull-out forces decrease to 188 N for the NBR sample, 214 N for the SBR sample and 245 N for the NR(A) sample. Hence, the adhesion performances using the automated coating process were not as good as for the manual coated wires but in general still usable. Further, the reproducibility of the measurements was improved as the standard deviations were reduced by half. These worsened adhesion properties using the automated wire-coating machine originate very probably from the cross-linking and drying step. The automated wire-coating machine features a tube furnace and not a closed drying chamber as used for the manual coating procedure. Consequently, the condensation reaction – by which the silanes are bonded to the hydroxyl-groups of the activated wire surfaces – is not that efficient and has still potential to be optimized. Beside this, also crack formation may impair the adhesion performance when rolling up the coated wire on the take-up reel. However, again, the adhesion performance was preserved after thermal aging. Further, after the pull-out tests, the degree of coverage for the automatically coated wires is 0 and for the untreated as well as manually coated wires 1 (only NBR showed no rubber residues on the untreated wire sample after the pull-out tests). So for the untreated and manually coated wires the bonding strength between wire and rubber exceeds partially the cohesive strength of the rubber whereas for the automated coated wires the adhesion completely fails between rubber and the metal surface.

It could not be clarified, why the adhesion performance is in some cases best for NR(A) and sometimes for SBR. Probably they can be seen as equivalent as they exhibit very large standard deviations.

In a second step, the polysulfide silane adhesion system was tested on zinc-plated steel wires (Figure 75).

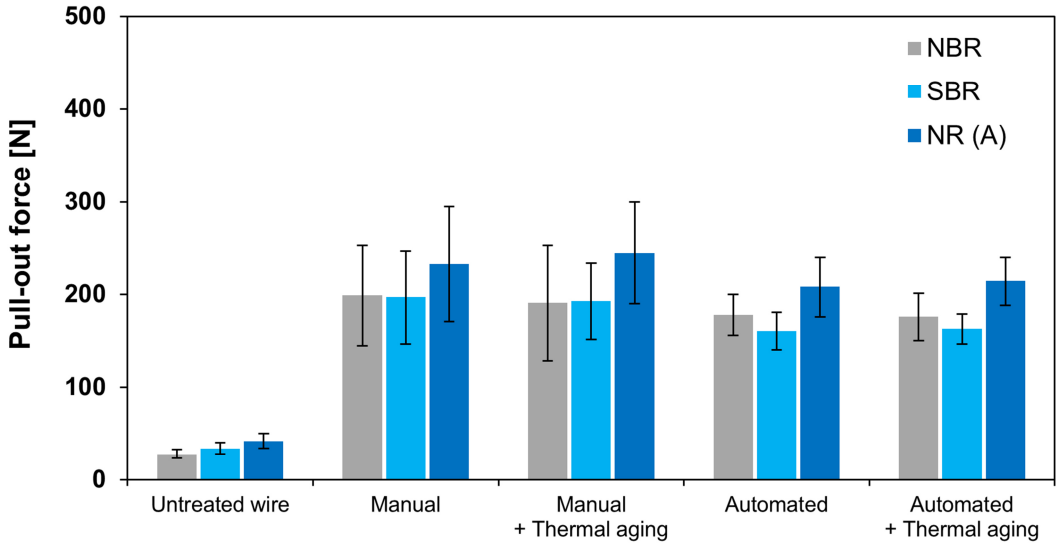

Figure 75 Adhesion strengths of NBR, SBR, and NR(A) to untreated zinc-plated steel wires as well as to wires coated with polysulfide silanes (S_4-Si:A=3:1, 40 min @ 160°C) whether by manual or automated dip-coating as well as after thermal aging for 7 days at 70°C. The numbers in the lower part of the columns correspond to the degree of coverage after the T-test experiments, whereas columns showing no number correspond to a coverage of 0.

The untreated wire samples show pull-out forces between 28 and 42 N and no real adhesion to the different rubber types. However, the silane coated wires show pull-out forces between 201 and 247 N, depending on the type of rubber. Here, the relative improvement of the adhesion strength is six- to sevenfold. This is again a considerable advancement of the adhesion performance using this chemical bonding system. Furthermore, compared to the brass-plated steel wires, the adhesion strength does not decrease significantly using the automated wire-coating machine. The pull-out forces are still in the range of 172 and 222 N and the standard deviations decrease down to one third compared to the values obtained with the manually coated wires. Also thermal aging does not influence the adhesion strength of the bonding system. Consequently, it can be assumed that the manual and automated dip-coating procedures do not differ significantly for the zinc-plated steel wires.

But, compared to brass-coated steel wires, one has to consider that the pull-out forces for the manually coated brass-plated steel wires are considerably higher than for the zinc-coated wires. The reason for that might be an improved adhesion performance of silanes on plasma activated copper oxide (which can be found on the surface of the brass layer) than on activated zinc oxide [57]. This would also correlate very well with the decreased adhesion strength of the automatically coated brass-plated steel wires. There the adhesion also fails due to an ill-defined bonding of the silane groups on the metal surface, caused by an incomplete drying and crosslinking step in the tube furnace. However, since the wire samples are of technical quality the conclusions have to be considered carefully.

In Figure 75 one can further see that NR(A) has in general slightly higher pull-out forces as the other rubber types. This could be due to the higher amounts of double bonds in the rubber backbone compared to NBR and SBR, which partially contain nitrile- and styrene-substituents instead of double bonds. Thus, more double bonds are available to bind on and the absence of substituents on the polymer backbone avoids sterical effects. The reason, why the increased adhesion of NR(A) to zinc cannot be seen for the brass-coated wires may be that there the pull-out forces are generally higher so that these effects are not evident. Further, the degree of coverage are identical to the brass-plated steel wires, only for the untreated zinc-plated wires the coverage is for each sample 0.

5.4.2 Blocked isocyanatesilane

After testing the adhesion promoter based on polysulfide silanes it was focused on the question, which other functional groups could be used to bind the molecule on the various rubber macromolecules? One perfect candidate would have been the isocyanate group. Isocyanates are highly reactive and possess the ability to bind on allyl-hydrogen atoms [1], which can be found on many rubber types as NR, NBR, SBR as well as EPDM. Unfortunately, isocyanates have a serious disadvantage namely their very great moisture-sensitivity. Consequently – by applying such isocyanates in real rubber products – there would appear major problems during transportation, storage but especially during the coating process. Thus, the reactivity of the isocyanate groups is reduced by using blocking-groups.

This bifunctional adhesion promoter can be synthesized via a one-step reaction. Only two starting substances are needed which are both commercially available. The turnover of the reaction is 99% and can be easily monitored using IR-spectroscopy.

Principle

In order to bind rubber via chemical bonds on the metal wires first of all the wires have to be dip-coated in the blocked isocyanatesilane (MEKO blocked 3-(triethoxysilyl)propyl isocyanate) solution according to Chapter 4.2.4. As soon as the bifunctional molecules are covalently bonded to the metal surface via the silane groups the wires can be incorporated into the rubber compound (Figure 76).

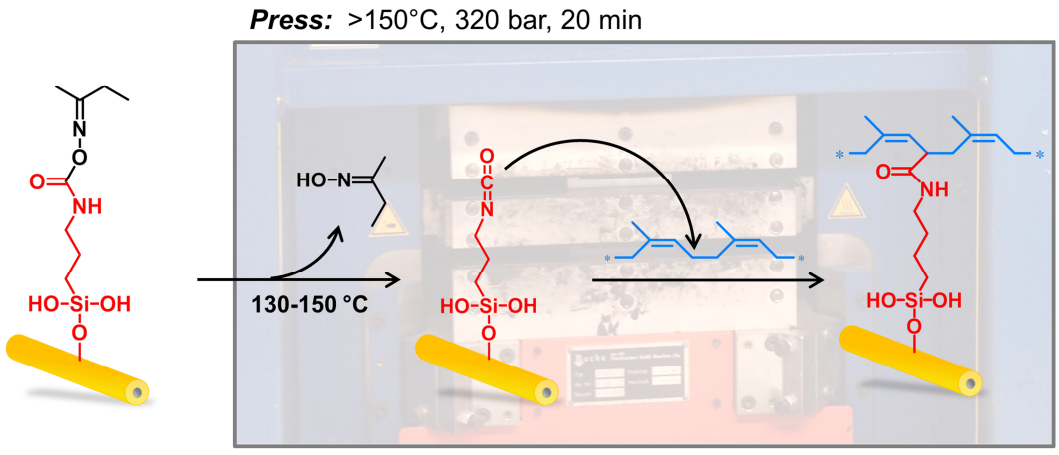

Figure 76 Principle of the isocyanatesilane adhesion system.

Thus, the uncured rubber compound as well as the coated wires are placed in the T-test mold and subsequently positioned in the heating press. There, the blocking groups escape at elevated temperatures, as detected by thermo gravimetric analysis (Figure 77). These measurements lead to the conclusion that deblocking of the isocyanate group occurs at temperatures between 130 and 210°C. However, due to a dynamic temperature increase during the thermo gravimetric measurements it can be assumed that deblocking takes place at temperatures between 130 and 150°C. This correlates very well with the data from literature [275].

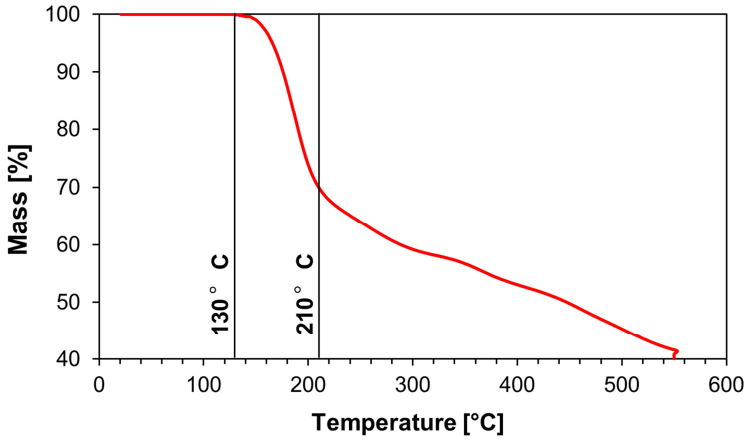

Figure 77 Mass loss of the MEKO blocked isocyanatesilane due to splitting-off MEKO at elevated temperatures detected by thermo gravimetric analysis (TGA).

In a further step, IR-spectroscopy was used to monitor the deblocking reaction of the MEKO blocked isocyanatesilane. As illustrated in Figure 78, after heating the blocked organofunctional silane solution to 150°C for 20 minutes in an inert gas atmosphere (N_2) most of the isocyanate groups are again deblocked. However, the isocyanate-peak (2275-2250 cm^{-1}) does not grow to the size of the starting reagent because of the formation of uretdiones (1779 cm^{-1}) in solution. If the isocyanates are bonded on the metal surface these reactions should be reduced. Further, at increased temperatures as during the vulcanization reaction the equilibrium of mono-, di-, and trimers shifts to the side of the monoisocyanate, for which reason these effects should not affect the adhesion performance [275].

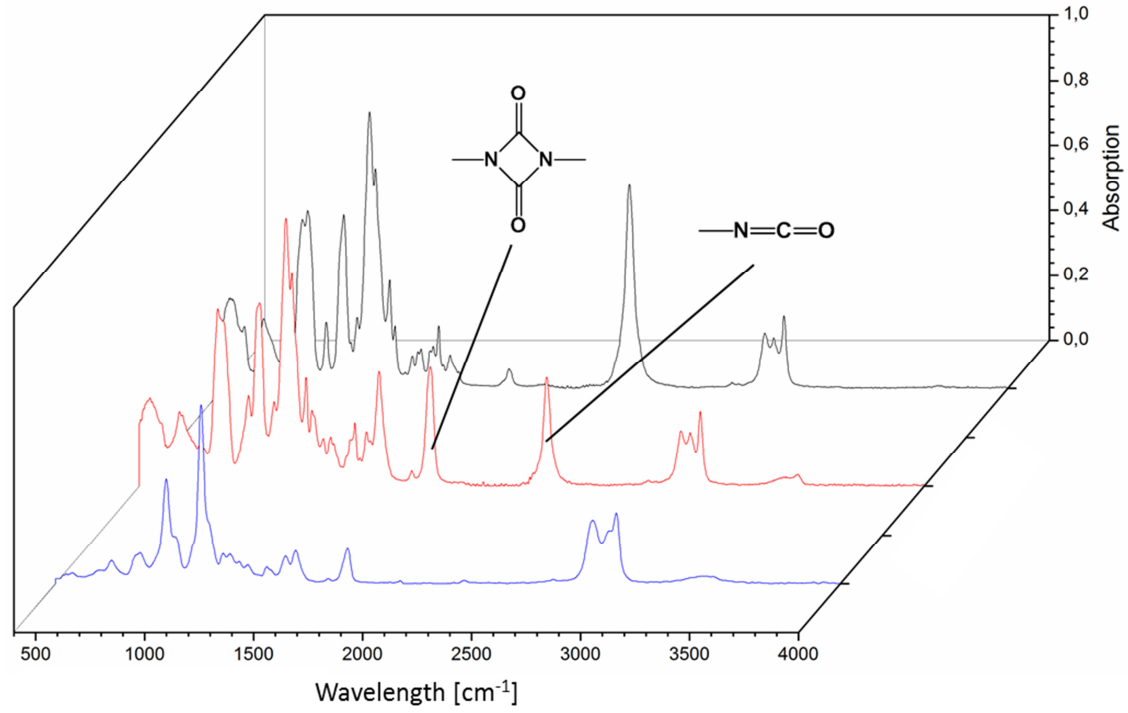

Figure 78 IR-spectra of the isocyanatesilane as obtained by Sigma Aldrich (black line), the MEKO blocked isocyanatesilane (blue line) and the isocyanatesilane after deblocking at 150°C (red line).

Since the vulcanization of rubber products is generally performed at temperatures higher than 150 °C, MEKO fits perfectly as protecting group for this application. After several minutes in the heating press, the isocyanate groups are unblocked and can bind to the allyl-hydrogen atoms (or some other functional groups) of the rubber macromolecules. Thus, the rubber gets linked to the wire surface via chemical bindings.

Optimization of the process parameters

To achieve good adhesion strengths between rubber and metal wires the mixture and process parameters had to be optimized. In the course of this, as a first step, the mixture ratio of the blocked isocyanatesilane and aminosilane solution was adjusted for the manual coating procedure (Figure 79). Thus it was observed that mixture ratios between 2 to 1 and 4 to 1 lead to the same quality of adhesion. Therefore, all further experiments were performed using a mixture ratio of 3 to 1. In a next step, the crosslinking temperature was optimized. Here, 100 °C was found to be the best compromise because to low temperatures lead to a binding of the silane groups to the activated metal surface and to high temperatures unprotect the MEKO protected isocyanate groups before they get incorporated into the rubber compound. As optimal crosslinking time 60 to 80 minutes was observed whereas a silane-layer thickness of 8 µm led to the best results.

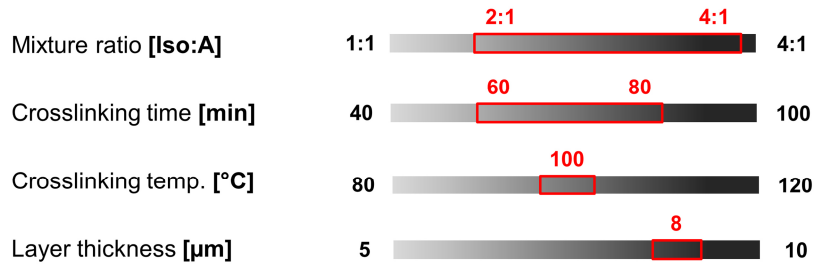

Figure 79 Optimized parameters for the adhesion system based on a mixture of MEKO blocked isocyanatesilanes (Iso) and aminosilanes (A) obtained via manual dip-coating.

For the automated coating process almost the same optimized parameters were obtained as for the manual procedure. As shown in Figure 80, the silane mixture ratio of 3 to 1 correlates well with the optimum of the manual coating. However, crosslinking times of 44 to 58 minutes led already to applicable adhesion strengths, which corresponds to a driving rate of 7 and 9 mm/min, respectively. Conversely, the optimal crosslinking temperature was again 100 °C and the layer thickness of 7 µm is also very close to the optimum of the manual procedure.

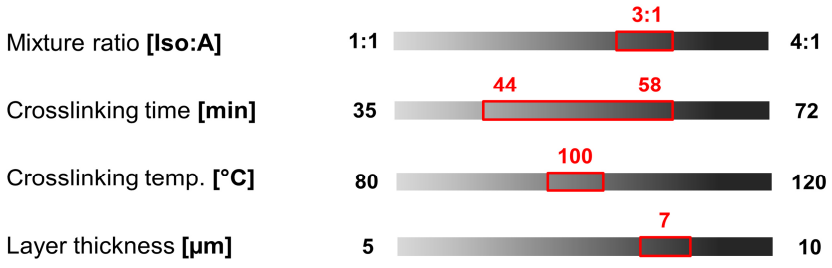

Figure 80 Optimized parameters for the adhesion system based on a mixture of MEKO blocked isocyanatesilanes (Iso) and aminosilanes (A) obtained via automated dip-coating.

Results

The pull-out forces of the brass-plated wire samples prepared by using blocked isocyanatesilane coupling agents are summarized in Figure 81.

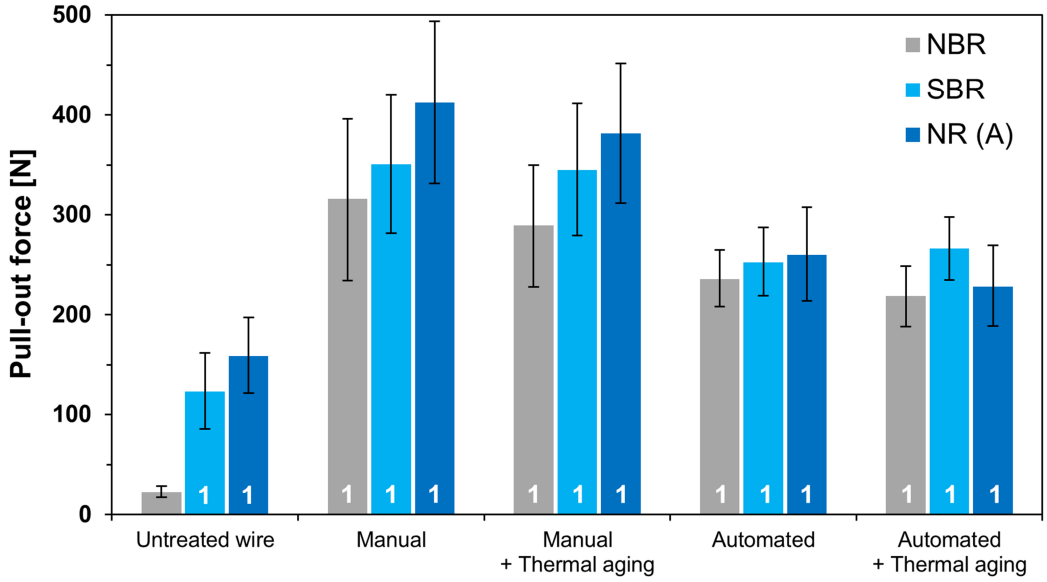

Figure 81 Adhesion strengths of NBR, SBR, and NR(A) to untreated brass-plated steel wires as well as to wires coated with blocked isocyanatsilanes (Iso:A=3:1, 1h @ 100°C) whether by manual or automated dip-coating as well as after thermal aging for 7 days at 70°C. The numbers in the lower part of the columns correspond to the degree of coverage after the T-test experiments, whereas columns showing no number correspond to a coverage of 0.

Here, it can be seen very clearly that the pull-out forces drastically increase using the manual coating procedure, namely up to values between 315 N and 413 N. NBR reaches a pull-out strength of 315 N, which is an increase by the factor 14 compared to the untreated wire. The adhesion strength between the brass-plated steel wire and SBR increases by the factor 3 using blocked isocyanatesilanes, which refers to a pull-out force of 351 N. However, the best results are obtained for the natural rubber mixture. With a factor of 2.5 the adhesion performance of the NR(A) sample increases, in relative terms, not that much compared to the other rubber types but it reached the highest absolute value of 413 N. The higher adhesion strength of the NR(A) sample may result – as already mentioned previously – from an increased number of double bonds found on the polymer backbone as natural rubber has no substituents compared to NBR and SBR. Additionally, the substituents may hinder the isocyanate group to bind on the polymer due to steric hindrance. Nevertheless, the pull-out strengths measured for all rubber types are already technologically relevant and consequently suitable for the use in real rubber products. Further, these adhesion strengths survive to a high

extend during thermal aging which is another big advantage. As already observed for the polysulfide silane coupling agent, the adhesion performances decrease down to adhesion strengths between 236 and 260 N by using the automated coating procedure. This is caused very probably by an incomplete crosslinking and drying step of the silane coating as an open tube furnace and not a closed drying chamber is used in the automated coating machine but may also be related to crack formation when rolling up the coated wire on the take-up real. Further, the limited process window requires an accurate parameter control, which may not be given permanently.

The degree of coverage after the T-test experiments was for all coated wire samples 1, so the bonding strength between the wire and rubber exceeds partially the cohesive strength of the rubber. However, this adhesion system shows high potentials for commercial usage, although the automation still has to be optimized.

In a subsequent step, the blocked isocyanatesilane adhesion system is tested on zinc-coated steel wires. The results of the corresponding pull-out tests can be seen in Figure 82.

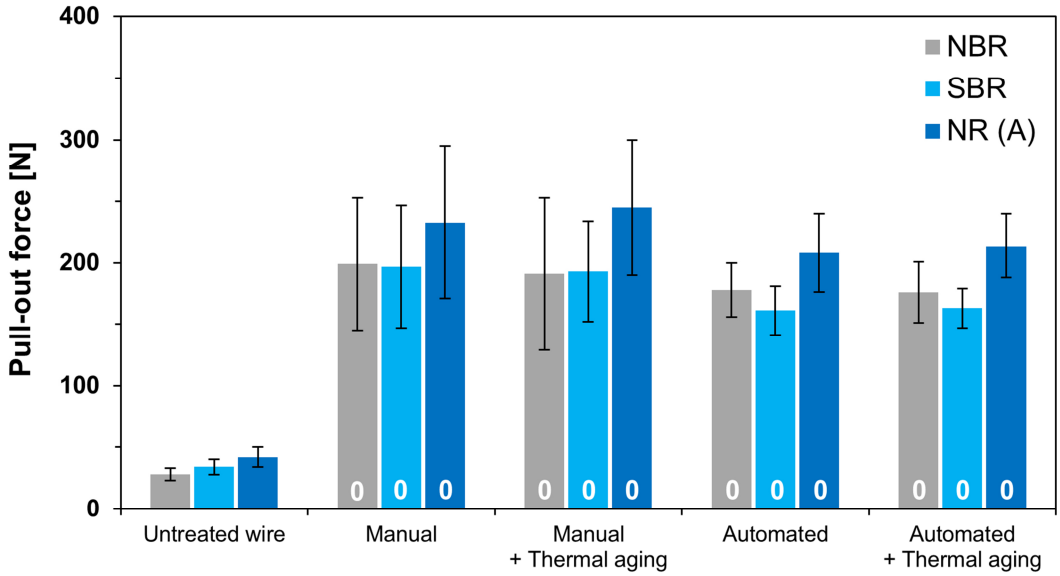

Figure 82 Adhesion strengths of NBR, SBR, and NR(A) to untreated zinc-plated steel wires as well as to wires coated with blocked isocyanatsilanes (Iso:A=3:1, 1h @ 100°C) whether by manual or automated dip-coating as well as after thermal aging for 7 days at 70°C. The numbers in the lower part of the columns correspond to the degree of coverage after the T-test experiments, whereas columns showing no number correspond to a coverage of 0.

Using isocyanatesilanes as adhesion promoters between rubber and plasma activated zinc the pull-out forces increase to values between 200 and 233 N. This roughly

corresponds to an increase of the adhesion strengths by factors between 7 for NBR and 5.5 for NR(A). Again – as for the brass-coated steel wires – thermal aging does not deteriorate the adhesion performance and the utilization of the automated coating procedure leads to decreased results. Beside this it is obvious to see that NR(A) leads to the best adhesion performance. In average, the adhesion strengths for NR(A) are 40 to 50 N higher than for SBR and NBR. However, the overall adhesion performance between rubber and brass-plated steel wires is significant higher than between rubber and zinc. This correlates very well with the coverage of the wire surfaces after the pull-out tests. The degree of coverage for the zinc-coated steel wires is always 0. Conversely, for the brass-plated steel wires the coverage is for each sample 1. Consequently one can conclude that in case of the zinc-coated wires the adhesion fails mostly between the silane anchor groups and the zinc oxide surface, which correlates well with observations of similar experiments in literature. Nevertheless, these results are very satisfactory and may be further improved by using alternative activation methods or metal substrates.

5.4.3 Blocked isocyanate phosphonic acid

Principle

In a further approach, phosphonic acids (PAs) were used as anchor groups instead of silanes for the bifunctional isocyanate based adhesion promoter (Figure 83). It is generally known that phosphonic acids bind very well to copper oxide [62] and zinc oxide[276], which can normally found on the surface of the brass-coated and zinc-coated steel wires, respectively. In principle, there is one big difference between the use of phosphonic acids and silanes as anchor groups, namely phosphonic acids form self-assembled monolayers on the wire surface and not networks as in the case of silanes. Thus, higher efficiencies in the material usage can be achieved. The principal bonding mechanism of the MEKO blocked isocyanate group to the rubber macromolecules is similar to the MEKO blocked isocyanatesilanes as explained in Chapter 5.4.2.

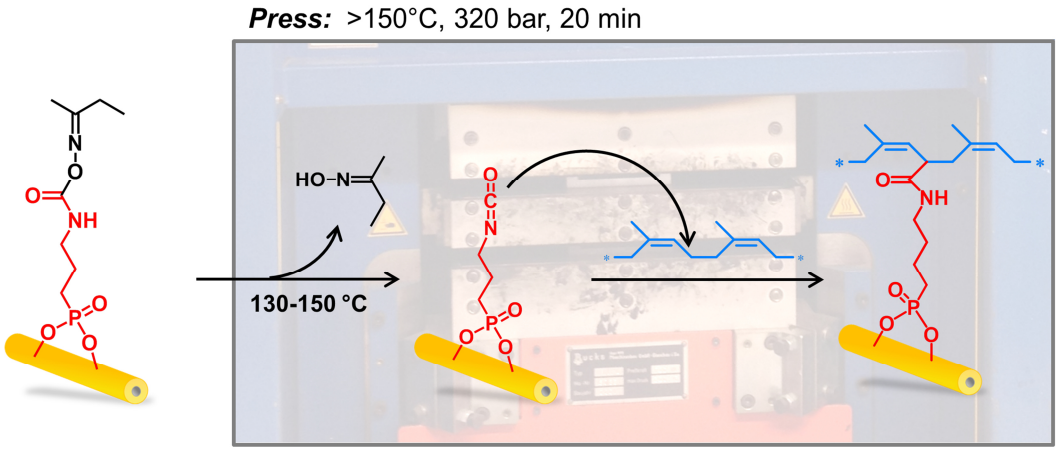

Figure 83 Principle of the blocked isocyanate-PA adhesion system.

In order to investigate the deblocking temperature of the blocked isocyanate-PA thermo gravimetric analysis was performed. As shown in Figure 84, using a dynamic temperature increase the isocyanate group is deblocked at temperatures between 120 and 265°C. But as mentioned before, during the real vulcanization procedure – where the temperature is rapidly increased and maintained at the final temperature – the MEKO group escapes already entirely at temperatures in the range of 120 and 150°C which correlates again very well with the observations from the blocked isocyanatesilane (Figure 77) and with the literature.

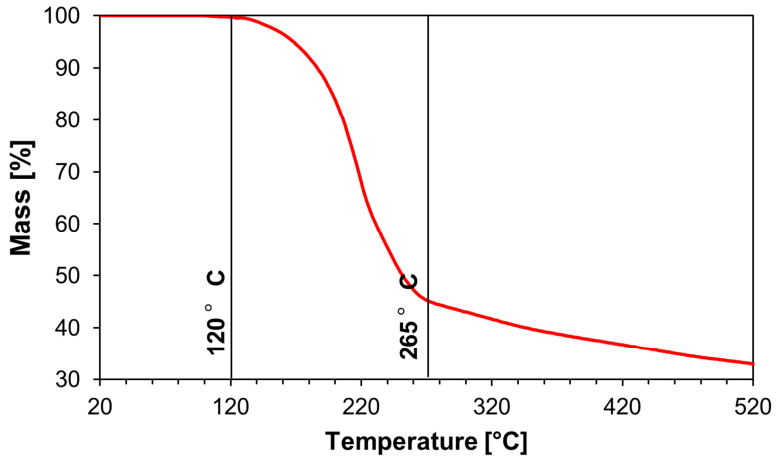

Figure 84 Mass loss of the MEKO blocked isocyanate-PA due to splitting-off MEKO at elevated temperatures detected by thermo gravimetric analysis (TGA).

Optimization of the process parameters

As already mentioned, phosphonic acids do not form sol-gel networks but self-assembled monolayers on metal oxides. Further, no catalyst is required to bind the phosphonate groups to the wire surface. Because of this the blocked isocyanate-PA is simply solved in MeOH in which 5 mg/ml was found to be an optimal concentration for the dip-coating process (Figure 85). Using contact angle measurements (water, diiodomethane) on brass-platelets, a full coverage of the brass surface with blocked isocyanate-PAs was observed after 12 hours dipping. Hence, the dip-time was set to 12 hours. In principle - after rinsing and drying - the freshly dip-coated wires could be used already for the T-test experiments. However, it was further investigated if an additional tempering step for 60 minutes at 90°C in a drying chamber improves the adhesion performance for which reason the coated wire samples were subjected to a heating step.

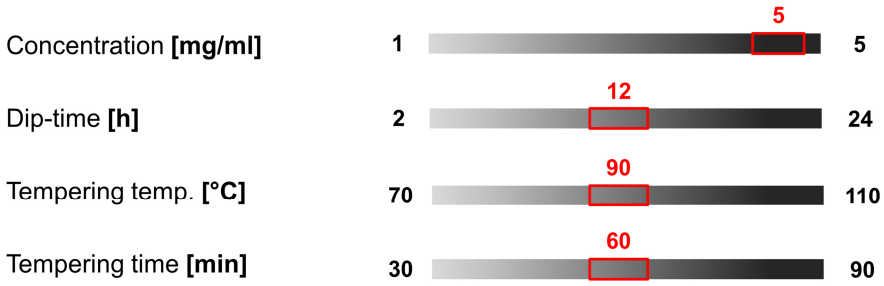

Figure 85 Optimized parameters for the blocked isocyanate-PA adhesion system obtained via the manual coating process.

For the blocked isocyanate-PA adhesion system the in-house constructed automated wire coating machine was not suitable. During the coating process the coating solution was not able to keep as clean as necessary for the production of well-defined self-assembled monolayers and the driving rate was not able to reduce so that the dip-time would be 12 hours for each wire section. Therefore, these adhesion systems were only processed manually.

Results

Figure 86 depicts the results of the blocked isocyanate-PA adhesion system. The performance of these bifunctional molecules was investigated for brass- and zinc-plated steel wires.

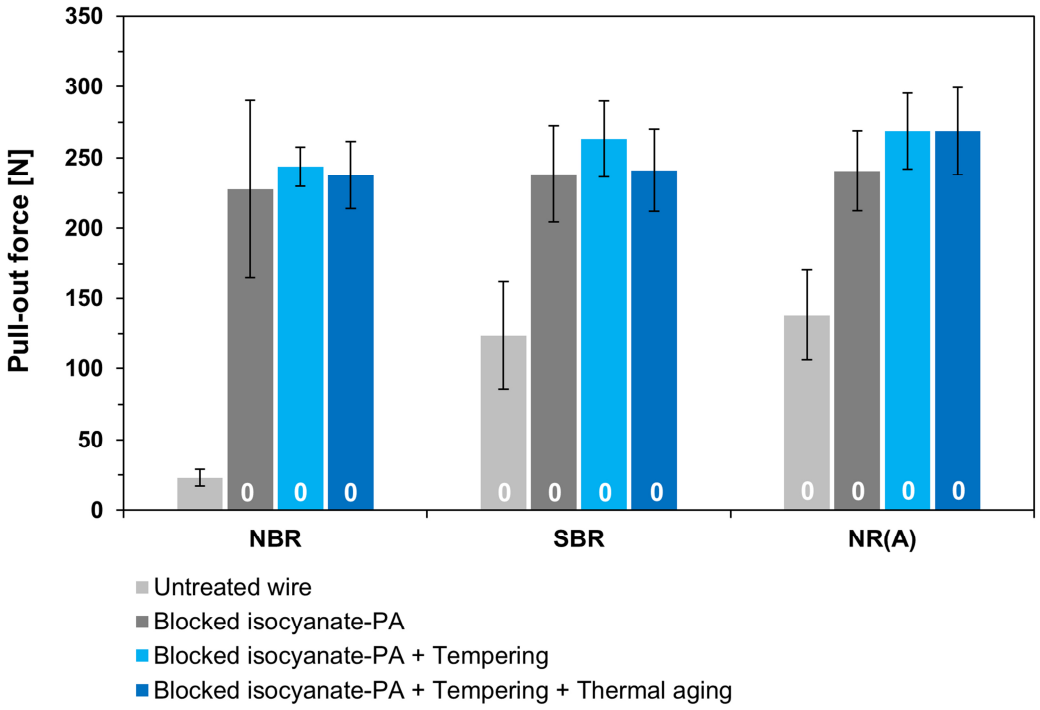

Figure 86 Adhesion strengths of NBR, SBR, and NR(A) to untreated zinc-plated steel wires as well as to wires coated with blocked isocyanate-PA (5 mg/ml), with and without tempering for 1 hour at 90°C by manual dip-coating as well as after thermal aging for 7 days at 70°C. The numbers in the lower part of the columns correspond to the degree of coverage after the T-test experiments, whereas columns showing no number correspond to a coverage of 0.

But as the adhesion between zinc and rubber failed completely, only the results of the brass-plated wires are discussed. By comparing the pull-out forces of the coated wire samples after tempering and thermal aging no big differences can be seen. All samples show at each stage of the coating procedure as well as after thermal aging a pull-out force between 227 N and 269 N with partially very high standard deviations. However,

compared to the untreated wires the adhesion between the different rubber types and brass wires could be improved significantly namely tenfold for NBR and doubled for SBR and NR(A). Hence, this adhesion promoter is also quite powerful but not as strong as the isocyanate system with the silane instead of the phosphonic acid as anchor group. Due to the fact, that the coverage of the wire surface after the pull-out tests is 0 for all samples and because no phosphor is detected on the uncovered brass surface one may conclude that the adhesion fails between the wire surface and the phosphonic acid group. Also tempering does not significantly improve the adhesion performance, for which this after-treatment could eventually be neglected as it is another energy and time consuming step in the coating procedure. Another reason for the lower adhesion performance of coupling agents based on phosphonic acids compared to the silane based adhesion promoter may be that in case of the silanes polymer chains interdiffuse into the silane network, which further improves its adhesion performance [56]. Nevertheless, this adhesion system features useful bonding properties, which may be of great interest for applications within and outside the area of rubber technology.

5.4.4 Acyl acide phosphonic acid

Principle

As an alternative to the blocked isocyanate coupling agents the capability of acyl azides as functional groups in adhesives was investigated. This system is based on the same principle as the blocked isocyanate, namely an unprotected isocyanate group is formed at elevated temperatures. Compared to the blocked isocyanate group, in the case of the acyl azide group the isocyanate is formed by splitting of nitrogen (N_2) at temperatures above 40 °C (Figure 87). This reaction is also known as the Curtius rearrangement [277-279]. The low deblocking temperature of the isocyanate group is a significant disadvantage compared to the MEKO blocked isocyanates as temperatures above 40 °C can appear very easily during transportation and coating processes. However, after the transformation of the acyl azide group to the isocyanate group it is highly reactive and can bind to the allyl-hydrogen atom of the rubber macromolecules.

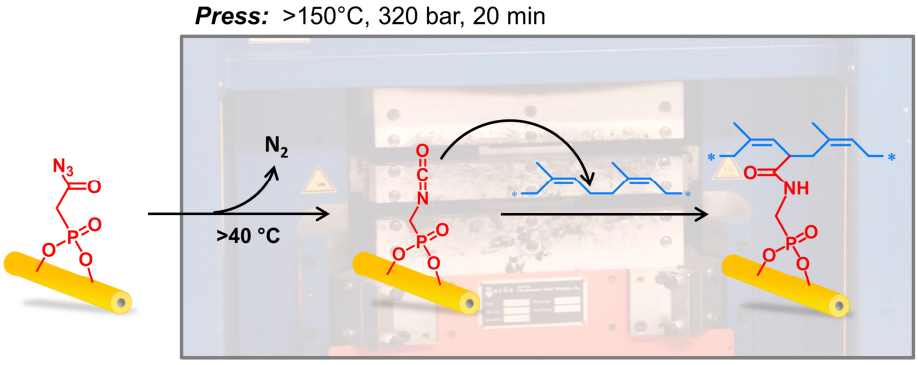

Figure 87 Principle of the acyl azide-phosphonic acid adhesion system.

The synthetic rout which was used to obtain this new bifunctional molecule is rather time-consuming (five steps) and leads with 15.8% to very low yields. The final molecule has to be handled carefully because at temperatures above 40°C it already loses its functionality.

Optimization of the process parameters

Identically to the blocked isocyanate-PAs the acyl acide-PAs form self-assembled monolayers on surfaces. Consequently, the O_2-plasma activated wires were dip-coated for 12 hours in a solution containing 5 mg acyl azide-PA per ml MeOH (Figure 88). Here, tempering of the wire sample after dip-coating was not reasonable because the acyl azide group is already transformed to isocyanate at temperatures higher than 40°C.

Figure 88 Optimized parameters for the acyl azide-PA adhesion system obtained via manual dip-coating.

Results

Compared to the other adhesion systems developed for sulfur crosslinkable rubber mixtures acyl azide-PAs show the worst performances (Figure 89).

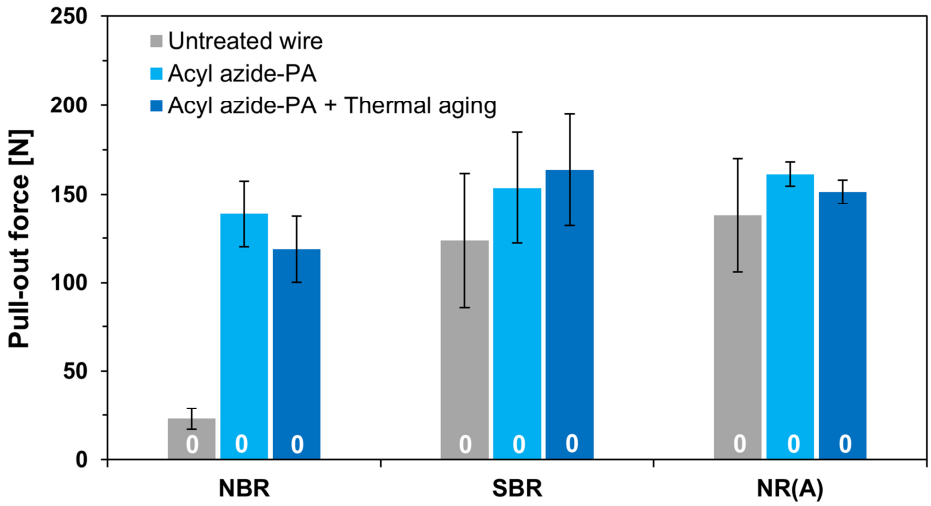

Figure 89 Adhesion strengths of NBR, SBR, and NR(A) to untreated zinc-plated steel wires as well as to wires coated with acyl azide-PAs (5 mg/ml) by manual dip-coating before and after thermal aging for 7 days at 70°C. The numbers in the lower part of the columns correspond to the degree of coverage after the T-test experiments.

For NBR pull-out forces of 139 N were obtained, which is – in relative terms – six times higher than for the untreated wire. The adhesion performance of SBR and NR(A) were only slightly improved by the acyl azide-PA molecules since their pull-out strengths increase for only 20 to 30 N compared to the untreated wires. Nevertheless, these values do not decrease noteworthy by reason of thermal aging. Consequently, transforming of the acyl azide groups to isocyanates is not that effective as the unblocking reaction of the MEKO blocked isocyanate groups. Further, coverages of 0 indicate that the adhesion failed between brass and the phosphonic acid anchor group. However, these experiments led to the conclusion that the adhesion performance of the acyl azide adhesion system is not very efficient and therefore it is ill-suited as adhesion promoter between rubber and metal substrates for technical processes, but in principle functionally.

5.4.5 Methacrylatesilane

In order to chemically link radically crosslinkable polymers to the wire surface methacrylate silanes were investigated. These bifunctional molecules were already patented by Milliken & Company in 2002 for a very similar application [280]. They used these molecules to promote the adhesion between textiles and rubber. Interestingly, they did not investigate the performance of this adhesion system on metallic substrates. Further, without the use of an additional resin layer on the methacrylate coating the bonding strengths were pretty poor. However, the commercially available methacrylatesilanes used in this study are applied for the first time on metals to enhance the adhesion on rubber.

Principle

As depicted in Figure 90, methacrylate was used as functional group to link the bifunctional molecule to the rubber polymers. Based on the results of the previously investigated adhesion systems (Chapter 5.4.1 to 5.4.4) silanes were selected as anchor groups. First, the methacrylate silanes are linked to the plasma-activated wire surface via manual dip-coating. Afterwards, the coated metal wires are incorporated into the rubber compound and placed in the heating press. However, during the radical crosslinking of the rubber macromolecules at elevated temperature and pressure various binding reactions occur. For instance, an activated initiator radical snaps the allyl-hydrogen atom of the e.g. natural rubber (cis-polyisoprene) and consequently a radical remains on the polymer backbone. On this radical, the methacrylate-group can bind chemically via the terminal double bond. In doing so, the rubber is linked to the metallic wire surface by means of a chemical bonding mechanism.

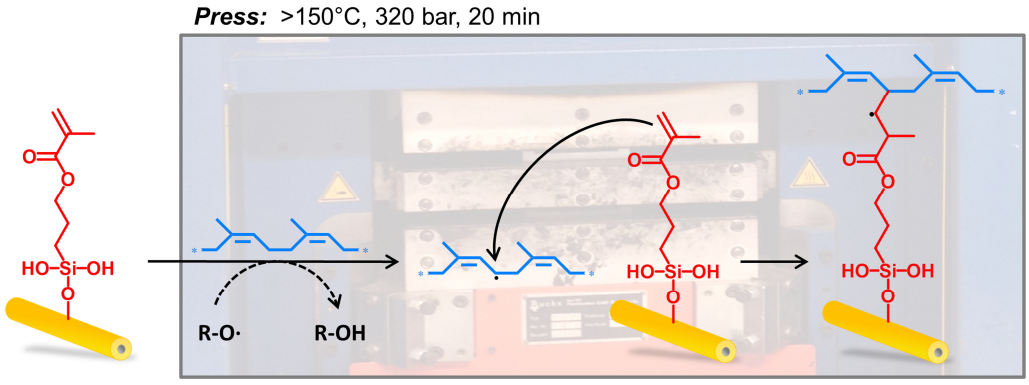

Figure 90 One possible binding mechanism of the methacrylate silane adhesion system.

Optimization of the process parameters

The methacrylate silane coupling agent for radical crosslinkable polymers was applied by the same way as the polysulfide silane as well as the blocked isocyanatesilane adhesion systems. As catalyst and drying auxiliary for the formation of the silane film bis[3-(trimethoxysilyl)propyl]amine was used. Thus it was observed that the grade of adhesion is best at mixture ratios between 2 to 1 and 4 to 1 (Figure 91). The optimal crosslinking time was found to be 40 to 80 minutes and the preferred crosslinking temperature was observed between 100 and 160 °C. Further, these optimized process conditions show a wide process window. This is a very great advantage of this system as the process conditions do not have to be set to a specific value, which facilitates their use on large-scales. However, the perfect layer thickness for satisfying adhesion strengths was located at 8 µm.

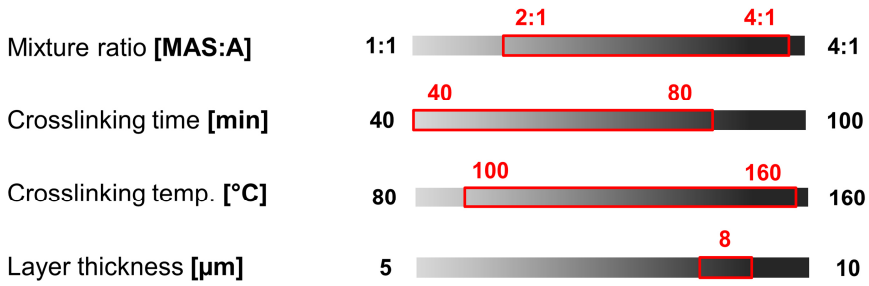

Figure 91 Optimized parameters for the methacrylate silane (MAS) adhesion system obtained via manual dip-coating.

Results

The adhesion performance of the methacrylate silane was tested to a simple EPDM mixture (Table IX).

Table IX Compound composition of EPDM in phr.

	EPDM mixture
EPDM rubber	100
Carbon black	67.5
Silitin N85	20.5
Zinc salts	1
White oil	30
Peroxide	6.5

As can be seen in Figure 92, both, the untreated brass- and zinc-coated steel wires show with pull-out strengths of 15 N and 21 N, respectively, no adhesion to the EPDM rubber polymers. Though, using methacrylate silanes as adhesion agents the adhesion forces increase drastically, namely up to values of around 430 N for the brass-plated steel wires and 246 N for the zinc-plated one. These excellent adhesion properties – especially for the brass-plated wires – remain unchanged during thermal aging.

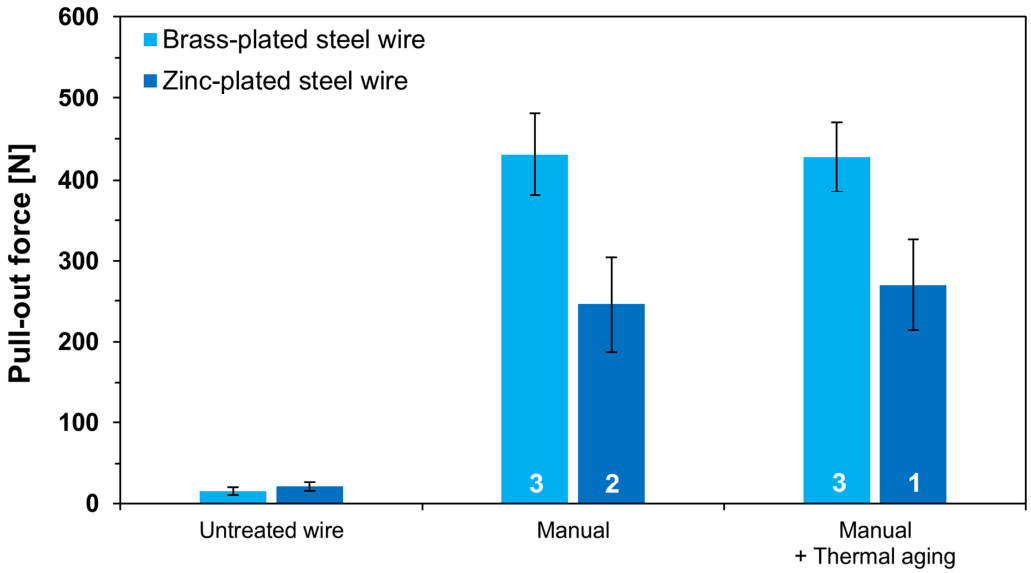

Figure 92 Adhesion performance of EPDM-rubber to untreated brass-plated and zinc-plated steel wires as well as to wires coated with methacrylatsilanes (MAS:A=3:1, 40 min @ 160°C) by manual dip-coating before and after thermal aging for 7 days at 70°C. The numbers in the lower part of the columns correspond to the degree of coverage after the T-test experiments, whereas columns showing no number correspond to a coverage of 0.

There is one big difference in the results between the methacrylate silane bonding system and the approaches used for the sulfur crosslinked rubber compounds. The samples where the methacrylate silane was used to improve the adhesion strength between EPDM and the metal wires have a coverage between 2 and 3 after the manual coating procedure. For the brass-plated wires, the degree of coverage is also preserved after thermal aging. Therefore it may be concluded that the strength of the bonding between the brass surface and the silane anchor group as well as the linkage of the methacrylate group to the rubber polymer exceeds the strength of the cured rubber network. Consequently, the real adhesion strength is still higher than the measured one. Nevertheless, these results are highly promising and path the way for a commercial use in radical crosslinked rubber systems.

In a further experiment, the adhesion performance of the bifunctional methacrylate-silane was investigated on zinc-coated cables. With a diameter of 10 mm the cables are used mostly in conveyor belts incorporated into EPDM rubber compounds. For the coating procedure the same process parameters were used as for the wire samples.

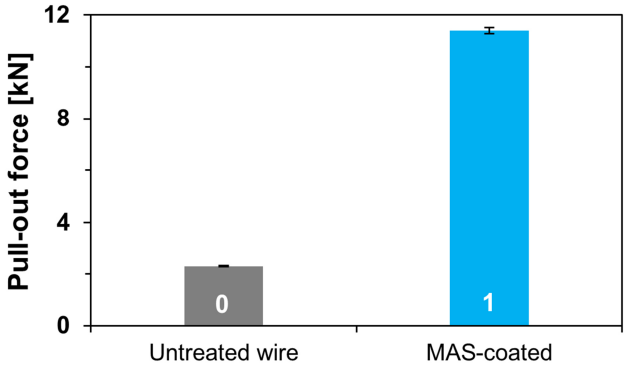

Figure 93 Adhesion performance of EPDM-rubber to untreated zinc-plated steel cords as well as to cords coated with methacrylatsilanes (MAS:A=3:1, 40 min @ 160°C) by manual dip-coating. The numbers in the lower part of the columns correspond to the degree of coverage after the T-test experiments.

As shown in Figure 93, using methacrylatsilanes the pull-out force increases from 2.3 kN (untreated wire) to 11.4 kN (MAS-coated wire), which is an increase by a factor of 5. Consequently, the methacrylatsilane adhesion system is highly suitable to be applied in real rubber products if the costs are competitive with the conventional systems.

5.4.6 Conclusion

Several bifunctional adhesion promoters were synthesized and tested regarding their bonding performance to various rubber compounds. Thus, the switch from the typical mechanically interlocking bonding mechanism between rubber and metal devices to an adhesion system based on chemical linkage was generally successful for all investigated types of rubber, whether they are vulcanized by sulfur or peroxides. For the sulfur crosslinked rubber mixtures as NR, NBR, and SBR the best working bifunctional coupling agent was the MEKO blocked isocyanatesilane followed by the polysulfide silane and MEKO blocked isocyanate-PA. The worst adhesion properties were definitely observed for the acyl azide-PAs. This is on the one side because the transformation of the acyl azide to the isocyanate group is too sensitive as it appears already at 40°C and on the other side due to the phosphonic acid group, which showed relatively poor adhesion performances to the wire surfaces, especially to zinc-plated steel wires. However, the MEKO blocked isocyanatesilanes take advantage of both, a very sensitive but well protected functional group as well as an anchor group, which shows good bonding performances to metallic substrates. Compared to the blocked isocyanate silane, the polysulfide silane is not that efficient in binding the rubber polymers and the blocked isocyanate-PA cannot bind strong enough to the wire surface. Therefore, the blocked isocyanatesilane is the preferential binding promoter for real rubber products, also because it is not limited to polymers containing double bonds as long as the polymers exhibit an allyl-hydrogen atoms other functional substituents as alcohols, amines or carboxylic acids, just to name a few. Unfortunately, isocyanates are highly toxic in their unprotected state which may complicate the technical realization.

The application area of the MEKO blocked isocyanatesilane could further be expanded by varying the blocking group, which enables to deblock the isocyanate group at different temperatures [275].

The best results were achieved for the adhesion agent developed for radical cured rubber systems. Thus, pull out forces of 430 N were obtained for the brass-plated wire sample and 11.4 kN for the zinc coated cables. Further, the degree of coverage for the brass-coated steel wires after the pull-out tests was found to be 3 and 2 for the zinc-coated wires. Therefore, one can conclude that the real pull-out forces are even greater than the measured one. However, the fact that the methacrylate silane coupling agent

leads to coverages up to 3 and the blocked isocyanatesilanes as well as the polysulfide silanes at the utmost to 1, it can be concluded that the blocked isocyanate and the polysulfide groups may hinder the silane groups to bind efficiently on the wire surface. Consequently, there is still room for optimizations.

In addition, all adhesion systems maintain their adhesion performances during thermal aging, which is very valuable for technical elastomer products. Although some bonding systems show already excellent adhesion performances after manual dip-coating, the automated wire-coating procedure still needs to be improved.

Another big advantage is that the rubber-metal adhesion is not limited to brass- or zinc coated reinforcing devices. By using a suitable substrate pretreatment also other metals such as aluminium or even steel could be used.

Further, the experiments showed that the bonding properties of the chemical adhesion systems are not really dependent on the compound composition as in case of the rubber-to-brass bonding. Thus, low sulfur and cobalt loadings can be applied. Hence, the rubber mixtures can be optimized in order to achieve good mechanical properties, which leads to improved product performances.

In summary, the observed performances of the in-house developed adhesion systems based on organofunctional molecules – especially the bifunctional silanes – are a major step in the right direction concerning the elastomer-metal adhesion due to its simplicity, performance, and broad applicability. Where they will find their place in rubber products depends finally on the cost efficiency, processibility in large scales, and environmental compatibility.

6 SUMMARY AND OUTLOOK

The aim of this thesis was to investigate the rubber-to-metal adhesion and to develop new adhesion promoter based on bifunctional molecules. Since many products for automotive, aerospace and technical applications need mechanical reinforcements to achieve the required performances, the elastomer-metal bonding is a crucial topic in rubber technology.

It is generally known that the adhesion performance depends on many parameters, especially on the composition of the rubber compounds as well as on the wire properties. Therefore, the first task of this work was first to investigate seven (**W1**-**W7**) wire samples, which have according to their manufacturer the same specifications but differ in their adhesion properties.

By watching the optical and morphological appearance of the wire surfaces using optical as well as scanning electron microscopy no significant differences were observed. Therefore, the specimens were investigated regarding their elemental composition by EDX and XRD. Thus, no linear correlation between the brass composition and the pull-out forces was detected. However, it was shown that adhesion fails if the Cu level of the brass layer is over 70 wt%. Additionally, it could be shown that the appearance of β-brass has a negative impact on the rubber-brass adhesion because compared to α-brass it is rather brittle and consequently detaches easily from the wire surface. On closer inspection, a Cu rich phase in α-brass was detected using XRD. Thus, it was observed that the adhesion performance increases with decreasing amount of the Cu rich phase in α-brass. This could be attributed to the Kirkendall effect, which states that the homogeneity of an alloy depends on the diffusion coefficients of the single components as well as on its production parameters. As a consequence, the brass layer is inhomogeneously formed and may get so called Kirkendall voids. This inhomogeneous brass layer could be the reason for a faulty build-up of the rubber-brass adhesion interface since the formation of the Cu_xS-structures strongly depends on the diffusion behavior of the copper and zinc ions in the brass layer. Hence, the wires showing bad adhesion properties exhibit high percentages of Cu rich phase in the brass layer, which is very likely caused by ill-defined parameter control during the wire manufacturing process.

In the second part of this thesis, the influences of various rubber mixtures on the rubber-brass adhesion interface were investigated using the olefin-metathesis method. Thus, in a first step, the focus was set on the investigation of different rubber types as NR, NBR and SBR. Due to steric and blocking effects of various functional groups on the rubber macromolecules the olefin-metathesis degradation time varies considerably, namely 6 hours for NR, 4 hours for NBR and only 1 hour for SBR. Beside this it was shown that the reaction of sulfur with the brass layer leads in case of NR and SBR to the build-up of a well-defined and structured adhesion interface. As a consequence, rubber mixtures based on NR and SBR show generally good adhesion performances.

However, well defined sulfur structures and thus satisfying adhesion properties between NBR and brass can just be achieved using high silica loadings. Experiments with real NBR compounds demonstrated the dependence of the adhesion performance on the amount of nitrile groups in the rubber compound as well as on the silica content. The more silica and the less nitrile groups in the rubber mixture the better the NBR-brass bonding characteristics. However, further experiments using model systems, which were based on low molecular nitrile compounds led to the assumption that nitrile groups prevent the formation of Cu_xS-structures by degrading the brass-coating of the steel wire. Evidences to support this assumption are increased Fe-contents in the EDX spectra as well as indentations on the brass surface when the brass-plated steel wires get in contact with nitrile groups (low molecular weight compounds or NBR). This observations correlate well with the fact that by using silica NBR forms well-defined adhesion interfaces because the silanol groups (Si-OH) form hydrogen bonds with the nitrile groups (-CN) preventing the degradation of the brass layer and enabling the formation of Cu_xS-structures. Consequently, that is the reason why NBR mixtures with 50 phr silica reach pull-out forces of 334 N and not just 23 N as in the case without the use of silica.

But not only differences in the polymer structure, also typical additives and fillers used in rubber chemistry can influence the olefin-metathesis reaction as well as the build-up of the rubber-brass adhesion interface. Thus - in a second series - NR-compounds with different additives (Co-stearate, silica, and formaldehyde resin) were compared. All samples showed similar degradation times of 6 hours, which leads to the conclusion that

the quality and velocity of the olefin-metathesis is not influenced by commonly applied fillers, adhesion promoters or other auxiliaries.

Comparing the SEM pictures of these NR samples with different additives, one can see that all samples differ in their microstructures. However, all interfaces show a structured and partially well-defined surface morphology typically observed in such adhesion layers. Also the EDX-values for sulfur between 6 to 8 atom% are pointing towards Cu_xS-structures. Although the different additives lead to variable pull-out forces and microstructures, no general trend between these two properties could be observed.

The third topic of this thesis was to develop new bonding systems which are based on organic bifunctional molecules. Thereby, the rubber-metal adhesion is not achieved by mechanical interlocking of the rubber macromolecules in the brass layer but by chemical linkage. This was accomplished by using bifunctional molecules, which feature a functional group (head group) to bind the adhesive to the polymer and an anchor group (terminal group) that links the adhesion promoter to the inorganic substrate.

For the sulfur cross-linked rubber, mixtures as NR, NBR, and SBR the best working bifunctional coupling agent to brass-plated steel wires was the MEKO blocked isocyanatesilane (413 N) followed by the polysulfide silane (310 N), and MEKO blocked isocyanate-PA (269 N). With 164 N acyl azide-PA showed definitely the worst adhesion properties. This is on the one side because the transformation of the acyl azide to the isocyanate group is too sensitive as it appears already at 40°C and on the other side due to the phosphonic acid group, which showed relatively poor adhesion performances to the wire surfaces, especially to zinc-plated steel wires. However, the MEKO blocked isocyanatesilanes take advantage of both, a very sensitive but well protected functional group as well as an anchor group, which shows good bonding performances to metallic substrates. Therefore, the blocked isocyanatesilane is the preferential binding promoter for real rubber products, also because it is not limited to polymers containing double bonds as long as the polymers exhibit allyl-hydrogen atoms or other functional substituents as alcohols, amines and carboxylic acids where the isocyanate group can connect. Unfortunately, isocyanates are highly toxic in their unprotected state which may complicate the technical realization.

The reason for the lower adhesion performance of coupling agents based on phosphonic acids (SAMs) compared to the silane based adhesion promoter (Sol-Gel networks) may be that in case of the silanes rubber polymer chains interdiffuse into the silane network, which improves the adhesion performance. Further, networks are able to bind generally stronger on substrates than single molecules. Consequently, networks are more suitable as rubber-brass adhesion promoter than monolayers.

The best results were achieved for the adhesion promoter developed for peroxide cured rubber systems, the methacrylatesilane. Here, pull out forces of 430 N were obtained for the brass-plated wire sample and 11.4 kN for the zinc-coated cables. Further, the degree of coverage for the brass-coated steel wires after the pull-out tests was found to be 3 and 2 for the zinc-coated wires. Therefore, one can conclude that the real pull-out forces are even greater than the measured one, which signifies that this adhesion system provides very strong adhesion performances.

However, all adhesion systems maintain their adhesion performances during thermal aging, which is very valuable for technical elastomer products. Although some bonding systems show already excellent adhesion performances after manual dip-coating, the here used automated wire-coating procedure has still to be improved. The experiments indicate that the heating step in the automated procedure is ineffective because an open tube furnace is used and not a closed drying chamber as in the manual coating procedure.

One of the biggest advantages of these systems is that the rubber-metal adhesion is not limited to brass- or zinc coated reinforcing devices. By using a suitable substrate pretreatment also other metals such as aluminium or even steel could be used. Thus, the area of application is considerably extended.

Additionally, the experiments demonstrated that the bonding properties of the chemical adhesion systems do not really dependent on the compound composition as in case of the rubber-to-brass bonding. Thus, low sulfur and cobalt loadings might be applied and the rubber mixtures might be optimized in order to achieve good mechanical properties. As a consequence, product performances can be drastically improved.

In summary, the observed performances of the in-house developed adhesion systems based on bifunctional molecules – especially the bifunctional silanes – may be quickly established in rubber technology due to its simplicity, efficiency, and wide applicability.

In which technical field they will be implemented first depends finally on the cost efficiency, processibility in large scales, and environmental compatibility.

This thesis forms a basis for many possible continuing and detailed studies. The mechanism of the brass layer degradation caused by NBR has still not been clarified for which also here detailed investigations are necessary. Additionally, the corrosion protection behavior of the silane and phosphonic acid coatings has to be investigated because this would have a significant impact on the lifetime of the elastomeric commodities. And of course, up to the point of product maturity, the bifunctional adhesion promoter still have to be optimize to be competitive with the conventional adhesion systems.

7 REFERENCES

[1] Röthmeyer F, Sommer F (2006) Kautschuk Technologie; Carl Hanser Verlag: München, Wien, pp 8

[2] Statista, Weltweiter Verbrauch von Natur- und synthetischem Kautschuk in den Jahren 1990 bis 2013: http://de.statista.com/statistik/daten/studie/200677/umfrage/weltweiter-verbrauch-von-natur-und-synthetischem-kautschuk-seit-1990 (26.07.2015)

[3] Halladay JR,Warren PA (2003) Handbook of Rubber Bonding; Rapra Technology Limited, pp 57-58

[4] Kretschmar T, Hofer F, Hummel K (1992) Kaut Gummi Kunst 45:1038

[5] Kim J, van Ooij WJ (2002) Rubber Chem Technol 75:199

[6] Van Ooij WJ (1977) Kaut Gummi Kunst 30:739; 30:833

[7] Davies JR (1984) Kaut Gummi Kunst 37:493

[8] Jeon GS, Kang UI, Jeong SW, Choi SJ, Kim SH (2005) J Adhes 19:1325

[9] Van Ooij WJ, Kleinhesselink A (1980) Appl Surf Sci 4:324

[10] Giridhar J, van Ooij WJ (1992) Surf Coating Tech 52:17

[11] Giridhar J, van Ooij WJ (1992) Surf Coating Tech 53:243

[12] Van Ooij WJ, Giridhar J, Ahn JH (1991) Kaut Gummi Kunst 44:348

[13] Shemenski RM, Su Y-Y (2003) Gummi Fas Kunstst 56:777

[14] Van Ooij WJ (1984) Rubber Chem Technol 57:421

[15] Fulton WS (2005) Rubber Chem Technol 78:426

[16] Fulton WS, Wilson JC (2003) Handbook of Rubber Bonding; Rapra Technology Limited, pp 197-212

[17] Chandra AK, Mukhopadhyay R, Konar J, Ghosh TB, Bhowmick AK (1996) J Mater Sci 31:2667

[18] Maemers G, Mollet J (1978) J Elastom Plast 10:241

[19] Van Ooij WJ (2003) Handbook of Rubber Bonding; Rapra Technology Limited, pp 163-195

[20] Ziegler E, Macher J, Gruber D, Pölt P, Kern W, Lummerstorfer T, Feldgitscher C, Holzner A, Trimmel G (2012) Rubber Chem Technol 85:264

[21] Kretschmar T, Hofer F, Hummel K, Sommer F (1993) Kaut Gummi Kunst 46:710

[22] Goodyear C (1844) Improvement in India-Rubber Fabrics. US Patent 3633 A, Jun 15, 1844

[23] Morrison NJ, Porter M (1984) Rubber Chem Technol 57:63

[24] Skinner TD (1972) Rubber Chem Technol 45:182

[25] Kapur RS, Koenig JL, Shelton JR (1974) Rubber Chem Technol 47:911

[26] Coran AY (1964) Rubber Chem Technol 37:679

[27] Luyt AS (1991) J Appl Polym Sci 48:449

[28] Kok CM (1985) Eur Polym J 21:579

[29] Ghosh P, Katare S, Patkar P, Caruthers JM, Venkatasubramanian V, Walker KA (2003) Rubber Chem Technol 76:592

[30] Versloot P, Haasnoot JG, Reeddijk J, Duin MV, Put J (1995) Rubber Chem Technol 68:563

[31] Ignatz-Hoover F (1999) Rubber Chem Technol 72:318

[32] Ikeda Y, Yasuda Y, Ohashi T, Yokohama H, Minoda S, Kobayashi H, Honma Tetsuo (2015) Macromolecules 48:462

[33] Ostromislensky II (1915) J Russ, Phys Chem 47:1467

[34] Loan LD (1967) Rubber Chem Technol 40:149

[35] Hofmann W (1987) Kaut Gummi Kunst 40:308

[36] Keller RC (1988) Rubber Chem Technol 61:238

[37] Baldwin FP, Verstrate G (1972) Rubber Chem Technol 45:709

[38] Hamed GR, Donatelli T (1983) Rubber Chem Technol 56:450

[39] Orband A, Anthoine G, Roebuck H (1986) Kaut Gummi Kunst 39:37

[40] Kim JM, van Ooij WJ (2003) J Adhes Sci Technol 17:165

[41] Evans LR, Hope JC, Okel TA (1996) Gummi Fas Kunstst 49:128

[42] Jeon GS, Han MH (1999) J Adhes Sci Technol 13:153

[43] Waddell WH, Evans LR, Goralski EG, Snodgrass LJ (1996) Rubber Chem Technol 69:48

[44] Rooke M (2003) Handbook of Rubber Bonding; Rapra Technology Limited, pp 81-120

[45] Jeon GS (2009) J Adhes sci 23:913

[46] Van Ooij WJ, Harakuni PB, Buytaert G (2009) Rubber Chem Technol 82:315

[47] Chandra AK, Biswas A, Mukhopadhyay R, Bhowmick AK (1994) J Adhes 44:177

[48] Hamed GR, Huang J (1991) Rubber Chem Technol 64:285

[49] Van Ooij WJ, Biemond MEF (1984) Rubber Chem Technol 57:686

[50] Hotaka T, Ishikawa Y, Mori K (2007) Rubber Chem Technol 80:61

[51] Ling CY, Hirvi JT, Suvanto M, Bazhenov AS, Ajoviita T, Markkula K, Pakkanen TA (2015) Chem Phys 453-454:7

[52] Fulton WS, Smith GC, Titchener KJ (2004) Appl Surf Sci 221:69

[53] Darwish NA, Shehata AB, Abou-Kandil AI, Abd El-Megeed AA, Lawandy SN (2013) Int J Adhes Adhes 40:135

[54] Patil PY, van Ooij WJ (2005) Rubber Chem Technol 78:155

[55] Magg H (1993) Kaut Gummi Kunst 46:139

[56] Ebnesajjad S (2014) Surface Treatment of Materials for Adhesive Bonding, Second Edition; Elsevier Inc: Amsterdam, 301-307

[57] Picard L, Phalip P, Fleury E, Ganachaud F (2015) Prog Org Coat 80:120

[58] Guerrero G, Mutin PH, Vioux A (2001) Chem Mater 13:4367

[59] Pellerite TD, Boardman LD Wood EJ (2003) J Phys Chem B 107:11726

[60] Pawsey s, McCormick M, De Paul S, Graf R, Lee YS, Reven L, Spiess HW (2003) J Am Chem Soc 125:4174

[61] Gao W, Dickinson L, Grozinger C, Morin FG, Reven L (1996) Langmuir 12:6429

[62] Queffélec C, Petit M, Janvier P, Knight DA, Brujoli B (2012) Chem Rev 112:3777

[63] Schreiber F (2000) Prog Surf Sci 65:151

[64] Wang D, Bierwagen GP (2009) Prog Org Coat 64:327

[65] Van Der Aar CPJ, van Ooij WJ (2000) Rubber to metal bonding by silane coupling agents US 6,409,874 B1, Oct 23, 1997

[66] Jayaseelan SK, van Ooij WJ (2003) Gummi Fas Kunstst 56:497

[67] Görl U (1998) Gummi Fas Kunstst 51:416

[68] Van Ooij WJ, Jayaseen SK, Mee EA (2005) Silane coatings for bonding rubber to metals US 6,919,469 B2, Jul 19, 2005

[69] Van Ooij WJ, Sorenson M, Stacy MB (2011) Silane compositions and methods for bonding rubber to metals US 8,029,906 B2, Oct 4, 2011

[70] Pan G, Schaefer DW, van Ooij WJ, Kent MS, Majewski J, Yim H (2006) Thin solid Films 515:2771

[71] Zhu D, van Ooij WJ (2004) Electrochim Acta 49:1113

[72] Mutin H (2009) Organophosphorous compounds having polysulfide bridge US 7,476,700 B2, Jan 13, 2009

[73] Najari A, Lang P, Lacaze PC, Mauer D (2009) Prog org coat 64:392

[74] Evonik Industries, Dynasylan®MEMO: organofunctional silanes, https://www.dynasylan.com/product/dynasylan/en/Pages/default.aspx (24.07.2015)

[75] Li S, Michiels DFM (2002) Adhesive compositions and methods of use thereof US 6,444,322 B1, Sep 3,2002

[76] Grela K (2014) Olefin Metathesis: Theory and Practice, John Wiley & Sons, New Jersey.

[77] Grubbs RH, Wenzel AG, O'Leary DJ, Khosravi E (2015) Handbook of Metathesis 2nd ed. John Wiley & Sons, New Jersey.

[78] Leitgeb A, Wappel J, Slugovc C (2010) Polymer 51:2927

[79] Banks RL, Bailey GC (1964) Ind Eng Chem Prod Res Dev 3:170

[80] Mol JC (2004) J Mol Catal A Chem 213:39

[81] Schuster M, Blechert B (1997) Angew Chem Int Ed Engl 36:2036

[82] Bose S, Ghosh S (2014) Proc Indian Nat Sci Acad 80:37

[83] Natta G, Dall'Asta G, Bassi IW, Carella G (1966) Makromol Chem 91:87

[84] Schrock RR (1990) Acc Chem Res 23:158

[85] Vougioukalakis GC, Grubbs RH (2010) Chem Rev 110:1746

[86] Kress S, Blechert S (2012) Chem Soc Rev 41:4389

[87] Schrock RR, Hoveyda AH (2003) Angew Chem Int Ed 42:4592

[88] Deraedt C, d´Halluin M, Astruc D (2013) Eur J Inorg Chem 4881

[89] Dall'Asta G (1974) Rubber Chem Technol 47:511

[90] Dounis P, Feast WJ, Kenwright AM (1995) Polymer 36:2787

[91] Katz TJ, Lee SJ, Acton N (1976) Tetrahedron Lett 47:4247

[92] Schleyer PvR, Williams JE, Blanchard KR (1970) J Am Chem Soc 92:2377

[93] Allinger NL, Sprague JT (1972) J Am Chem Soc 94:5734

[94] Hérisson PJ-L, Chauvin Y(1970) Makromol Chem 141:161

[95] Dimonie M, Coca S, Teodorescu M, Popescu L, Chipara M, Dragutan V (1994) J Mol Catal 90:117

[96] Keitz BK, Fedorov A, Grubbs RH (2012) J Am Chem Soc 134:2040

[97] Bielawski CW, Grubbs RH (2007) Prog Polym Sci 32:1

[98] Streck R (1989) Chemtech 19:498

[99] Warel S (1987) Erdöl Erdgas Kohle 103:238

[100] Evonik Industries, Vestenamer 8012: The rubber additive with unique properties, http://www.struktol.com/pdfs/Vestenamer%208012-Evonik.pdf (05.05.2015)

[101] Meisenheimer H, Steiger R, Marbach A, Diedrich KM, Dunn J, Karall G (2011) Encyclopedia of industrial chemistry, Wiley-VCH Verlag, Weinheim (Rubber, 6. Synthesis by Radical and Other Mechanisms)

[102] Dräxler A (1981) Kaut Gummi Kunst 34:185

[103] Calderon N, Ofstead EA, Judy WA (1967) J Polym Sci Part A Polym Chem 5:2209

[104] Katz TJ, Lee SJ, Acton N (1976) Tetrahedron Lett 47:4247

[105] Dimonie M, Coca S, Teodorescu M, Popescu L, Chipara M, Dragutan V (1994) J Mol Catal 90:117

[106] Katz TJ, Han CC (1982) Organometallics 1:1093

[107] Preishuber-Pflugl P, Buchacher P, Eder E, Schitter RM, Stelzer F (1998) J Mol Catal A Chem 133:151

[108] Shea KJ, Kim JS (1992) J Am Chem Soc 114:3044

[109] Walker R, Conrad RM, Grubbs RH (2009) Macromolecules 42:599

[110] Delaude L, Szypa M, Demonceau A, Noels AF (2002) Adv Synth Catal 6:344

[111] Martinez H, Ren N, Matta ME, Hillmyer MA (2014) Polym Chem 5:3507

[112] Scheider WA, Mueller MF (1988) Makromol. Chem. 189:2823

[113] Anderson AW, Merckling NG (1955) Polymeric Bicyclo-(2,2,1)-2-heptene. US Patent 2,721,189, Oct 18, 1955

[114] Ohm RF, Vial TM (1987) J Elastom Plast 10:15

[115] Banasiak DS, Mozdzen EC, Byers JD (1987) Metallotetradecadiene compounds US Patent 4,687,867 A, Aug 18, 1987

[116] Dimonie M, Coca S, Teodorescu M, Popescu L, Chipara M, Dragutan V (1994) J Mol Catal 90:117

[117] Kress J, Wesolek M, Osborn JA (1982) J Chem Soc Chem Commun 514

[118] Kress J, Osborn JA, Greene RME, Ivin KJ, Rooney JJ (1987) J AM Chem Soc 109:899

[119] Schrock RR, Feldman J, Cannizzo LF, Grubbs RH (1987) Macromolecules 20:1172

[120] Floros G, Saragas N, Paraskevopoulou, Psaroudakis N, Koinis S, Pitsikalis M, Hadjichristidis N, Mertis K (2012) Polymers 4:1657

[121] Murdzek JS, Schrock RR (1987) Organometallics 6:1373

[122] Bazan GC, Schrock RR, Cho HN, Gibson VC (1991) Macromolecules 24:4495

[123] Heroguez V, Fontanille M (1994) J Polym Sci (Part A) 32:1755

[124] Hatjopoulos JD, Register RA (2005) Macromolecules 38:10320

[125] Schwab B, France MB, Ziller JW, Grubbs RH (1995) Angew Chem Int Ed Engl 34:2039

[126] Hafner A, Schaaf van der PA, Mühlebach A (1996) Chimia 50:131

[127] Truett WL, Johnson DR, Bobinson IM, Montague BA (1960) J Am Chem Soc 82:2337

[128] Gilliom LR, Grubbs RH (1986) J Am Chem Soc 108:733

[129] Wallace KC, Liu AH, Dewan JC, Schrock RR (1988) J Am Chem Soc 110:4964

[130] Brumaghim JL, Girolami GS (1999) Organometallics 18:1923

[131] Dounis P, Feast WJ, Kenwright AM (1995) Polymer 36:2787

[132] Dall'Asta G, Mazzanti G, Natta G, Porri L (1962) Makromol Chem Rapid Comm 56:224

[133] Natta G, Dall´Asta G, Porri L (1965) Makormol Chem 81:253

[134] Wu Z, Wheeler DR, Grubbs RH (1992) J Am Chem Soc 114:146

[135] Dounis P, Feast WJ, Kenwright AM (1995) Polymer 36:2787

[136] Dimonie M, Coca S, Teodorescu M, Popescu L, Chipara M, Dragutan V (1994) J Mol Catal 90:117

[137] Flook MM, Jiang AJ, Schrock RR, Müller P, Hoveyda AH (2009) J Am Chem Soc 131:7962

[138] Natta G, Dall'Asta G, Porri L (1965) Makromol Chem 81:253

[139] Wu Z, Grubbs RH (1994) J Mol Catal 90:39

[140] Dimonie M, Coca S, Teodorescu M, Popescu L, Chipara M, Dragutan V (1994) J Mol Catal 90:117

[141] Natta G, Dall´Asta G, Mazzanti G (1964) Angew Chem Int Ed 3:723

[142] Günther P, Haas F, Marwede G, Nützel K, Oberkirch W, Pampus G, Schön N, Witte J (1970) Angew Makromol Chem 14:87

[143] Dall'Asta, Scaglione P (1964) Rubber Chem Technol 18:1235

[144] Trzaska ST, Lee L-BW, Register RA (2000) Macromolecules 33:9215

[145] Haas F, Nützel K, Pampus G, Theisen D (1970) Rubber Chem Technol 43:1116

[146] Hejl A, Schermann OA, Grubbs RH (2005) Macromolecules 38:7214

[147] Vasile C (2000) Handbook of Polyolefins 2nd ed., Marcel Dekker, New York, S 131

[148] Baughman TW, Wagener KB (2005) Adv Polym Sci 176:1

[149] Bachler PR, Wagener KB (2015) Monatsh Chem 146:1053

[150] Wagener KB, Boncella JM, Nel JG (1991) Macromolecules 24:2649

[151] Wagener KB, Nel JG, Duttweiler RP, Hillmyer MA, Boncella JM, Konzelman J, Smith DW, Puts R, Willoughby L (1990) Rubber Chem Technol 64:83

[152] Zuech EA, Hughes WB, Kubicek DH, Kittleman ET (1970) J Am Chem Soc 92:528

[153] Dall'Asta G, Stigliani G, Greco A, Motta L (1973) Chimica e Industria 55:142

[154] Brosse JC, Campistron I, Derouet D, Hamdaoui el A, Houdayer S, Reyx D, Ritoit-Gillier S (2000) J Appl Polym Sci 78:1461

[155] Maughon BR, Grubbs RH (1997) Macromolecules 30:3459

[156] Perrott MG, Novak BM (1996) Macromolecules 29:1817

[157] Schneider MF, Gantner C, Obrecht W, Nuyken O (2010) Macromol Rapid Commun 31:1731

[158] Smit T, Müller K, Dahmen S, Negrete L, Sturm B (2012) Rubber material with barrier material made of cycloolefin copolymers WO 2014026865 A1, Aug 13, 2012

[159] Buchmeiser MR, Ahmad I, Gurram V, Kumar PS (2011) Macromolecules 44:4098

[160] Bornand M, Chen P (2005) Angew Chem Int Ed 44:7909

[161] Torker S, Müller A, Sigrist R, Chen P (2010) Organometallics 29:2735

[162] Lichtenheldt M, Wang D, Vehlow K, Reinhardt I, Kühnel C, Decker U, Blechert S, Buchmeiser MR (2009) Chem Eur J 2009, 15, 9451

[163] Cetinkaya S, Karabulut S, Imamoglu Y (2007) NATO Science Series 243:355

[164] Cetinkaya S, Karabulut S, Imamoglu Y (2005) Eur Polym J 41:467

[165] Karabulut A, Cetinkaya S, Imamoğlu Y (2005) Appl Organometal Chem 19:997

[166] Gringolts ML, Denisova YI, Shandryuk GA, Krentsel LB, Litmanovich AD, Finkelshtein ES, Kudryavtsev YV (2015) RSC Adv 5:316

[167] Otsuka H, Muta T, Sakada M, Maeda T, Takahara A (2009) Chem Commun 1073

[168] Ast W, Rheinwald G, Kerber R (1976) Makromol Chem 177:1341

[169] Tian Q, Larock RC (2002) J Am Oil Chem Soc 79:479

[170] Spurcaciu B, Buzdugan E, Nicolae C-A, Dragutan I, Dragutan V (2007) NATO Science Series 243:347

[171] Jeong W, Mauldin TC, Larock RC, Kessler MR (2009) Macromol Mat Eng 294:756

[172] Caster KC, Walls RD (2002) Adv Synth Catal 344:764

[173] Hillmyer MA, Grubbs RH (1993) Macromolecules, 25:872

[174] Thomas RM, Grubbs RH (2010) Macromolecules 43:3705

[175] Ji S, Hoye TR, Macosko CW (2004) Macromolecules 37:5485

[176] Pitet LM, Hillmyer MA (2011) Macromolecules 44:2378

[177] Annunziata L, Fouquay S, Michaud G, Simon F, Guillaume SM Carpentier J-F (2013) Polym Chem 4:1313

[178] Mathers RT McMahon KC, Damodaran K, Retarides CJ, Kelley DJ (2006) Macromolecules 39:8982

[179] Brzezinska KR, Wagener KB, Burns GT (1999) J Polym Sci A Polym Chem 37:849

[180] Nubel PO, Lutman CA, Yokelson HB (1994) Macromolecules 27:7000

[181] Tamura H, Maeda N, Matsumoto R, Nakayama A, Hayashi H, Ikushima K, Kuraya M. (1999) J Macromol Sci A Pure Appl Chem 36:1153

[182] Brzezinska KR, Deming TJ (2001) Macromolecules 34:4348

[183] Schwendeman JE, Wagener KB (2009) Macromol Chem Phys 210:1818

[184] Ast W, Hummel K (1970) Naturwissenschaften 57:545

[185] Seifert K, Taube R, Dahlke M (1981) Ester group-terminated polyolefins. Ger. East Pat. 146,053, Jan. 21, 1981.

[186] Marmo JC, Wagener KB (1993) Macromolecules 26:2137

[187] Marmo JC, Wagener KB (1995) Macromolecules 28:2602

[188] Chasmawala M, Chung TC (1995) Macromolecules 28:1333

[189] Solanky SS, Campistron I, Laguerre A, Pilard J-F (2005) Macromol Chem Phys 206:1057

[190] Sadaka F, Campistron I, Laguerre A, Pilard J-F (2013) Polym Degrad Stabil 98:736

[191] Tlenkopatchev MA, Gutièrrez S (2009) Rev LatinAm Metal Mater S1:1463

[192] Saetung N, Campistron I, Pascual S, Pilard J-F, Fontaine L (2011) Macromolecules 44:784

[193] Martìnez A, Gutièrrez S, Tlenkopatchev MA (2013) Natural Science 5:857

[194] Martìnez A, Gutièrrez S, Tlenkopatchev MA (2012) Molecules 17:6001

[195] Fomine S, Tlenkopatchev MA (2010) Organometallics 29:1580

[196] Gutìerrez S, Tlenkopatchev MA (2011) Polym Bull 66:1029

[197] Thorn-Csanyi E, Ruhland K (1999) Macromol Chem Phys 200:1662

[198] Thorn-Csanyi E, Hammer J, Zilles JU (1994) Macromol Rapid Commun 15:797

[199] Reyx D, Campistron I (1997) Angew Makromol Chem 247:197

[200] Tlenkopatchev MA, Barkenas A, Fomine S (2001) Macromol Theo Simul 10:441

[201] Fainleib A, Pires RV, Lucas EF, Soares BG (2013) Polìmeros 23:441

[202] Obrecht W, Müller JM, Nuyken O, Berke H, Meca L, Triscikova L (2008) Method for the degradation of nitrile rubber by metathesis in the presence of Ruthenium- or Osmium-based catalysts. US Patent 7,470,750 B2, Dec 30, 2008

[203] Guèrin F (2004) Process for the preparation of low molecular weight hydrogenated nitrile rubber. US Patent 6,673,881 B2, Jan 6, 2004

[204] Stelzer F, Hobisch G, Pongratz T, Hummel K (1988) J Mol Catal 46:433

[205] Zhan Z-YJ (2012) Methods of modifying polymers with highly active and selective metathesis catalysts. US 2012/0252982 A1, Oct 4, 2012.

[206] Hummel K (1985) J Mol Catal 28:381

[207] Thorn-Csanyi E, Perner H (1979) Makromol Chem 180:919

[208] Hummel K, Ast W (1973) Makormol Chem 166:39l

[209] Lorber F, Hummel K (1973) Makromol Chem 171:257

[210] Thorn-Csanyi E, Perner H (1986) J Mol Catal 36:187

[211] Hummel K (1982) Pure Appl Chem 54:351

[212] Thummer R, Stelzer F, Hummel K (1975) Makromol Chem 176:1703

[213] Stelzer F, Hummel K, Graimann C, Hobisch J, Martl MG (1987) Makromol Chem 188:1795

[214] Ast W, Bosch H, Kerber R (1979) Angew Makromol Chem 76:67

[215] Kumar VNG, Hummel K, Hönig H (1981) Angew Makromol Chem 96:93

[216] Korshak YV, Tlenkopatchev MA, Dolgoplosk BA, Avdeikina EG, Kuterov DF (1982)J Mol Catal 15:207

[217] Hummel K, Kiattanavith N, Bernard E (1993) Angew Makromol Chem 207:137

[218] Alimuniar A, Yarmo MA, Rahman MZA Kohjiya S, Ikeda Y, Yamashita S (1990) Polym Bull 23:119

[219] Wagener KB, Puts RD, Smith Jr DW (1991) Makromol Chem Rapid Commun 12:419

[220] Thorn-Csanyi E (1994) Rubber Chem Technol 67:786

[221] Craig SW, Manzer JA, Coughlin EB (2001) Macromolecules 34:7929

[222] Sedransk KL, Kaminski CF, Hutchings LR, Moggridge GD (2011) Polym Degrad Stabil 96:1074

[223] Sashuk V, Peeck LH, Plenio H (2010) Chem-Eur J 16:3983

[224] Wolf S, Plenio H (2011) Green Chem 13:2008

[225] Ouardad S, Peruch F (2014) Polym Degrad Stabil 99:249

[226] Hummel K, Groyer S, Lechner H (1982) Kaut Gummi Kunst 35:731

[227] Grießer H, Hummel K (1980) Colloid & Polymer Sci 258:467

[228] Stelzer F, Hummel K, Sommer F, Baumegger E, Lesiak MC (1987) Rubber Chem Technol 60:600

[229] Hummel K, Raithofer G (1976) Angew Makromol Chem 50:183

[230] Hummel K, Stelzer F, Hobisch G, Hartmann B (1987) Angew Makromol Chem 155:143

[231] van Ooij WJ, Harakuni PB, Buytaert, G (2009) Rubber Chem Technol 82:315

[232] Leimgruber S, Kern W, Hochenauer R, Melmer M, Holzner A, Trimmel G (2015) Rubber Chem Technol, 146:1081

[233] Stelzer F, Hummel K, Sommer F, Baumegger E, Lesiak MC (1987) Rubber Chem Technol 60:600

[234] Zümreoglu-Karan B, Bozkurt C, Imamoglu (1992) Polymer J 24:25

[235] Demel S (2003) PhD Thesis, Technical University Graz, page 116

[236] Wolf S, Plenio H (2013) Green Chem 15:315

[237] Zirngast M, Pump E, Leitgeb A, Albering JH, Slugovc (2011) Chem Com 47:2261

[238] Rodriguez-Carvajal J (1992) Physica B 192:55

[239] FIZ Karlsruhe Inorganic Crystal Structure Database: http://www.fiz-karlsruhe.de/ (09.07.2015)

[240] Gottlieb HE, Kotlyar V, Nudelman A (1997) J Org Chem 62:7512

[241] Youssef H.A., El-Hofy H.A., Ahmed M.H. (2011) Manufacturing Technology: Materials, Processes, and Equipment; CRC Press: Boca Raton, pp 75-77

[242] Kirkendall E, Thomassen L, Upthegrove C (1939) Transactions of the AIME 133:186

[243] van Ooij WJ (1979) Rubber Chem Technol 52:650

[244] Van Ooij WJ (2001) Handbook of Rubber Bonding; RAPRA Technology: Shrewsbury, Chap. 6

[245] Van Ooij WJ, Weening WE, Murray PF (1981) Rubber Chem Technol 54:227

[246] Jeon GS, Han MH, Seo G (1999) Korean J Chem Eng 16:434

[247] Ishikawa Y, Hotaka T (2004) Gummi Fasern Kunstst 57:642

[248] Maeseele A, Debruyne E (1969) Rubber Chem Technol 42:613

[249] Haemers G, Mollet J (1978) J Elastom Plast 10:241

[250] Yamauchi MT, Shimuzu T, Doi M, Yasunaga D, Nakayama T, Okumura K (2003) Rubber Chem Technol 76:1045

[251] Hotaka T, Ishikawa Y, Mori K (2005) Rubber Chem Technol 78:175

[252] Kim J (2005) Rubber Chem Technol 78:844

[253] Hammer GE (2001) J Vac Sci Technol A 19:2846

[254] Van Ooij (1977) Surf Sci 68:1

[255] Ball JJ, Gibbs HW, Tate PER (1990) J Adhes 32:29

[256] Hamed GR, Paul R (1997) Rubber Chem Technol 70:541

[257] Patil PY, van Ooij WJ (2004) Rubber Chem Technol 18:1367

[258] Jeon GS (2008) J Adhes Sci Technol 22:1223

[259] Buytaert G, Coornaert F, Dekeyser W (2009) Rubber Chem Technol 82:430

[260] Buytaert G, Liang H, Pax G, Reis P (2010) Rubber Plast News 14

[261] Ziegler E, Kern W, Hochenauer R, Holzner A, Trimmel G (2012) Proceeding of the International Rubber Conference, Jeju-si, South Korea

[262] Zümreoglu-Karan B, Bozkurt C, Imamoglu Y (1992) Polym J 24:25

[263] Reyx D, Campistron I (1997) Angew Makromol Chem 247:197

[264] Craig SW, Manzer JA, Coughlin EB (2001) Macromolecules 34:7929

[265] Zümreoglu-Karan B, Bozkurt C, Imamoglu Y (1992) Polym J 24:25

[266] Fulton WS, Smith GC, Titchener KJ (2005) Appl Surf Sci 221:69

[267] Steiner UB, Caseri WR, Suter UW (1992) Langmuir 8:2771

[268] Loo BH, Frazier DO (1985) J Phys Chem 89:4672

[269] Lopez-Dellamary T, Sampedro JA, Carlos G, Fontes M, Ogura T (1978) Transit Metal Chem 3:342

[270] Falcomer VAS, Lemos SS, Martins GBC, Casagrande GA, Burrow RA, Lang ES (2007) Polyhedron 26:3871

[271] Yan H, Sun K, Zhang Y, Zhang Y (2005) Polym Test 24:32

[272] Choi S-S (2000) J Appl Polym Sci 79:1127

[273] Loo BH, Kato T (1993) Surf Sci 284:167

[274] Lin DG, Sedliarova SN, Vorobieva EV (2003) J Adhesion Sci Technol 17:633

[275] Wicks DA, Wicks Jr. ZW (1999) Prog Org Coat 36:148

[276] Hotchkiss PJ, Malicki M, Giordano AJ, Armstrong NR, Marder SR (2011) J Mater Chem 21:3107

[277] Curtius T (1890) Ber Chem Ges Berl 23:3023

[278] Curtius T (1894) J prakt Chem 50:275

[279] Scriven EFV, Turnbull K (1988) Chem Rev 88:297

[280] Li S, Michiels D (1999) Bonding rubber to textile substrate; using organosilicon compound. US Patent US 6,444,322 B1, Sep 3, 2002